

TECTONIC HISTORY OF THE GREATER ONTONG JAVA PLATEAU AND
ERRATA-BASED CORRECTION OF MARINE GEOPHYSICAL TRACKLINE DATA

A DISSERTATION SUBMITTED TO THE GRADUATE DIVISION OF THE
UNIVERSITY OF HAWAII IN PARTIAL FULFILLMENT
OF THE REQUIREMENTS FOR THE DEGREE OF

DOCTOR OF PHILOSOPHY
IN
GEOLOGY AND GEOPHYSICS

DECEMBER 2011

By
Michael Thomas Chandler

Dissertation Committee:

Pål Wessel, Chairperson
Fernando Martínez
Richard Hey
Dietmar Müller
Michael Mottl

Acknowledgements

Professor Pål Wessel was responsible for my recruitment and also served as my academic adviser throughout my graduate studies. Dr. Wessel's role in this work and in my education can not be overstated. His was, without exception, a productive and positive work environment where all forms of inquiry were encouraged and where impediments to progress were always speedily addressed. The $\sim 4,275$ e-mails that passed between Dr. Wessel and myself were exceeded only by the number of trackline surveys I reviewed and perhaps by his cumulative consumption of caffeinated beverages. I am a very fortunate and appreciative recipient of Dr. Wessel's outstanding guidance. Research funding was provided by the National Science Foundation, J. Watumull Scholarship, International Association for Mathematical Geosciences, Leonida Family Scholarship, Korea Ocean Research and Development Institute and the University of Hawai'i Graduate Student Organization. I thank Brian Taylor, Fernando Martínez, Kiseong Hyeong and the Hawai'i Mapping Research Group for involving me in numerous research topics and seagoing expeditions. Chapter 2 benefited greatly from collaborative contributions by Dietmar Müller, Maria Seton, Brian Taylor, Seung-Sep Kim and Kiseong Hyeong. I thank William Sager for his encouraging review of Chapter 3. Dan Metzger, John Campagnoli and George Sharman of the National Geophysical Data Center provided exceptional support toward the global trackline data review. I thank Edgar Lobachevskiy, Seung-Sep Kim, Seunghye Lee, Todd Bianco, Kolja Rotzoll and Jonathan Weiss and the rest of my contemporaries for making my time away from the computer so interesting. And last but not least, I thank the world-class faculty and staff of the GG department to whom I promise to donate should I ever get a job.

Abstract

The plate tectonic revolution of the 1960s and 1970s is said to mark the Earth Sciences' transition from data-driven discovery to hypothesis testing. This is largely the case in marine geoscience as modern research expeditions focus on isolated study areas rather than globe spanning surveys typical of the past. Although the onus among scientists is generally to explore new problems by gathering new sets of data, I contend that we have not yet fully digested existing data sets. During my doctoral studies, I engaged in researches that examined large amounts of previously collected data. I utilized paleolatitude measurements in my attempts to constrain the past movements of the Ontong Java, Manihiki and Hikurangi oceanic plateaus. Through my resultant familiarity, I was able to discover a pattern within the paleolatitudes that suggested significant rotation of the plateaus. This rotation may explain why Ontong Java's paleo-pole does not agree with other coeval Pacific paleo-poles and with the Pacific apparent polar wander path in general. This inference further implies that Ontong Java may have been decoupled from the Pacific plate during the past or that, speculatively, the entire Pacific plate was rotated by $\sim 30^\circ$ – 50° to coincide with Ontong Java's paleo-orientation. I further immersed myself in the entirety of the National Geophysical Data Center's marine geophysical trackline archive in an effort to identify and correct large-scale and systematic errors in marine gravity, magnetic, and single/center beam depth measurements. I produced 5,203 "E77" correction tables pertaining to along-track analysis of each of the archived surveys. Initial inspection of discrepancies at intersecting tracks indicates improvements in median crossover errors from 27.3 m to 24.0 m, 6.0 mGal to 4.4 mGal, and 81.6 nT to 29.6 nT for depths, free air gravity anomalies, and residual magnetic anomalies, respectively.

Contents

Acknowledgements	ii
Abstract	iii
List of Tables	vi
List of Figures	viii
Preface	ix
1 Introduction	1
2 Reconstructing Ontong Java Nui: Implications for Pacific absolute plate motion, hotspot drift and true polar wander	10
2.1 Introduction	11
2.2 Analysis	15
2.2.1 Reconstruction of the OJN breakup	15
2.2.2 Absolute reconstruction of OJN origin	19
2.3 Discussion	24
2.4 Conclusion	28
3 Analysis of Ontong Java Plateau Paleolatitudes and Evidence for Rotation since 123 Ma	42
3.1 Introduction	43
3.2 Analysis	44
3.3 Results	48
3.4 Discussion	50
3.5 Conclusion	55

4	Errata-based correction of marine geophysical trackline data	67
4.1	Introduction	68
4.2	Errata Review Process	70
4.3	Results	75
4.3.1	Effects of along-track analysis on global crossovers	75
4.3.2	E77 errata table review	76
4.4	Discussion	81
4.5	Conclusion	85
5	Conclusions	97
5.1	Pacific absolute plate motion	97
5.2	Hotspot drift	97
5.3	True polar wander	98
5.4	Rotation of the Ontong Java Plateau	99
5.5	Coupling of Ontong Java–Pacific	100
5.6	The Greater Ontong Java Plateau Hypothesis	101
5.7	Errata-based correction of trackline data	104
	Literature Cited	105

List of Tables

2.1	Ontong Java Nui breakup rotation poles	30
3.1	Published ODP drill locations and paleomagnetism	56
3.2	Ontong Java paleomagnetic analysis results	56
3.3	Inter-site latitude and paleolatitude differences	57
4.1	Along-track analysis outlier thresholds	86
4.2	Sample E77 errata table for HIG cruise 08040004	86
4.3	List of invalid trackline surveys.	87
4.4	List of Scripps cruises with two-way travel wrap-around errors.	88
4.5	The largest systematic gravity offsets	89

List of Figures

1.1	Raff and Mason magnetic anomaly map	3
1.2	Plumes and large igneous provinces	6
1.3	The Taylor [2006] Ontong Java–Manahiki–Hikurangi reconstruction	7
2.1	Ontong Java, Manihiki, and Hikurangi regional bathymetry	31
2.2	KORDI Leg NAP09-3 multibeam, backscatter and magnetic data	32
2.3	Ontong Java Nui relative rotations	33
2.4	Ellice Basin bathymetry compilation and fracture zone traces	34
2.5	Ellice Basin magnetic anomaly map	35
2.6	Illustration of absolute plate motion models used in this study	36
2.7	Total reconstructions of the Ontong Java Nui breakup	37
2.8	Modeled ODP site latitude and plateau rotation histories.	38
2.9	Modeled ODP site longitude histories.	39
2.10	123 Ma reconstruction and paleolatitude comparison	40
2.11	Louisville hotspot drift predicted by the OMS-05 APM	41
3.1	Ontong Java basement drilling locations	57
3.2	Ontong Java diverges from the Pacific apparent polar wander path	58
3.3	Illustration of the observed Δ paleolatitude vs Δ latitude slope bias	59
3.4	Invalid paleolatitudes indicated by Δ paleolatitude vs inter-site distances	60
3.5	Map view illustration of rotation method	61
3.6	Map view illustration of the undisturbed rotation case	62
3.7	χ^2 misfit vs rotation angle	63
3.8	Observed versus modeled paleolatitudes at optimum rotation angles	63
3.9	Removing the slope bias using optimum rotations and tilt corrections	64
3.10	123 Ma Ontong Java Nui reconstructions	65

3.11	Effect of tilt correction on Δ paleolatitude vs inter-site distances . . .	65
3.12	Effect of tilt correction on slope bias	66
4.1	Distribution of NGDC bathymetry tracks	90
4.2	Sample E77 review plot for HIG cruise 08040004.	91
4.3	Depth, free air gravity, and magnetic anomaly COE histograms. . . .	92
4.4	Effects of magnetic anomaly recalculation on crossover errors	93
4.5	Median gravity COE map before and after correction.	94
4.6	Median depth COE map before and after correction.	95
4.7	Median magnetic COE map before and after correction.	96
5.1	Which model for Ontong Java rotation is correct?	100
5.2	Variations on a theme by Taylor [2006]	103

Preface

This work began as a data analysis exercise centered around improving erroneous trackline geophysical data archived at the National Geophysical Data Center. The aims were to identify systematic error sources and to initiate an errata-based data correction system that preserves original data while enabling on-the-fly correction of data sets. Project components included software development, along-track data exploration/review, crossover error analysis, and correction dissemination. Development and calibration of analytical software and the errata format comprised much of my Master's work. I was invited to continue as a doctoral candidate so that I might complete the remaining ~5,000+ cruise reviews and crossover error analyses.



The author aboard R/V *Ka'imikai O Kanaloa* in August of 2011.

The data review project, though vastly important, did not in itself possess sufficient breadth and scope for a Doctor of Philosophy degree. In addition, funding

constraints inhibited supplemental funding of this project which furthered the need to pursue alternative research topics. Fortunately my adviser was able to provide funding for a tectonic investigation of the Ontong Java–Manihiki–Hikurangi super-plateau hypothesis. This investigation proved to be fruitful as I encountered large differences in reconstructions predicted by published absolute plate motion models. Comparisons of plateau reconstructions to published paleolatitudes also allowed us to consider important topics such as hotspot drift and true polar wander. Through this investigation a new Pacific absolute plate motion model was derived that is in better agreement with Pacific paleolatitudes.

By comparing super-plateau reconstructions to published paleolatitudes for Ontong Java Plateau, I was able to become sufficiently familiar with the paleolatitudes to notice the pattern that their differences were generally twice the magnitude of their drill site latitude differences. This observation initiated an exciting period of data exploration as my adviser and I attempted to gain an understanding of the phenomenon. This investigation quickly developed into a distinct project with important implications for Ontong Java and Pacific plate histories.

Although the global crossover analysis portion of the trackline review project remains as future work, the time-intensive stage requiring manual review of all individual cruises is now complete. Along with the super-plateau reconstruction and paleolatitude analysis projects, it is my hope that these endeavors constitute an achievement worthy of a doctoral degree in Geology and Geophysics.

Chapter 1

Introduction

Prior to the deployment of naturalists aboard 19th century exploration voyages, marine science consisted largely of the study of tides, currents, navigation and cartography. These skills enabled the settlement of remote locations such as Iceland and Greenland by the Vikings as well as the diffuse islands of Oceania by Micronesians, Melanesians, and Polynesians. Nautical science played an eminent role in the development of the modern inter-connected world we live in today.

While naturalists made early geologic observations at sea (e.g., Charles Darwin's insight that atolls form as coral reefs continue to grow upward as islands subside), the earliest dedicated marine science expeditions included America's 90,000 mile Exploring Expedition (1839–1843) and Britain's Challenger Expedition (1872–1876). The latter voyage first located the Mariana Trench using leadline fathometry.

Vening Meinesz became one of the earliest marine geophysicists by deploying his pendulum gravimeter onboard Dutch submarines in the 1920s–1930s. These expeditions took him to the opposite side of the globe where he mapped the first negative gravity anomalies over ocean trenches [e.g., Vening-Meinesz, 1948].

Observations of submarine mountain chains and trenches perplexed many scientists working under the then standard paradigm in which continents and ocean basins were not subject to lateral displacement. Alfred Wegener's revolutionary continental drift hypothesis [Wegener, 1915] rocked the geologic community by being the first hypothesis to present compelling evidence for the past movement of continents. His hypothesis lacked a physically plausible mechanism for such movement, however, and was not readily accepted.

Massive investment in geophysical instrumentation occurred during World War II

as sonars, magnetometers and positioning systems proved essential in struggles for naval superiority. Significant investment in marine geophysics was continued after the war, primarily by the United States. Instrumentation rapidly improved and expanded to include marine seismology and perhaps the fulcrum of all marine science, drilling of the deep sea floor. Costly drill cores recovered from the seafloor are analyzed by virtually every sub-discipline within the marine sciences.

Remanent magnetization is particularly relevant to the understanding of Earth history. Remanent magnetization is the process by which the Earth's magnetic field orientation is frozen into molten iron-bearing rock as it cools or in sedimentary settings as iron-bearing clasts are deposited and subsequently lithified in orientations imposed by the Earth's geomagnetic field. The study of the remanent magnetic field orientations preserved in undisturbed volcanic rocks [e.g., Runcorn, 1956; Irving, 1956] yielded important estimates of sample latitudes at the time of their emplacement (a.k.a, paleolatitude). By measuring paleolatitudes for chronological sequences of rock, drift histories through time known as apparent polar wander paths (APWP) were constructed. Radiometric dating of rock samples constrained these drift histories. APWP were compiled around the world and all results indicated that continents had moved in the past.

In the marine setting, fluxgate magnetometers were first deployed behind ships off the U.S. west coast in the 1950s [Raff and Mason, 1961]. The resulting zebra pattern magnetic anomaly (Fig. 1.1) was not understood until Morley [2001] and Vine and Matthews [1963] combined the seafloor spreading hypothesis [Hess, 1962; Dietz, 1961], where mantle convection currents are thought to rise and form new oceanic crust at mid-ocean ridges then slowly sink with age before eventually subducting back into the mantle at ocean trenches, with the reversing nature of the Earth's paleomagnetic field [i.e., Brunhes, 1906; Matuyama, 1929] to produce the alternately magnetized pattern shown in Figure 1.1.

ters of the Nazca, Cocos and Philippine Sea plates, most of the world's ocean basins share passive margins with continents. The Pacific, therefore, has no easily accessible outcrops for APWP determination.

As a work around, the past motions of the Pacific plate have been investigated thoroughly by analyzing the geometries of hotspot seamount trails such as Hawai'i and Louisville and others. By assuming that hotspot plumes are fixed in the mantle, scientists interpret bends in seamount chains (e.g., the classic Hawaiian Emperor Bend) as resulting from past changes in plate motion. These seamount trends relative to a fixed hotspot reference frame have long been used to generate Pacific absolute plate motion models (APM) [e.g., Duncan and Clague, 1985; Koppers et al., 2001; Wessel and Kroenke, 2008].

The Pacific APM derived from hotspot trail geometries is currently being revised due to paleolatitude measurements at several Emperor Seamounts that are well north of the Hawaiian hotspot's current latitude [Tarduno et al., 2003]. These measurements question the validity of the fixed hotspot assumption. Under the new interpretation, the Hawaiian Emperor Bend is thought to reflect southward motion of the plume until ~ 50 Ma when its position is thought to have stabilized. This new interpretation was additionally supported when an African plate based motion model projected to the Pacific via the Africa–East Antarctica–West Antarctica–Pacific plate circuit was used to model the Hawaiian-Emperor chain [Steinberger et al., 2004]. Results of this study did not produce the pronounced bend so apparent in bathymetry and gravity maps indicating that changes in plate motion were not responsible for the Hawaiian Emperor Bend.

Preliminary results from the recently completed IODP Leg 330 drilling expedition along the Louisville seamount trail presented at this December's American Geophysical Union conference indicate $\sim 2^\circ$ or less of north-south movement of the Louisville Hotspot in the last ~ 70 My. This drift history differs from coeval samples from the

Emperor chain, and given observed great-circle distances between coeval Emperor and Louisville volcanoes [Wessel and Kroenke, 2009] it suggests that both true polar wander and hotspot drift might have played a role [e.g., Steinberger et al., 2011]; more work is needed to constrain true polar wander versus hotspot drift. This new evidence suggesting a fixed Louisville plume supports fixity of hotspots and implies that the motion of the Hawai‘i plume prior to 50 Ma could be considered a temporary perturbation brought about by interaction of the plume with a migrating ridge, for example, rather than behavior typical of mantle plumes as pronounced as Hawai‘i.

That scientists are currently debating whether hotspots drift or not and whether the Earth underwent true polar wander indicates to some extent the uncertainties involved in attempting to determine plate motion histories. A great deal of work remains toward understanding the history of plate motions. Another important element in the hotspot debate is whether large igneous provinces (LIP) and hotspot chains can be formed from the same plume (see Figure 1.2). There exist many hotspot seamount chains and many LIPs but the two rarely appear to have a genetic relationship. Connecting LIPs to their prospective hotspot sources has proven challenging [Clouard and Bonneville, 2001].

At the center of many of these questions is the Ontong Java Plateau (OJP), which is thought to have erupted rapidly between ~ 125 – 120 My ago. OJP is the world’s largest LIP with anomalously thick crust and largely homogenous seismic and geochemical structure. It is thought that OJP was erupted during the plume head phase of hotspot volcanism [e.g., Tarduno et al., 1991]. OJP’s only existing potential hotspot source is the Louisville. Louisville seamounts older than ~ 80 Ma have been subducted at the Tonga-Kermadec Trench thus limiting our ability to establish this connection.

Chapter 2 investigates the connection between OJP and the Louisville hotspot using both the Pacific and Africa-based APMs along with a hybrid Pacific APM

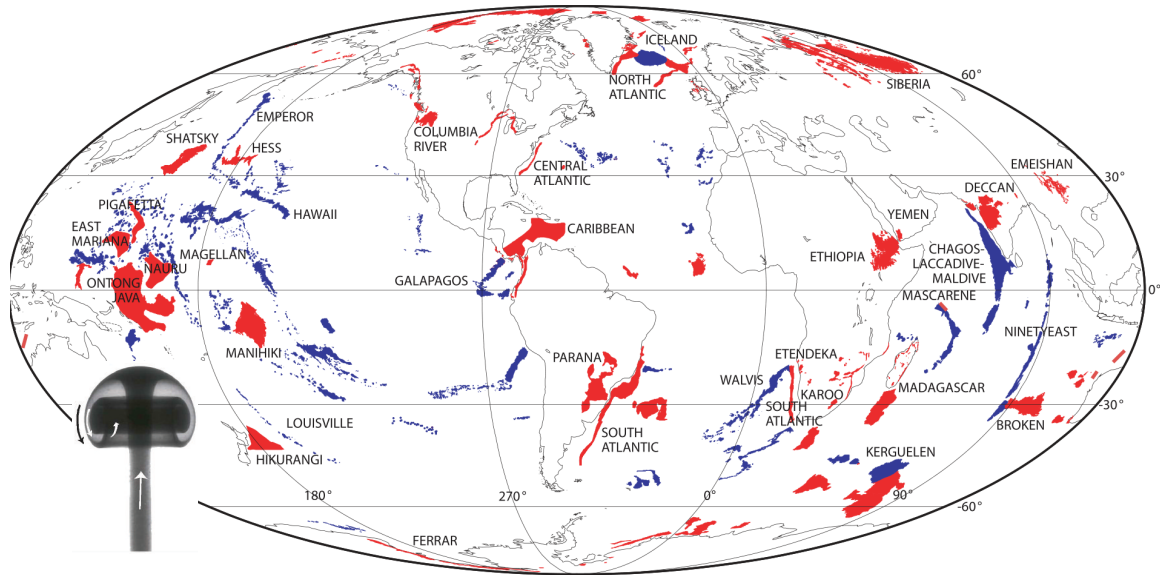


Figure 1.2: Map of the world's large igneous provinces (red) and volcanic chains (blue) (from Coffin et al. [2006]). According to the mantle plume hypothesis [e.g., Morgan, 1971; Campbell, 2005], large igneous provinces form rapidly by eruptions of plume heads whereas age-progressive hotspot chains form over much longer time frames as moving plates pass over hotspots.

that was developed for this research that includes Hawaiian hotspot drift during the Emperor stage. Whereas previous studies found excessive latitudinal discrepancies between OJP's reconstructed latitude and Louisville hotspot's current latitude, this study builds upon the recent hypothesis by Taylor [2006] (see Figure 1.3) which established the plausibility of an Ontong Java–Manihiki–Hikurangi super-plateau. The two additional plateaus, according to the hypothesis, were rifted away from OJP by seafloor spreading in the Ellice Basin and Osbourn Trough. Chapter 2 compares 123 Ma super-plateau reconstructions to the current position of the Louisville hotspot and published paleolatitudes for OJP. By comparing this array of information I am able to infer which models require true polar wander or hotspot drift and to determine which APM model is favored by the evidence.

Whereas Chapter 2 investigates the OJP–Louisville connection using OJP's mean paleolatitude, Chapter 3 details an in-depth internal analysis of OJP's paleolatitudes. In the course of my research, I became sufficiently familiar with the table of paleolat-

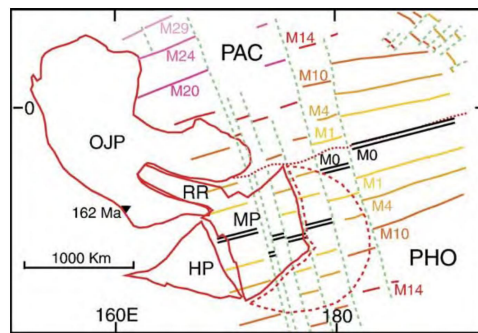
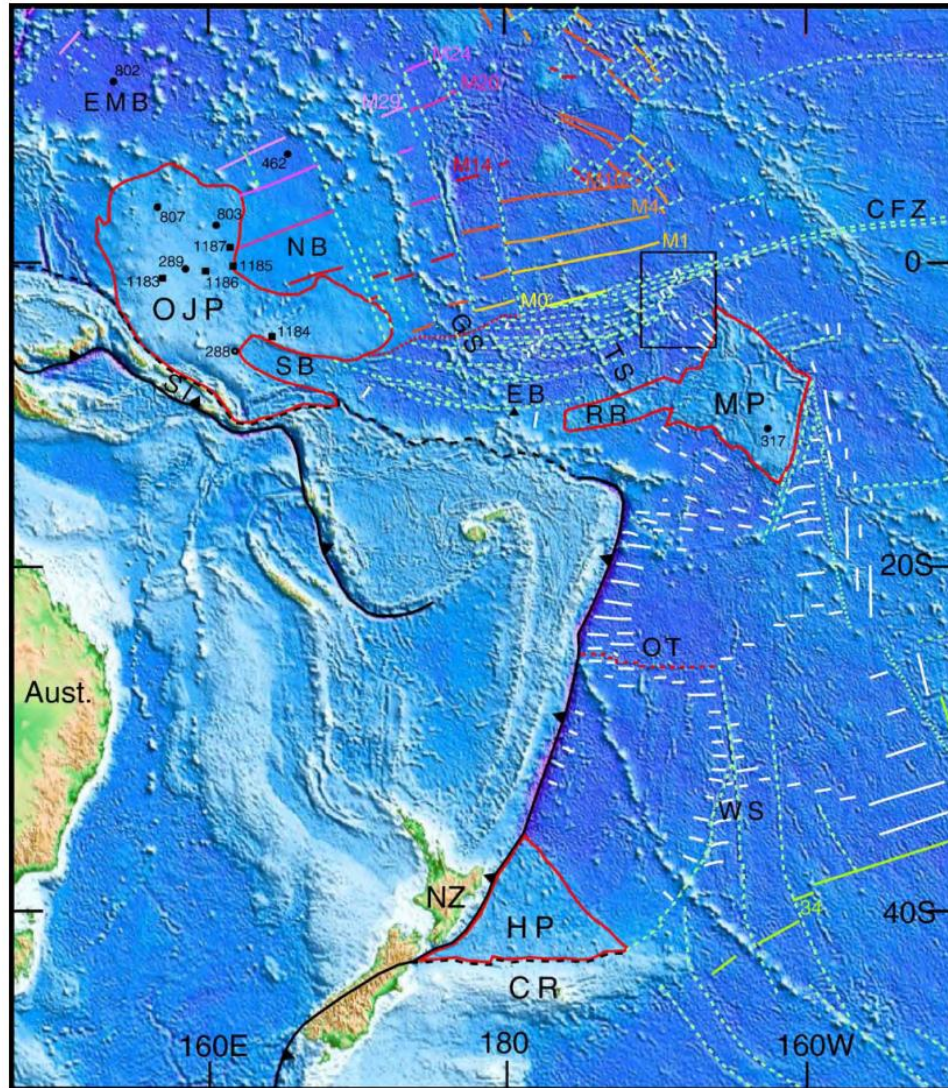


Figure 1.3: Taylor [2006] regional bathymetry map of the Western Pacific (top) and ~ 125 Ma reconstruction of the Ontong Java–Manahiki–Hikurangi super-plateau (bottom). This hypothesis suggests that Ontong Java (OJP) and Manihiki (MP) plateaus were rifted apart by seafloor spreading in the Ellice Basin (EB) and that Hikurangi Plateau (HP) was rifted away from MP by spreading at Osborn Trough (OT) [Lonsdale, 1997]. A second order feature of the model is that Robbie Ridge (RR) reconstructs into Stewart Basin (SB).

itudes published by Riisager et al. [2004] to finally recognize a bias between the published drill site latitudes relative to their paleolatitudes. I noticed that, for instance, the latitudinal distance between sites 807 and 1184 was 8.5° while the corresponding paleolatitude distance between these two sites was 16.5° . This pattern persisted as I examined differences for other sites. Chapter 3 details this intriguing observation and illustrates how the bias can be explained through rotation of the plateau as well as correction of two of OJP's paleolatitudes.

The modern geophysicist enjoys unencumbered access to a wide array of physical data served around the clock by online data centers. Although interpretations derived from these data are largely restricted by copyright of published research articles, the most important component of all, the empirical observations, are largely accessible to the public. It would not be far-fetched for intrepid non-scientists to access this information and to bring new insights to the forefront.

Instrument resolution and sampling frequencies continue to improve at rates that far exceed the growth rate of the international body of scientists. That scientists are not entirely able to keep up with the rising tide of information is not an unreasonable claim. However, the cost of marine research continues to escalate as does competition for increasingly scarce research funding. The globe-trotting days of the 1960s-1970s have been replaced by an era of focused research expeditions where every moment counts.

A large part of my graduate work involved the development of marine geophysical data quality control methods and the subsequent review of the 5,203 cruises presently archived by the National Geophysical Data Center. This archive is the largest in the world and houses the majority of single/center beam depth, magnetic, and gravity measurements gathered since the dawn of accurate marine positioning systems in the early 1950s. Wessel and Chandler [2007] and Chandler and Wessel [2008] describe the quality control methods that were developed in the course of this research. Chapter

4 describes how each cruise was reviewed along-track and gauges the effectiveness of the methods by comparing median measurement discrepancies at track intersections before and after correction. The resulting E77 errata tables are shown to improve data quality considerably.

Chapter 2

Reconstructing Ontong Java Nui: Implications for Pacific absolute plate motion, hotspot drift and true polar wander

Abstract

The Taylor [2006] hypothesis suggesting a common origin for the Ontong Java, Manihiki, and Hikurangi large igneous provinces provides an opportunity for a quantitative reconstruction and reassessment of the Ontong Java–Louisville hotspot connection. My plate tectonic reconstructions of the three plateaus into Ontong Java Nui, or greater Ontong Java, combined with models for Pacific absolute plate motion (APM), allowed an analysis of this connection. The Ontong Java Nui breakup model calls for rifting apart of Ontong Java and Manihiki plateaus in one stage, with a two-stage separation for Manihiki and Hikurangi plateaus. Using three different Pacific APMs, I reconstruct the Ontong Java Nui super plateau back to 123 Ma and compare its predicted location with paleolatitude data obtained from the Ontong Java and Manihiki plateaus. Discrepancies between my Ontong Java Nui reconstructions and Ontong Java and Manihiki paleolatitudes are largest for the fixed Pacific hotspot APM. Assuming a Louisville Hotspot source for Ontong Java Nui, remaining disparity between Ontong Java Nui’s paleo-location at 123 Ma and published paleomagnetic latitudes for Ontong Java plateau imply that 7° – 12° of Louisville hotspot drift or true polar wander may have occurred since the formation of Ontong Java Nui. However, the older portions of the Pacific APMs could easily be biased by a similar amount, making

a firm identification of the dominant source of misfit difficult. Prior studies required a combined 26° of hotspot drift, octupole bias effects, and true polar wander just to link the Ontong Java Plateau to Louisville. Consequently, I suggest the super plateau hypothesis and my new reconstructions have considerably strengthened the case for a Louisville plume origin for Ontong Java Nui.

2.1 Introduction

The largest and most voluminous of large igneous provinces, Ontong Java Plateau (OJP) (see Figure 2.1), is also thought to have had the highest emplacement rate [Coffin and Eldholm, 1994]. Formative volcanism may have triggered a global oceanic anoxic event and black shale deposition while ongoing volcanism likely contributed to the 30 m.y. mid-Cretaceous greenhouse period [Larson and Erba, 1999; Kerr, 1998; Erba and Tremolada, 2004]. Yet in spite of OJP's geologic prominence, its formation and tectonic history remain poorly understood.

Numerous studies tested OJP's link to existing hotspots, reaching differing conclusions based on an evolving set of paleolatitude evidence and Pacific plate motion models. Prior to the availability of oceanic paleolatitudes, Pacific reconstructions assuming hotspot fixity reconstructed OJP near Louisville hotspot thus providing a satisfactory history of the Louisville plume that was in accordance with observations at the time [e.g., Henderson and Gordon, 1981]. Subsequently, the accumulation of Pacific paleolatitude information gathered by the Deep Sea Drilling Project (DSDP) and Ocean Drilling Program (ODP) provided much needed constraints on plume history. For instance, Tarduno et al. [1991] suggested southward motion of the Louisville plume to account for discrepancies between plate motion models and OJP paleolatitude measurements at DSDP Site 289 and ODP Site 807. However, Louisville drift remains uncertain due to the lack of paleolatitude measurements along the Louisville

chain (such apparent drift could also be induced by errors in Pacific plate motion models). More recently, studies by Neal et al. [1997], Antretter et al. [2004] and Kroenke et al. [2004] were unable to link OJP with Louisville, suggesting either (a) that the largest igneous province was formed by a relatively short-lived hotspot whose plume trail has long been subducted or (b) that OJP was indeed formed over a Louisville hotspot that has since drifted south, in addition to requiring a combination of true polar wander and the long-term effects of octupole contributions to account for the large paleomagnetic discrepancies. Importantly, paleolatitude evidence along the Emperor seamount chain [e.g., Tarduno et al., 2003, 2009]) may necessitate a revision of Pacific motion models prior to ~ 50 Ma; such Pacific APM models accounting for Hawaiian plume drift should produce less southerly reconstructions of OJP and improved paleolatitude agreement.

Similarities in composition, seismic velocity structure, and age among Ontong Java and two other large igneous provinces, Manihiki (MP) and Hikurangi (HP) plateaus (Figure 2.1), have been widely cited in previous studies. After analyzing DSDP Leg 33 basalts (MP Site 317a), Jackson et al. [1976] determined MP's basement composition to be similar to OJP basalts retrieved at DSDP Site 289. Mortimer and Parkinson [1996] concluded that HP shared similar geochemical characteristics with OJP and MP after analyzing dredged rocks from HP's basement. Predominantly tholeiitic ocean-island like composition has consistently been reported for OJP [Tejada et al., 2002; Mahoney et al., 1993], MP [Timm et al., 2011; Ingle et al., 2007], and HP [Hoernle et al., 2010]. Hussong et al. [1979] investigated the crustal structure of OJP and MP and found nearly identical crustal seismic velocities for the two plateaus. Furthermore, analyses of ODP basement samples yielded similar ages for OJP as 121–125 Ma [Tejada et al., 2002], MP as 117.9 Ma [Ingle et al., 2007] or 124.6 Ma [Timm et al., 2011], and HP as 118 Ma [Hoernle et al., 2010].

Key observations that Manihiki and Hikurangi plateaus were rifted apart by

seafloor spreading centered at the Osbourn Trough [Lonsdale, 1997; Billen and Stock, 2000] and that OJP and MP appear to have rifted apart by \sim east-west spreading in the Ellice Basin [Taylor, 2006] allowed Taylor to propose that the three plateaus originated as one super plateau, here called Ontong Java Nui (OJN), meaning greater Ontong Java. The Taylor [2006] interpretation of Ellice Basin’s evolution identifies the Nova Canton Trough as a fracture zone [e.g., Joseph et al., 1992] as opposed to an earlier rift system interpretation by Larson [1997]. Taylor [2006] identified several unresolved issues with the super plateau model including a lack of lineated magnetic anomalies to better constrain the breakup which constrains the breakup to the Cretaceous normal superchron (\sim 124 to \sim 84 Ma [Walker and Geissman, 2009]) as well as the lack of an accepted geodynamic mechanism for the submarine emplacement of such a large igneous province. For instance, the plume separation model of Bercovici and Mahoney [1994] sought to explain the observation of secondary volcanism at several large igneous provinces including the Ontong Java Plateau. Ingle and Coffin [2004] speculated that OJP’s anomalous emplacement could be explained by a major bolide impact. However, Korenaga [2005]) considered OJP’s submarine emplacement due to both plume head and bolide events unlikely and proposed the entrainment of eclogite mantle at a fast spreading ridge to explain OJP’s submarine emplacement. While the widely established plume hypothesis is currently favored, the eclogite entrainment hypothesis may provide an interesting alternative should scientists eventually rule out a hotspot source for Ontong Java.

Considerable uncertainties exist in both attempting to reconstruct Ontong Java Nui back in time and in linking the plateau to its only geometrically plausible hotspot source, the Louisville. This is in part due to uncertainties associated with using Africa-based absolute plate motion models [O’Neill et al., 2005] projected to the Pacific via the Antarctica plate circuit or with using APM models relying on the assumption of hotspot fixity [Wessel and Kroenke, 2009; Tarduno, 2007]. Apparent

incompatibility between the current latitude of Louisville ($\sim 51^\circ$ S) and the mean ODP paleolatitude of OJP (25.2° S) [Riisager et al., 2004] also contributes to the dilemma. Furthermore, regarding Louisville as a prospective source for OJN, although geochemists have not been able to unequivocally link OJP samples to current hotspots [e.g., Vanderkluyzen et al., 2007], geochemical variation between plume head and tail phases remains possible [Mahoney and Spencer, 1991]. A causal connection between the plateau and a plume source may also indirectly support the plume theory, which recently has come under increased scrutiny [e.g., Foulger and Natland, 2003].

A recent transit survey of central Ellice Basin by the Korea Ocean Research and Development Institute (KORDI), in collaboration with SOEST, has yielded new bathymetry revealing \sim east-west trending fracture zone fabric, \sim north-south oriented abyssal hill fabric, as well as southeasterly trending fracture zones possibly associated with a late stage spreading reorientation. I interpret these new data as evidence in favor of the large offset, short-segment spreading centers proposed by Taylor [2006] to accommodate the separation of OJP and MP. Here, using available physical evidence, including fracture zone signatures in Ellice Basin and the vicinity of Osbourn Trough, I aim to further constrain the OJN breakup.

APM rotations imply large plateau displacements and are the primary causes of discrepancies between OJN reconstructions, Louisville hotspot's current estimated position, and OJP/MP paleolatitude measurements. I therefore investigate the effects of two recent APMs available in the literature [Wessel and Kroenke, 2008; O'Neill et al., 2005], as well as a new hybrid APM based on a fixed Louisville and drifting Emperor-stage Hawaiian plume, on OJN reconstructions. Such a comparison is timely and necessary as these three APMs reflect the principal ideas and evidential refinements found in the current literature but also produce significantly different reconstructions. By reconstructing the reassembled OJN back in time using these different APM models, I attempt to shed light on the tectonic conditions during the

formation and breakup of OJN.

2.2 Analysis

2.2.1 Reconstruction of the OJN breakup

The reconstruction of the Ontong Java, Manihiki, and Hikurangi plateaus by Taylor [2006] was qualitative as no finite rotation model was determined. As OJP, MP and HP formed during the Cretaceous normal superchron, the interlying basins lack a reversing magnetic signal. I therefore use digitized outlines of the plateaus in lieu of magnetic isochrons in the tectonic reconstruction of the OJN plateau. Except in areas where geologic mapping provided insight, I relied on the 4,000 meter contour in delimiting plateau extents (as in previous studies, e.g., Fitton and Godard [2004] and Korenaga [2005]). Whereas Hellinger’s method for least squares on a sphere [Hellinger, 1981; Chang, 1987] typically uses conjugate magnetic isochrons as inputs for solving spherical reconstructions, I was limited to choosing complementary boundaries along each plateau instead of conjugate isochrons. Figure 2.3 illustrates how I determined OJN relative rotations. Uncertainties in plateau complementary boundaries were estimated at 21 km for Osbourn Trough spreading and 48 km for Ellice Basin spreading. By convention, HP was first rotated to MP using the MP–HP rotation pole (blue star), followed by a rotation of MP/HP to OJP about the OJP–MP pole (green star). Flowlines predicted by my single stage rotations, also shown in Figure 2.3 (dashed black curves), indicate first-order agreement with Ellice Basin fracture zone trends (fine black pen). However, single-stage flowlines in the Osbourn Trough vicinity show inadequate agreement with fracture zone constraints and require further refinement as described later in this section. A result of my method is that gaps between OJP–MP and between MP–HP apparent in the Taylor [2006] reconstruction are not found in my OJN reconstruction. I model MP \sim 350 km west

and HP ~ 200 km southeast of their Taylor [2006] counterparts. My model, however, positions HP ~ 250 km northwest (relative to MP) of HP's position predicted by the MP–HP reconstruction of Davy et al. [2008], and is therefore intermediate.

My digitized plateau outlines follow those of Taylor [2006], especially in their inclusion of Robbie Ridge as part of MP and Stewart Basin as part of OJP. I tested the effect of excluding these features from Ellice Basin conjugate borders. Omitting the Robbie Ridge–Stewart Basin fit in the modeling results in a $\sim 3^\circ$ displacement of the OJP–MP rotation pole (dark green star in Fig. 2.3) and increases rotational uncertainty (not shown) but does not rule out such a fit. In fact, omitting these features from the Ellice Basin reconstruction produces the same result, that Robbie Ridge fits into Ellice Basin. This result is not surprising as the same plateau borders, aside from Robbie Ridge and Stewart Basin, are used in both reconstructions. Due to their fit in both cases, I include these features in my remaining analyses. The OJP perimeter loosely follows the 4,000 m isobath along the northern margin as in prior studies [e.g., Korenaga, 2005] then follows the base of the plateaus steepest gradients in the vicinity of the Stewart Basin. Along the southern OJP margin, the perimeter has been extended to encompass the plateau's geologically mapped extents in the Solomon Islands [e.g., Tejada et al., 2002]. OJP's east rift margin, along which conjugate boundaries are drawn, are highly pronounced. Manihiki's perimeter is fairly straight forward and was visually interpreted to follow the base of the plateau's rift margins. In the Robbie Ridge vicinity, the perimeter loosely follows the 4,000 meter contour and terminates at a bathymetric channel which by coincidence yields a length comparable to that of the Stewart Basin. Hikurangi's perimeter follows plate boundaries to the south and west and is interpreted along the base northeast flank.

The lack of magnetic isochrons in Ellice Basin and in the vicinity of Osbourn Trough constrains the OJN breakup to have occurred within the Cretaceous normal superchron (~ 124 Ma to ~ 84 Ma). I was able to model plateau formation to have

occurred rapidly between ~ 125 Ma and ~ 120 Ma based on published ages of basement rocks at each plateau: 122 ± 3 Ma from OJP [Parkinson et al., 2003] and 124.6 ± 1.6 Ma from MP [Timm et al., 2011]. Evidence from rift structures along the MP and HP plateau margins [Davy et al., 2008] as well as the 120.4 Ma M0 isochron [Gradstein et al., 1994] north of Ellice Basin constrain my 120 Ma OJN breakup initiation age. I terminate spreading at 86 Ma in accordance with a proposed southerly docking of HP with Chatham Rise prior to the commencement of spreading at the Pacific-Antarctic ridge [Billen and Stock, 2000; Downey et al., 2007; Worthington et al., 2006].

To further constrain the breakup, I conducted a detailed analysis of Ellice Basin fracture zones utilizing 1 arc minute vertical gravity gradient data (Sandwell and Smith [2009], as in Fig 2.2) and a compilation of 30 arc second resolution predicted bathymetry [Becker et al., 2009] and available high resolution multibeam data. These maps were imported into Google Earth, enabling the digitization of fracture zones in accordance with guidelines for the new Global Seafloor Fabric and Magnetic Lineations Database project (GSFML) [Wessel et al., 2009]. Fracture zone digitization is subject to uncertainty in areas lacking high resolution shipboard data but fracture zones are well defined in the Nova-Canton Trough and NAP09-3 multibeam mapping areas. Fracture zone trends are dominantly \sim east-west in the western Ellice Basin and \sim east-northeast in the east. A zone of southeast trending fracture zones in the central basin may be related to a late stage spreading reorientation. If this is the case, paleo-spreading centers could possibly be found within the southeast trending zone. Ellice Basin fracture zones digitized in this study are shown in Figure 2.4 and will be submitted for inclusion in the GSFML Database.

Ellice Basin bathymetry coverage shown in Figure 2.4 is quite sparse, with previous surveys focusing on the Nova Canton Trough, northwest of MP [Joseph et al., 1992; Taylor, 2006], and the Gilbert Ridge [Koppers and Staudigel, 2005], among others. The more recent 2009 KORDI NAP09-3 survey mapped a portion of the central

Ellice Basin between the territorial waters of Tokelau and Gilbert islands (Figure 2.2), a very complex part of the Pacific. Additional multibeam and trackline bathymetry were downloaded from the National Geophysical Data Center's (NGDC) multibeam and trackline archives (<http://www.ngdc.noaa.gov/ngdc.html>). A comparison of Figures 2.2 and 2.4 illustrates that much of the spreading fabric is below the resolution of current global gravity grids. For instance, large-scale features such as fracture zones are barely discernible in the vertical gravity gradient data. Thus, if extinct spreading centers do exist in Ellice Basin, high resolution mapping expeditions will be needed to determine their locations. My reconstruction will therefore be both preliminary and approximate.

Ellice Basin magnetics were also analyzed as depicted in Figure 2.5. KORDI and NGDC magnetic anomalies were recomputed using the methods of Wessel and Chandler [2007] and involved removing the latest International Geomagnetic Reference Field from reported total field anomalies. This step was necessary as many magnetic datasets were submitted to NGDC with inaccurate anomalies computed using outdated reference fields [Chandler and Wessel, 2008]. Magnetic data were then adjusted vertically to remove constant offsets between data sets, median filtered, and interpolated using a nearest neighbor algorithm. In contrast to classic seafloor spreading crust north of Ellice Basin (highlighted in Fig. 2.5 using interpreted isochrons and fracture zones by Nakinishi et al. [1992]), Ellice Basin magnetic polarity appears to reverse across fracture zones (see Figure 2.2), resembling Cretaceous quiet zone anomaly patterns reported elsewhere [e.g., Verhoef and Duin, 1986]. A statistical comparison between the magnetic anomalies of the reversing and quiet zones was also performed (see the inset of Figure 2.5). Anomalies within the perimeter of the Ellice Basin were binned at 30 nT intervals and compared to those from within the study area of Nakinishi et al. [1992]. To avoid sampling rate artifacts, all tracklines were resampled to 1 km resolution along-track. As shown in the Figure 2.5 histogram,

Ellice Basin anomaly magnitudes (white bins) form a narrower distribution centered at ~ 50 nT. The broader Nakinishi et al. [1992] anomaly distribution (black bins) is centered at ~ 50 nT with some asymmetry, indicating either trackline distribution bias, insufficient samples, or increased negative polarity prevalence in their study area. The Ellice Basin distribution, however, shows no such asymmetry indicating that the distribution of normally magnetized quiet zone crust may be adequately described.

Plateau outlines, fracture zone traces, and derived rotation poles were then imported into an interactive plate tectonic visualization software, GPlates [Müller et al., 2011], for further refinement of rotations. Here, Ontong Java was considered fixed to the Pacific reference frame with Hikurangi moving relative to Manihiki and Manihiki moving relative to Ontong Java. Although flowline predictions indicate first order agreement with Ellice Basin fracture zone trends (Figure 2.3), it was necessary to refine Hikurangi-Manihiki spreading into a two pole solution (fine dot-dashed curves). The spreading change in this case is thought to have occurred at 100 Ma when spreading switches from being parallel to East Manihiki/West Wishbone Scarp to being parallel to the northern segment of the East Wishbone Scarp. This spreading change may be related to other 100 Ma changes evident in Pacific fracture zone trends [e.g., Matthews et al., 2011, in press]. The final rotation poles derived in this study are presented in Table 2.1.

2.2.2 Absolute reconstruction of OJN origin

I use my OJN relative rotations in conjunction with three models for absolute plate motion to determine paleo-locations of the plateau and to illustrate differences in the assumptions and predictions of the three APM models. Published paleolatitudes from Ontong Java and Manihiki allow us to test the predictions of each APM. I note that the consistency of OJP paleolatitude measurements [Riisager et al., 2004] justifies their use as a quantitative means for comparing and contrasting APM models. The

three APM models and their predictions for the Hawai'i-Emperor geometry are shown in Figure 2.6(a); the corresponding flowlines restoring OJP back in time are illustrated in Figure 2.6(b).

Pacific fixed hotspot model: WK08-A

The WK08-A model for Pacific plate motion [Wessel and Kroenke, 2008] is based on a fixed hotspot reference frame and models the contemporaneous bends in the Hawaiian-Emperor, Louisville and other chains believed to have resulted from major changes in absolute plate motion. Figure 2.7 shows selected frames of the OJN breakup with reconstructed plateau outlines and Louisville trail predictions color-coded according to APM. Ellice Basin fracture zones digitized in this study, reconstructed spreading centers and terranes (exported from the Seton et al. [2011, in press] model) as well as subduction zones [Gurnis et al., 2011] are also shown. In the 0 Ma frame, the red WK08-A predicted Louisville chain matches well with the observed chain as the WK08-A is constrained by the Louisville and other hotspot chains. Progressing back in time, large changes in APM are indicated by bends in the predicted Louisville seamount chain. These predicted bends were presumably subducted within the last 50 Ma, however, and have no observable seamount counterparts for comparison.

The WK08-A OJN reconstruction implies 4.1° of clockwise OJP rotation since 123 Ma, with initial spreading at Ellice Basin and Osbourn Trough oriented primarily east-west and north-south, respectively. Reconstructed ODP site latitude and rotation histories for the WK08-A APM are shown in Figure 2.8(a) whereas reconstructed ODP site longitude histories are shown in Figure 2.9(a). Hikurangi Plateau moves south throughout the breakup with a westward component prior to 100 Ma. At ~ 100 Ma, Hikurangi switches to eastward motion (and continues south) which it continues for the remainder of the breakup. Manihiki moves eastward throughout the breakup aside from slight westward motion between ~ 106 –100 Ma. MP's latitude is

relatively stable until ~ 100 Ma when the plateau begins moving north. HP's ~ 100 Ma motion change may be related to the MP's coeval northward motion but is likely also driven by the coeval spreading direction change at Osbourn Trough. As OJP is fixed to the Pacific plate throughout the breakup, these modeled OJP ODP latitude and longitude histories reflect Pacific plate motion and are hence nearly identical. A key observational constraint in the WK08-A model is the simultaneous fit to the Emperor and Louisville chains, implying a considerable amount of north-south Pacific absolute plate motion during the time the Emperor chain was formed. Consequently, my reconstructions utilizing the WK08-A APM place the super-plateau furthest south of all the APMs tested herein. I note that Hikurangi–Chatham Rise docking was constrained using the OMS-05 APM [O'Neill et al., 2005] embedded in the GPlates global rotation model.

At 123 Ma the WK08-A OJN model reconstructs 9° south of published Ontong Java paleolatitudes and 6° north of the Louisville hotspot (see Figure 2.10(a)). ODP/DSDP sites plotted as triangles are color coded according to published paleolatitude [Riisager et al., 2004; Cockerham and Jarrard, 1976] and overlay the OJN reconstruction colored according to WK08-A predicted paleolatitude. The 9° paleolatitude discrepancy is computed at OJN's center point (yellow circle in Fig. 2.10(a)) as the difference between extrapolated and reconstructed paleolatitude. The extrapolated value was determined through regression of OJP measurements. Although the OJP paleolatitude discrepancy is clear, Manihiki's DSDP Site 317 shows no apparent latitudinal discrepancy. However, Cockerham and Jarrard [1976] indicated that tectonic tilt may have affected the paleomagnetic inclination measurements of their basalt samples. Site 317's sedimentary paleolatitude was estimated at $\sim 20^\circ$ further north. If the Louisville plume did form OJN, this reconstruction implies that Louisville was $\sim 6^\circ$ – 7° further north at the time of OJN emplacement. Such drift estimates are subject to unknown uncertainty (i.e., Louisville's drift history prior to 78

Ma is unknown as is OJN’s actual eruption center) and are only presented as a first order indicator to gauge OJN’s proximity to a fixed Louisville plume. Furthermore, 9° of true polar wander is required to account for discrepancies between reconstructed and measured OJP paleolatitude. For comparison, Besse and Courtillot [2002] suggest $\sim 10^\circ$ of Pacific true polar wander since 123 Ma, while a more recent study by Steinberger and Torsvik [2008] implies negligible true polar wander for this vicinity.

Pacific drift-corrected model: WK08-D

The second Pacific APM, herein called the WK08-D APM, was developed for this research and is based on WK08-A but incorporates an Emperor-stage moving Hawaiian plume [Tarduno, 2007; Tarduno et al., 2009]. Specifically, I determined a stage rotation that (as WK08-A) reproduced the Louisville chain from its 50-Ma bend to the end of the trail at the Tonga-Kermadec trench. However, a second constraint was added that the stage rotation should predict a trail geometry with no discernible Hawai‘i-Emperor bend. Such a stage rotation pole was found to lie along the bisector great circle of the Louisville trail, at approximately (36°N , 53°W). I extended this rotation back to 83.5 Ma and used it to replace WK08-A rotations for the 83.5–47 Ma period. Older rotations were adjusted for the change in reference.

The WK08-D APM induces the most OJN rotation (dark green pen in Figure 2.7). Hikurangi therefore begins from a more westerly starting point at 123 Ma and continues its pronounced westward path until ~ 100 Ma (Figure 2.9(b)). HP’s southward motion continues throughout the breakup (Figure 2.8(b)). Manihiki’s latitude is again relatively stable prior to northward motion commencing at ~ 95 Ma with a similar eastward longitude history aside from slight westward motion around ~ 105 – 100 Ma. Again the HP course change coincides with the onset of northeasterly MP motion and the jump from southwesterly West Wishbone-parallel spreading to nearly north-south East Wishbone-parallel spreading at Osbourn Trough. In the WK08-D

scenario, Hikurangi docks west of Chatham Rise at 86 Ma. This discrepancy may be due to my juxtaposition of WK08-D OJN rotations with background terranes rotated by the GPlates OMS-05 global model.

This model implies 13° of counter-clockwise rotation since 123 Ma and results in a revised geometry where Ontong Java plateau is positioned $\sim 7^\circ$ further north than for the WK08-A reconstruction, while Manihiki ODP Site 317 reconstructs at approximately the same latitude as before (Figure 2.10(b)). Although OJP paleolatitude discrepancies are improved considerably, OJN now reconstructs $\sim 12^\circ$ north of Louisville hotspot's present estimated position. The WK08-D OJN model therefore requires twice the magnitude of Louisville drift. This model also plots just 4° south of the range required by OJP paleolatitudes. This paleolatitude discrepancy implies a small amount of true polar wander but this discrepancy is possibly insignificant (i.e., the mean OJP paleolatitude standard deviation is 3.6°).

Indo-Atlantic moving hotspot model: OMS-05

The third APM used herein derives from O'Neill et al [2005] and represents a moving-hotspot model that best describes the absolute motion of Africa. I projected this model via the East Antarctica-West Antarctica plate circuit. As this circuit only allows reconstruction back to 83.5 Ma, I extended the model back to 144 Ma using the WK08-A model adjusted for the change in reference. The three APM models share the same rotation history before 83.5 Ma and thus are not independent.

This APM implies 2.8° of counter-clockwise rotation intermediate of WK08-A and WK08-D and therefore imparts similarly intermediate westward and southerly components to the initial Hikurangi and Manihiki paths, respectively (blue pen in Figure 2.7). Hikurangi moves west until ~ 100 Ma (Figure 2.9(c)) when MP motion switches to from \sim east–west to \sim northeasterly motion and Osborn Trough's spreading direction switches from \sim southwest–northeast to \sim north–south. Manihiki's

latitude fluctuates around 45° S until ~ 105 Ma (Figure 2.8(c)) then begins rotating northward about the OJP–MP rotation pole prior to Pacific accretion. The predicted Louisville seamount chain shows poor agreement with the observed chain in the 0 Ma frame where a fixed Louisville hotspot is used, implying significant drift of the Louisville hotspot since ~ 80 Ma.

As shown in the 123 Ma reconstruction (Figure 2.10(c)), this model positions OJN 2° further south than OJP paleolatitudes would indicate, which is insignificant relative to OJP paleolatitude error magnitudes. However, the center of the plateau plots 13° north and 12° east of Louisville’s current estimated position. This model therefore implies 18° of hotspot drift since 123 Ma.

2.3 Discussion

Uncertainties in both Pacific APM reconstructions and in paleolatitude measurements moderate the significance of my quantitative model comparisons. While the 123 Ma WK08-A OJN reconstruction clearly minimizes modeled hotspot drift, Ontong Java paleolatitudes necessitate a more northerly reconstruction and hence require true polar wander. Both WK08-D and OMS-05 APMs reconcile paleolatitude discrepancies but require greater magnitudes of Louisville plume drift. Although paleolatitudes along the Louisville chain are preliminary at this time [Gee et al., 2011], the amount of Louisville drift implied by the OMS-05 model is unreasonable. I solved for this drift by backtracking the empirical age-progression for Louisville [Wessel and Kroenke, 2009] to 0 Ma using OMS-05. Figure 2.11 compares this OMS-05 predicted drift history (color worm with solid black center line) to Louisville drift predictions by Steinberger et al. [2004] (shorter color worm with white center line). WK08-A and WK08-D drift predictions are not shown due to their minor deviations about Louisville’s current location.

While data are limited, I find that Louisville seamount predictions and paleolatitude evidence best support the WK08-D APM. However, $\sim 12^\circ$ of hotspot motion is needed to locate Louisville under the center of the reconstructed OJN at 123 Ma. This result indirectly supports Hawaiian plume drift during the Emperor-stage as incorporated into the WK08-D APM and independently corroborated by the Indo-Atlantic OMS-05 model. However, misfits between Louisville hotspot and my OJN reconstructions could also be due to large uncertainties in older (i.e., pre-Emperor) parts of APM models that presently are hard to quantify.

The WK08-D and OMS-05 models support the notion of a drifting Hawaiian plume during the Emperor stage [Tarduno, 2007; Tarduno et al., 2009] by reducing OJP paleolatitude discrepancies. These more northerly OJN reconstructions would then, assuming Louisville as the OJN source, suggest a more northerly Louisville plume at 123 Ma. Such drift is possible given that there are no other constraints on Louisville motion prior to 78 Ma. However, up to 10° of true polar wander has been proposed previously to account for OJP paleolatitude discrepancies [Antretter et al., 2004], making a combination of plume drift and true polar wander a possibility. In either case, reconciling OJP paleolatitudes using true polar wander or hotspot drift would potentially introduce a discrepancy with Manihiki's paleolatitude. New constraints on the latitudinal history of the Louisville hotspot provided by the recently completed ODP Leg 330 indicates that the OMS-05 APM projected to the Pacific, which produces very different predictions for the Louisville trail (e.g., Fig. 2.7(c)–0 Ma), appears to be unrealistic although this may be related to plate circuit bias.

Both plume drift and true polar wander have been proposed as mechanisms that may explain paleolatitude anomalies relative to a fixed hotspot APM reconstruction. Pacific APMs traditionally tend to honor the Emperor chain whose geometry may be compromised by plume motion [Tarduno, 2007]. Since there is no clear evidence for significant true polar wander during the Emperor stage I decided to test APMs that

either ignored the Emperors (WK08-D) or were projected from another plate (OMS-05). Between the time of OJN formation and ~ 100 Ma there might have been true polar wander of up to 10° in the Pacific [Besse and Courtillot, 2002; Prevot et al., 2000]. However, the Steinberger and Torsvik [2008] model suggests negligible true polar wander for OJP during this time period. Hence, it is uncertain whether OJN paleolatitude anomalies may be used to infer true polar wander.

The contradictory true polar wander estimates cited above as well as unaccounted for Emperor stage Hawaiian plume drift detract from the plausibility of the WK08-A APM. Furthermore, the OMS-05 APM (perhaps due to plate circuit bias) requires considerable LV drift that is drastically different from preliminary paleolatitude estimates obtained by IODP Leg 330 and from mantle flow modeling by Steinberger et al. [2004] in order to fit the 0–78 Ma LV chain geometry and age progression. My analysis also finds that the easterly OMS-05 OJN reconstruction implies the most LV drift since 123 Ma ($\sim 18^\circ$). I therefore favor the WK08-D APM, which accurately reproduced the Louisville seamount chain, reconciled OJP paleolatitude discrepancies, requires a moderate 12° of Louisville hotspot drift between 123 and 78 Ma, and is based on current Pacific hotspot drift evidence.

As presented, this interpretation of the OJN breakup does not readily explain the coincidence of secondary volcanism at the three plateaus [Taylor, 2006; Hoernle et al., 2010; Timm et al., 2011]. My models show wide plateau separation during the ~ 90 Ma secondary phase and, if correct, do not favor the Bercovici and Mahoney [1994] explanation of secondary volcanism at OJP by way of plume head separation. Consequently, this volcanism would appear unrelated to the original plume source and could instead reflect decompressional melting following zones of weaknesses in the separated plateaus, possibly reactivated by stresses induced by changes in plate motion (i.e, Sykes [1978]; Sager and Keating [1984]). These results are also compatible with the interpretation by Joseph et al. [1992]; Taylor [2006] that the Nova-Canton

Trough is likely the westward extension of the Clipperton Fracture Zone. In addition, the near intersection of the Pacific–Ellice Basin suture boundary and Nova-Canton Trough north of Manihiki (Figure 2.4) suggests that left lateral motion along the suture boundary may have preferentially aligned along the Nova-Canton Trough.

By reuniting Ontong Java, Manihiki, and Hikurangi plateaus, I find that the plateau center reconstructs $\sim 15^\circ$ north of Louisville hotspot’s current estimated position at ~ 123 Ma. This is in contrast to the 26° latitudinal gap between Louisville ($\sim 51^\circ$ S) and OJP’s center ($\sim 25^\circ$ S) determined by Antretter et al. [2004]. Antretter et al. [2004] further speculated that a combination of 11° of true polar wander, 6° – 9° of hotspot drift and 7.5° due to octupole effects might explain the 26° offset and thus link OJP to a Louisville source. By relocating the center of volcanism from $\sim 25^\circ$ S to the middle of my preferred super-plateau reconstruction at $\sim 39^\circ$ S, I model 12° of Louisville drift (within published drift estimates for Hawai’i [Tarduno et al., 2003]) without requiring significant true polar wander or octupole effects, thereby increasing the likelihood that Louisville formed Ontong Java Nui.

Although this study assumes a Louisville Hotspot source for the OJN super-plateau, the debate is not yet settled. Alternative formational mechanisms include short duration plume volcanism as well as the eclogite entrainment mechanism proposed by Korenaga [2005]. Under a short duration plume scenario, all volcanic seamounts formed during the relatively brief plume tail phase (prior to ~ 80 Ma) would presumably have been subducted beneath the Australian Plate with no remaining trace. OJN’s 123 Ma reconstruction straddles the Pacific–Farallon ridge (Figure 2.7) thus could indicate a ridge capture cause for Louisville drift. However, this proximity to the paleo-ridge could also support the mantle entrainment hypothesis.

My OJN reconstruction has estimated area of $\sim 5 \times 10^6$ km² ($\sim 2/3$ the size of Australia) and volume of $\sim 1 \times 10^8$ km³. In agreement with Taylor [2006], the OJN

super-plateau potentially covered $\sim 1\%$ of Earth's surface at ~ 123 Ma, representing the largest known magmatic event. These may be minimum estimates, however, as an unknown proportion of Manihiki plateau has been rifted away and presumably subducted [Viso et al., 2005]. A larger OJN extending further south or east would displace my eruption center southward, potentially resulting in even better paleolatitude agreement. Such large-scale volcanism and resultant plate boundary reorganization occurring throughout the OJN breakup may have contributed to a geomagnetically stable regime wherein reversals of the geomagnetic field did not occur [e.g., Larson and Olson, 1991]. Current OJN breakup timing constraints favor the onset of OJN formation beginning at ~ 125 Ma with ongoing hotspot volcanism as well as seafloor spreading at Ellice Basin and Osbourn Trough occurring until ~ 86 Ma, spanning the entire Cretaceous normal superchron.

Although I was unable to determine actual basin opening rates due to the lack of magnetic reversal pattern, I estimate minimum full spreading rates of ~ 70 km/Myr (approximated as 22° longitude / 34 Myr) and ~ 90 km/Myr (28° latitude / 34 Myr) for Ellice Basin and Osbourn Trough spreading, respectively.

2.4 Conclusion

I have examined the Taylor [2006] Ontong Java–Manihiki–Hikurangi super plateau hypothesis and three models for Pacific absolute plate motion using paleolatitude and fracture zone data as constraints. I find that the WK08-D OJN reconstruction, which allows for drift of the Hawaiian plume during the Emperor stage, best satisfies OJN paleolatitudes, Louisville seamount trail geometry, and Ellice Basin/Osbourn Trough fracture zone traces. The WK08-A and OMS-05 APMs are based on assumptions that may compromise their accuracy (i.e., fixed hotspots versus projection via an Antarctic plate circuit); however I am unable to definitively rule them out due to

potentially large uncertainties in all APMs for ages greater than 83.5 Ma. Plume drift and true polar wander are not mutually exclusive processes, implying that a model allowing for both phenomena be considered. In either case, my reconstruction has made the connection between the OJN super plateau and the Louisville hotspot much more probable, and despite the shortcomings of my APM modeling I suggest the case of a Louisville plume origin for the OJN has been considerably strengthened.

Table 2.1: Rotation poles for Ontong Java Nui reconstructions. θ , λ , t_1 , t_2 , and ω are pole latitude, longitude, time interval (Ma), and rotation angle, respectively.

	θ	λ	t_1	t_2	ω
OJP–MP	32.54	182.35	120	86	-33.46°
MP–HP	1.20°	94.20°	100	86	8.86°
	3.87°	132.46°	120	100	31.24°

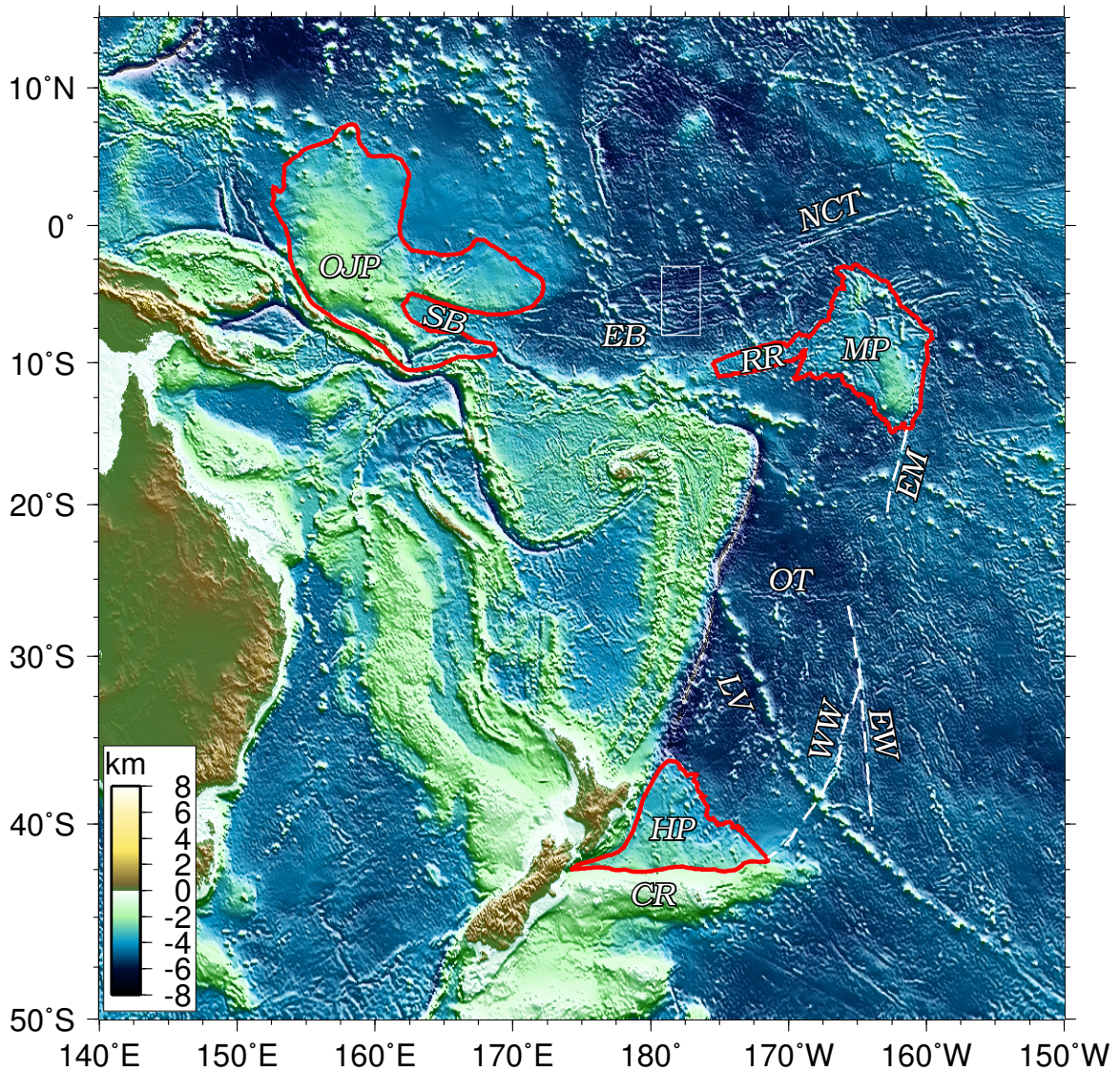


Figure 2.1: Regional bathymetry [Becker et al., 2009] map showing Ontong Java (OJP), Manihiki (MP), and Hikurangi (HP) plateaus outlined in red. Ellice Basin (EB) separates OJP and MP and exhibits a complex fabric of large offset fracture zones terminating at the Nova-Canton Trough (NCT) north of MP. The Osbourn Trough (OT) relict spreading center lies ~midway between MP and HP/Chatham Rise (CR), trending east-west. White dashed lines show the locations of the East Manihiki (EM), West Wishbone (WW), and East Wishbone (EW) scarps. Louisville Ridge (LV), Robbie Ridge (RR) and Stewart Basin (SB) are also shown. The white box indicates the location of high resolution data shown in Figure 2.2.

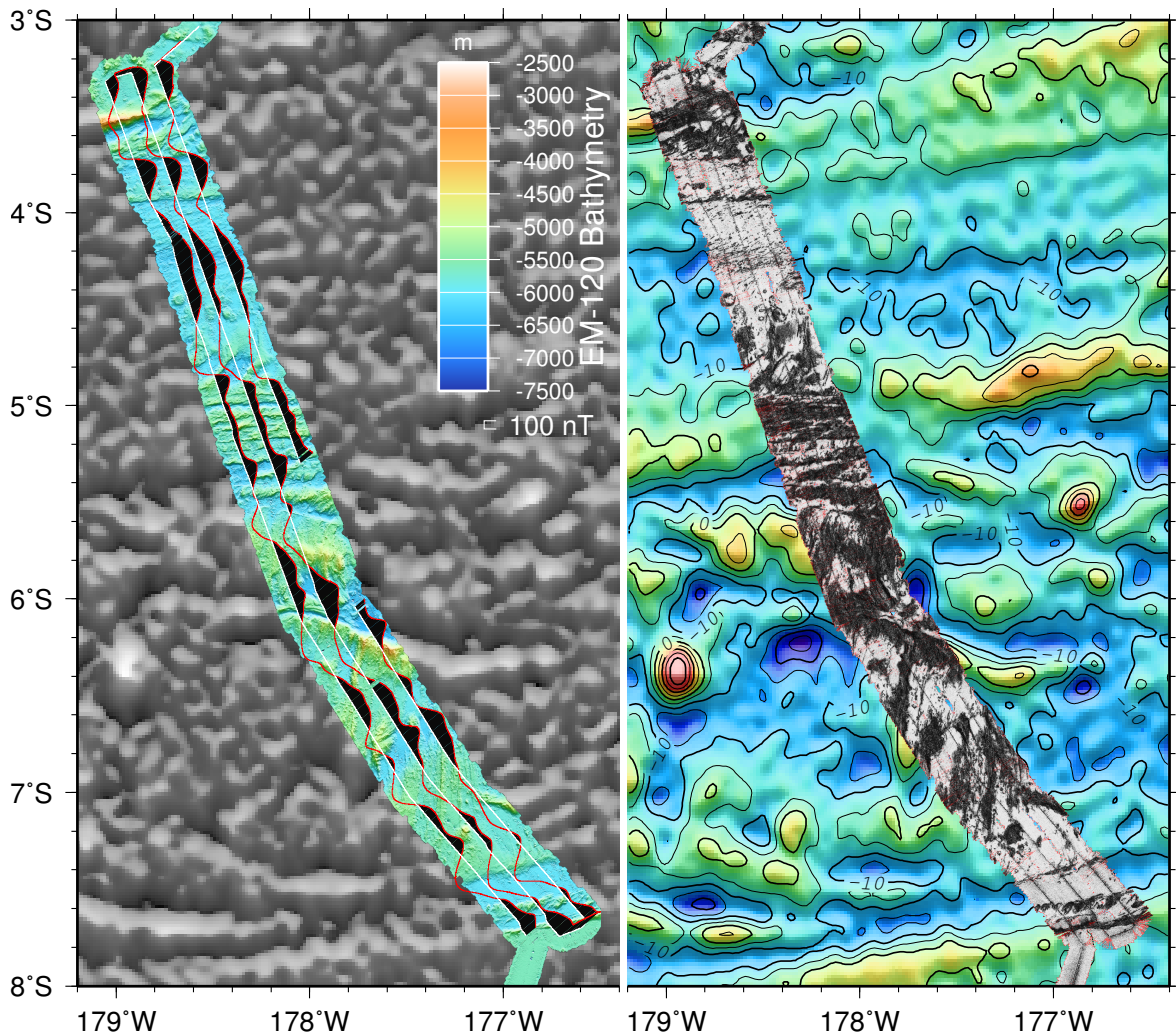


Figure 2.2: ~East-west fracture zone trends are apparent in new EM-120 bathymetry (left panel) and backscatter data (right panel). Shades of gray (right panel) indicate differing levels of backscatter intensity with lighter and darker shades corresponding to lower and higher intensity, respectively. Sandwell and Smith [2009] vertical gravity gradient data (left panel background) and free-air gravity data (right panel background) show similar trends. Southeasterly fabric possibly associated with a late stage EB spreading reorientation is also apparent. The shipboard data also exhibit ~north-south aligned fabric in the southern portion of the NAP09-3 Ellice Basin survey area, within the southeasterly trending realm. Although more mapping is clearly required, the large scale features visible in existing EB data appear to support the EB spreading hypothesis of Taylor [2006]. Magnetic wiggles overlay the bathymetry (positive anomalies shaded black) and show a ~north-south reversing pattern perpendicular to the apparent spreading direction which is presumably related to EB fracture zone topography rather than reversals of the geomagnetic field.

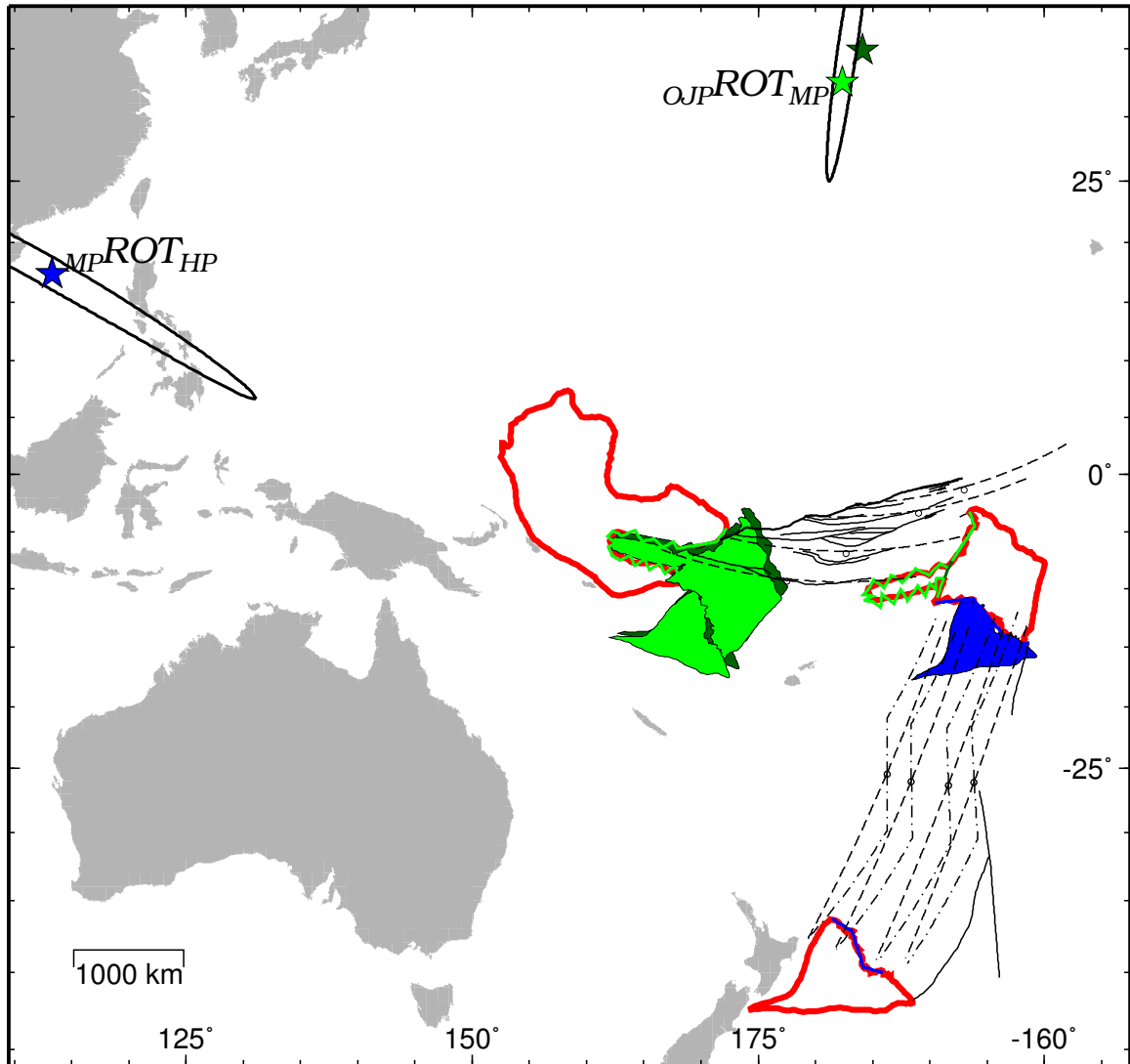


Figure 2.3: Illustration of OJN relative rotations. Conjugate plateau boundaries (jagged green and blue curves) are used to determine spherical rotations using the methods of Hellinger [1981] and Chang [1987]. By convention, I first rotate HP to MP (blue plateau) about the MP–HP pole (blue star), then rotate MP/HP to OJP (green plateau) about the OJP–MP pole (green stars). Although not shown here, rotations at intermediate times induce identical proportions of closure for the two basins. Light/dark green plateaus and poles show the effect of including/omitting the Stewart Basin–Robbie Ridge (SB and RR from Fig. 2.1) constraint in the modeling. Also shown are fracture zone traces (thin black curves), the Pacific–EB boundary (heavy black curve) and flowlines predicted by my single (dashed curves) and, in the vicinity of OT, two-stage (dot-dashed curves) rotations. Open circles indicate actual (OT) and potential (EB) extinct ridge locations used to generate flowlines.

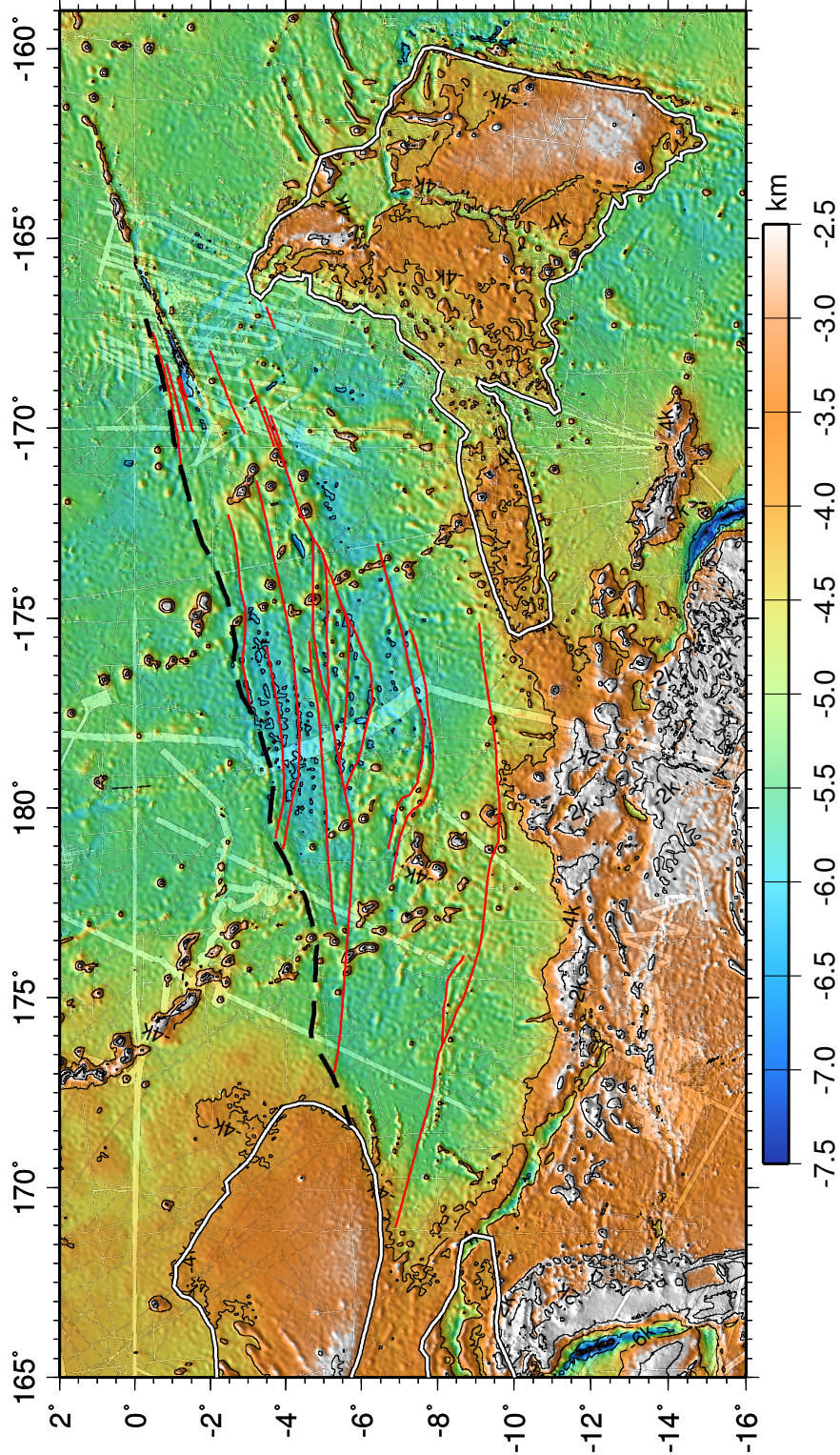


Figure 2.4: Ellice Basin bathymetry compilation including KORDI NAP09-3 and Taylor [2006] data as well as available multibeam and trackline data from NGDC overlaying Becker et al. [2009] predicted bathymetry. Features digitized in this study include EB fracture zones (red curves), plateau outlines (white) and the Pacific-EB suture boundary (dashed curve). Thin solid lines show 2 and 4 km isobaths.

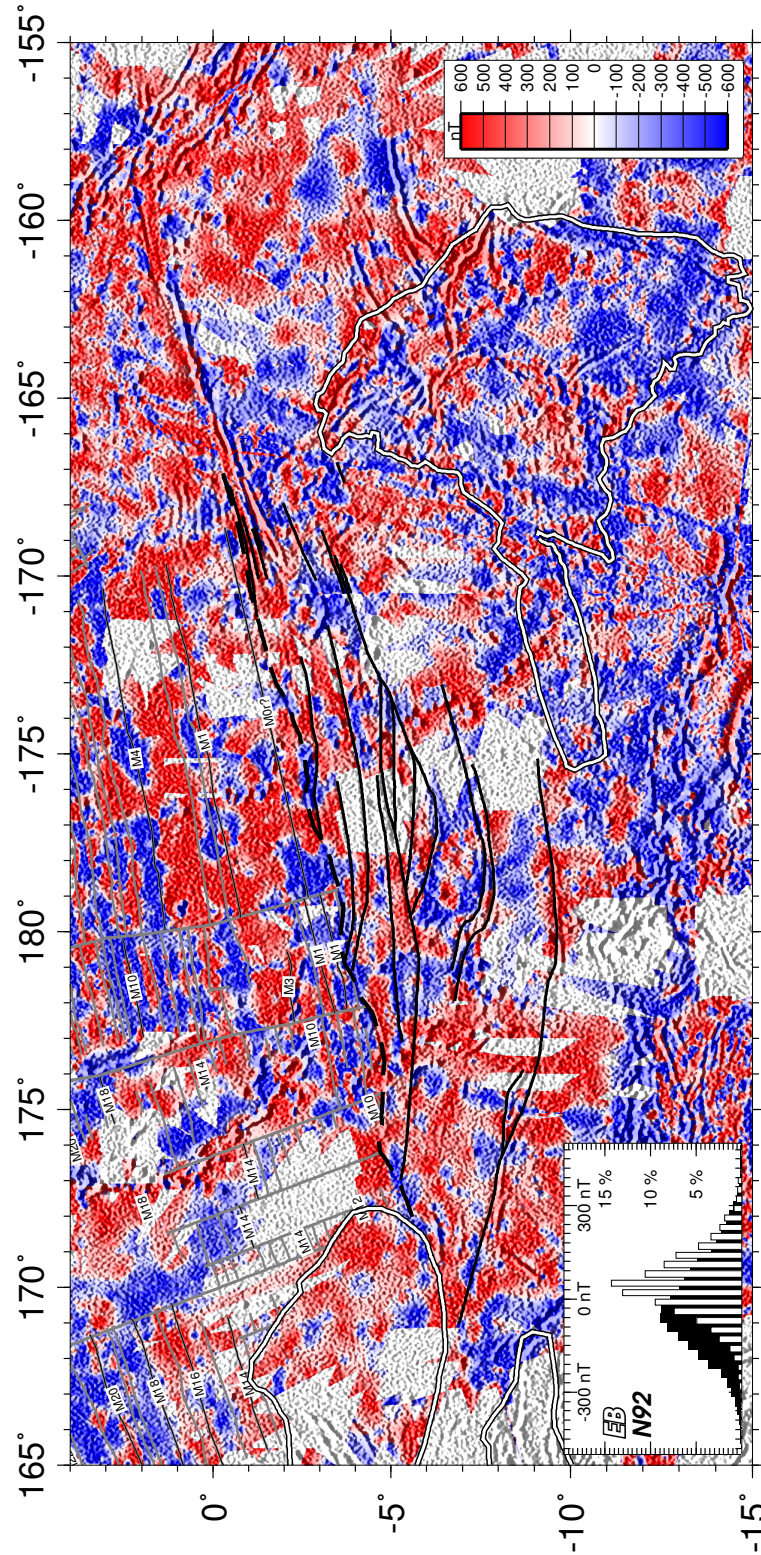


Figure 2.5: Compilation of KORDI and NGDC magnetic anomalies for the Ellice Basin vicinity. EB fracture zone trends (black) contrast sharply to those of Nakinishi et al. [1992] (gray) north of the dashed rift boundary. A comparison of anomaly distributions from within the EB and Nakinishi et al. [1992] (NK92) study areas (lower-left histogram) indicates a positive shift and narrowed distribution for EB anomalies.

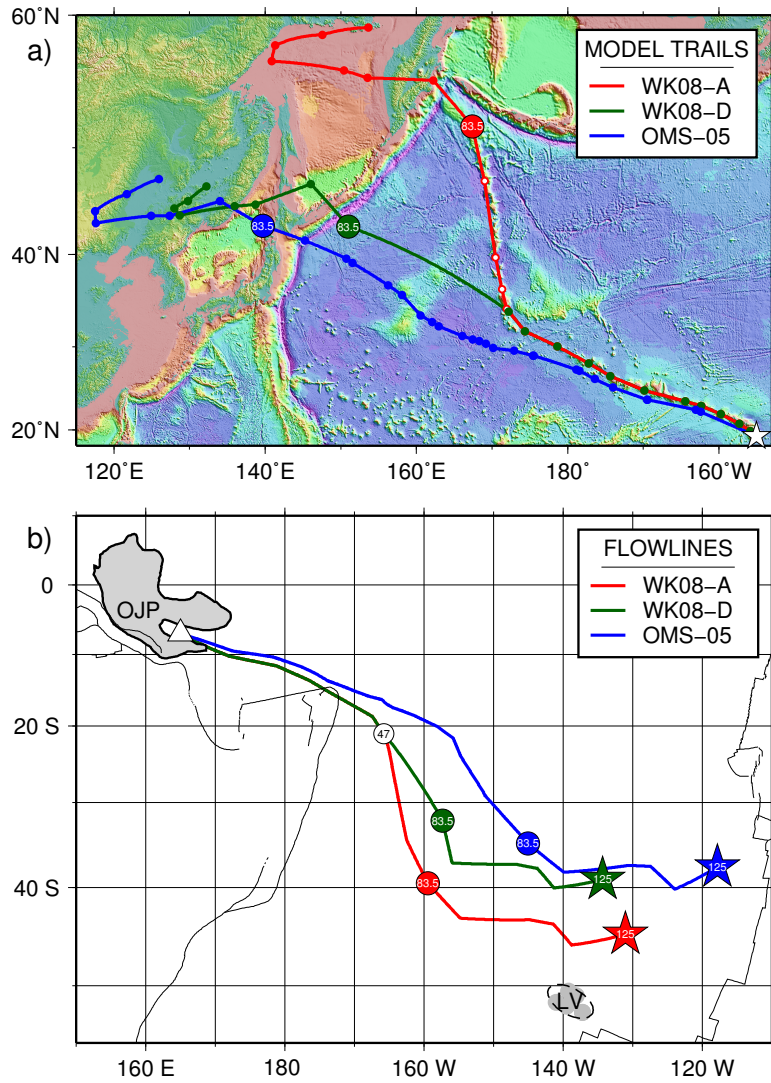


Figure 2.6: APM models tested herein differ considerably. WK08-A (red) assumes fixity of Pacific hotspots, hence its faithful reproduction of the HEB (a) and consequent southerly reconstruction of OJP nearest the present-day Louisville hotspot (LV) (b). WK08-A and WK08-D (green) are identical until 47 Ma when modeled drift of the Hawaiian plume begins to affect WK08-D, resulting in a Hawaiian chain-parallel Emperor prediction (a) and a less southerly OJP reconstruction (b). The Indo-Atlantic plate motion based OMS-05 (blue) also gives a Hawaiian-parallel Emperor-stage prediction (a) but reconstructs OJP further east (b). Dots in modeled seamount trails (a) correspond to changes in Pacific motion.

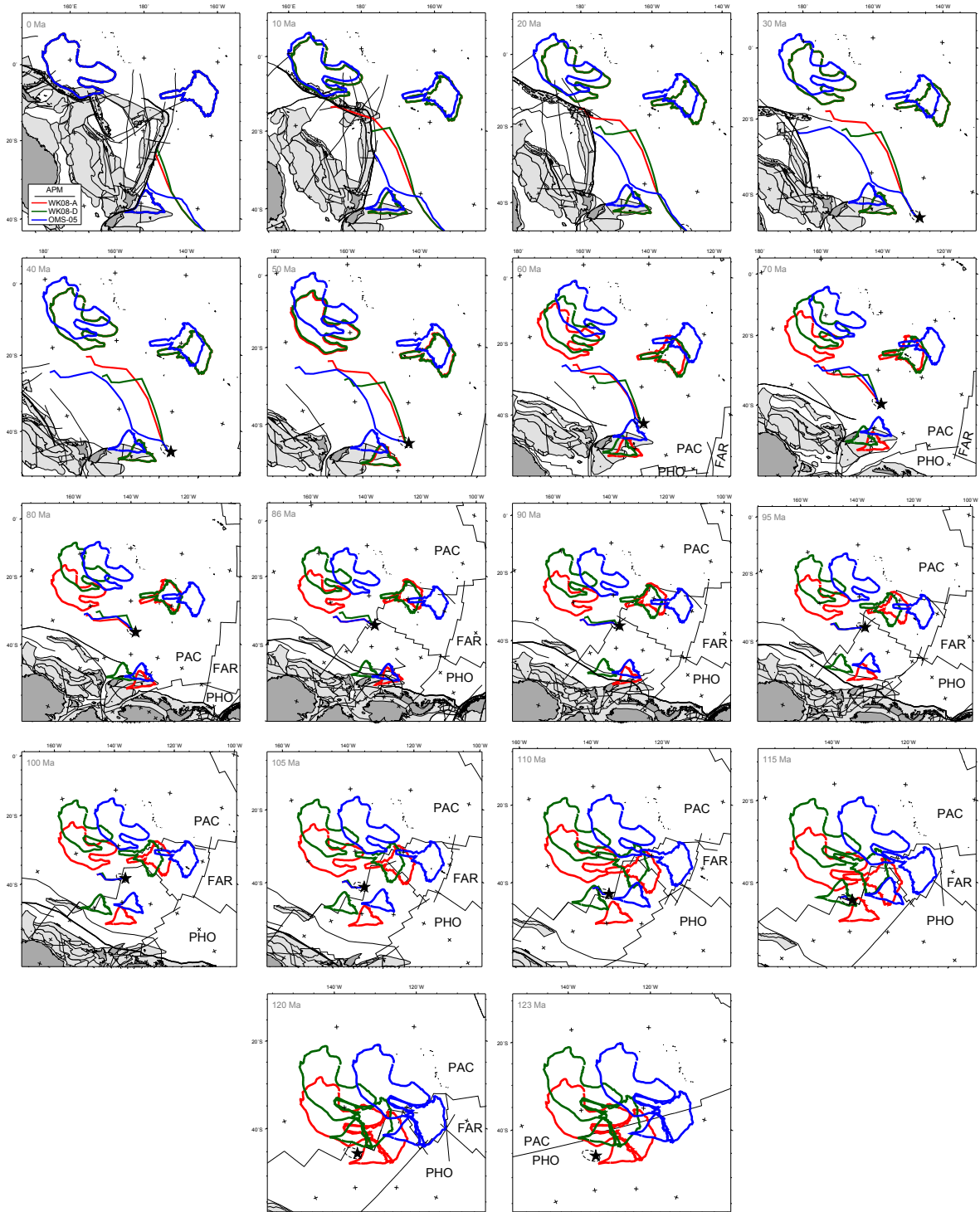
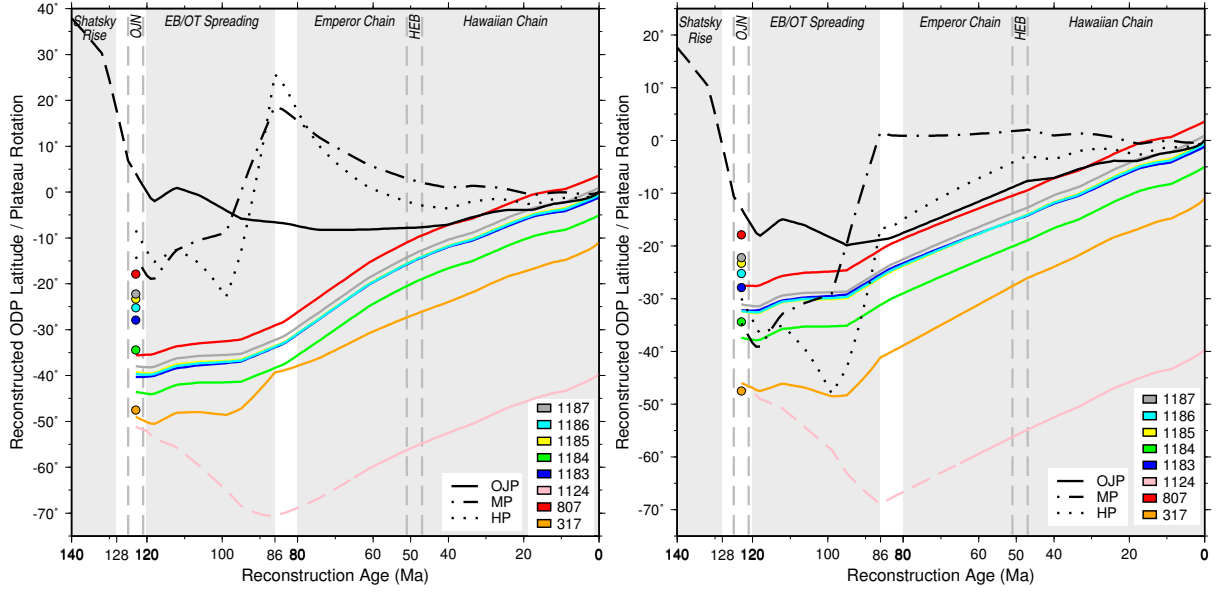
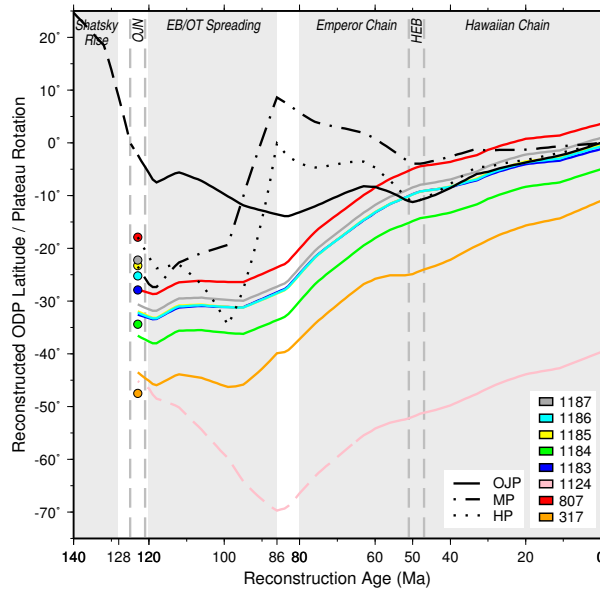


Figure 2.7: Absolute reconstructions of the OJN breakup from 123 Ma to the present. Red (WK08-A), green (WK08-D) and blue (OMS-05) plateau outlines and predicted Louisville seamount locations illustrate the effects of different APMs on the OJN breakup. Black star indicates Louisville hotspot's current estimated position. Also shown are subduction zones [Gurnis et al., 2011] along with plate boundaries (thin black pen), terranes (light gray) and coastlines (dark gray) [Seton et al., 2011, in press].



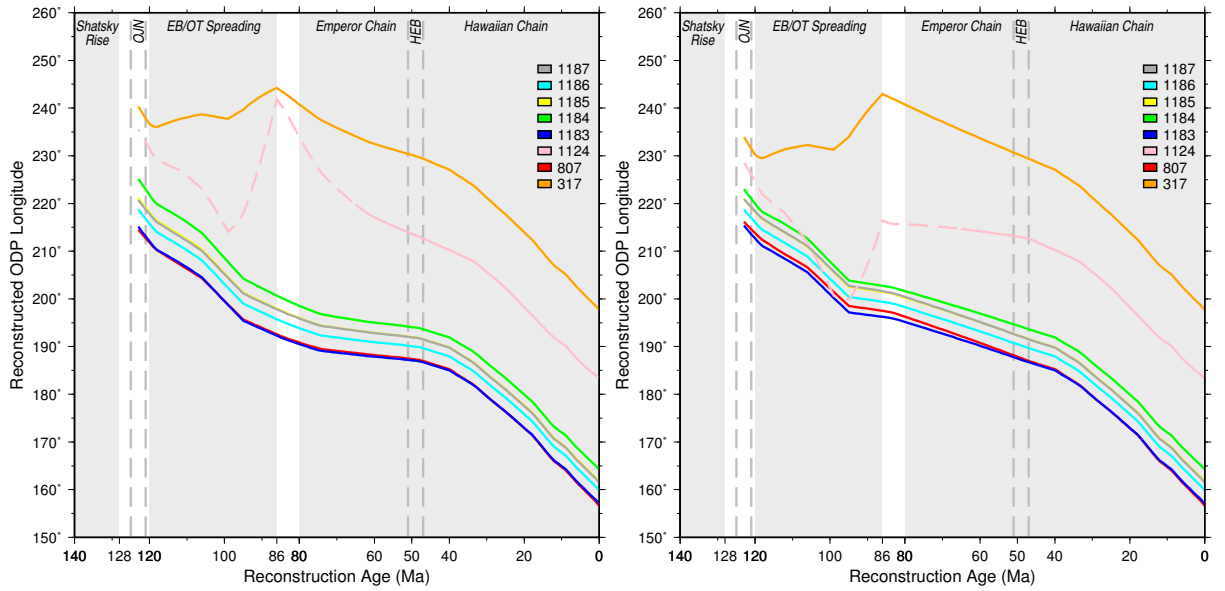
(a) WK08-A

(b) WK08-D



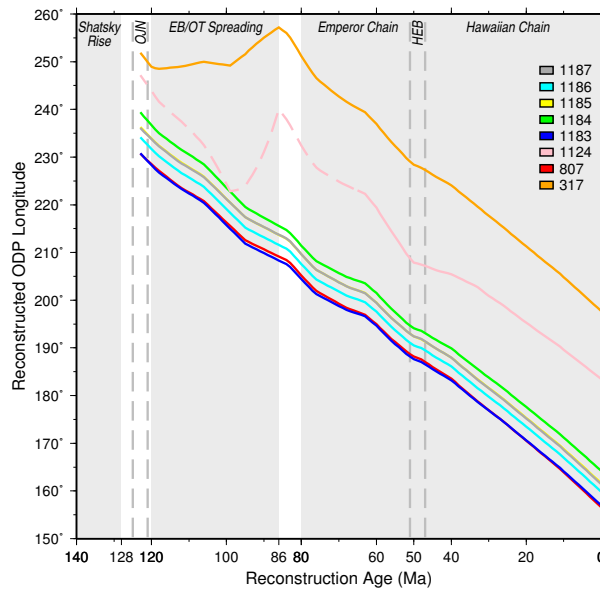
(c) OMS-05

Figure 2.8: Absolute reconstruction of ODP site latitudes (color curves) and plateau rotation angles (black curves) from 140 Ma to the present (OJN relative rotations included). Color-filled circles pertain to ODP/DSDP paleolatitudes and ages as published. MP Site 317’s basement paleolatitude is shown although Cockerham and Jarard [1976] also reported a similarly aged carbonate paleolatitude 20° further north. HP’s latitudinal history (Site 1124) is also reconstructed although no HP basement paleolatitudes have been reported to date.



(a) WK08-A

(b) WK08-D



(c) OMS-05

Figure 2.9: Absolute reconstruction of ODP site longitudes (color curves) from 140 Ma to the present (OJN relative rotations included). Sites 317 and 1124 pertain to MP and HP, respectively, while the remaining ODP sites pertain to OJP.

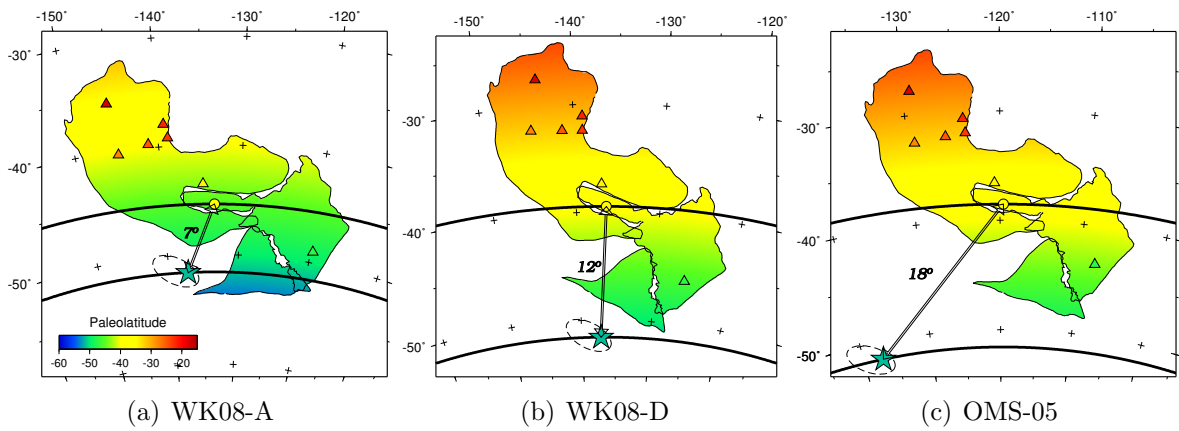


Figure 2.10: Comparison of three 123 Ma OJN reconstructions. Plateaus are color-coded according to reconstructed latitude while reconstructed ODP/DSDP sites (triangles) are colored according to their published paleolatitude. Distance estimates from Louisville (teal star) to the reconstructed OJN midpoint (open circle) are also shown. Differences in reconstructed plateau orientation, longitude/latitude range, and paleolatitude discrepancies are apparent. Bold lines highlight latitudinal positions of Louisville and OJN estimated mid point.

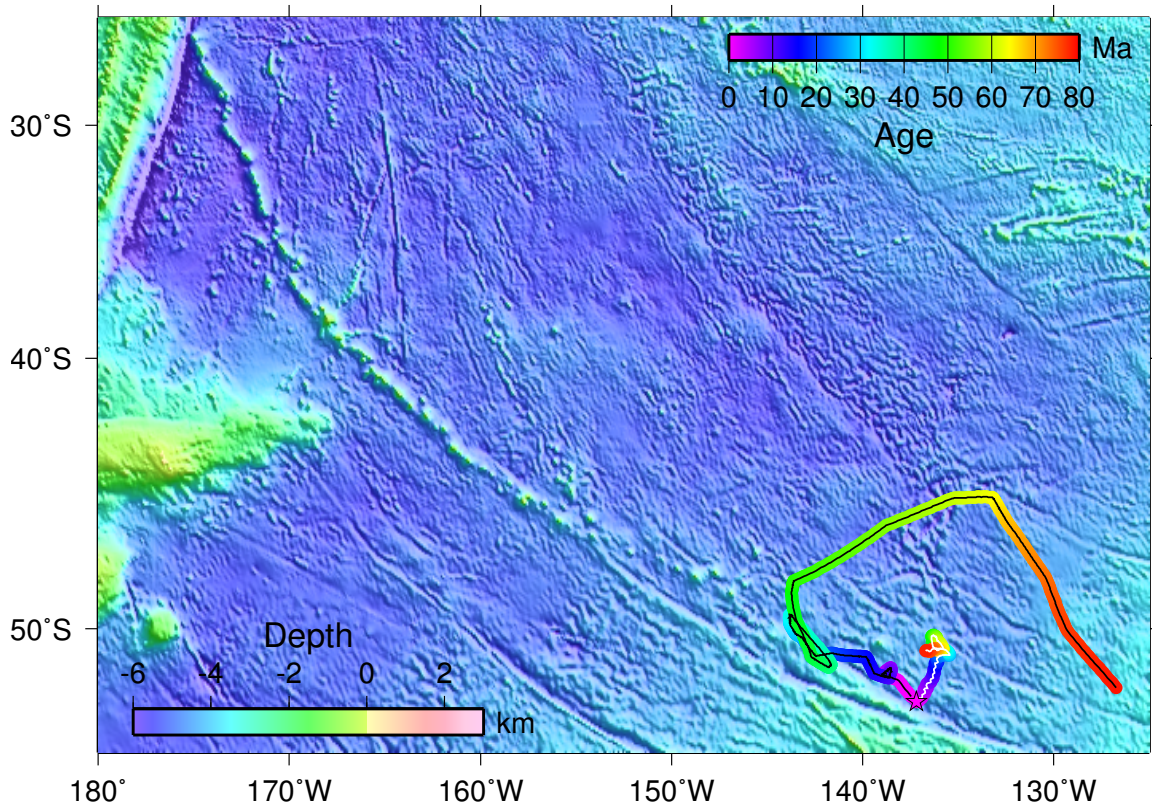


Figure 2.11: Louisville seamount age progression data backtracked using the OMS-05 APM predicts apparently excessive Louisville hotspot drift (black centered age-color curve) since 78 Ma as compared to the flow-model prediction by Steinberger et al. [2004] (white centered age-color curve). Louisville hotspot (star) is fixed at its current estimated position in both WK08-A and WK08-D APMs, hence only the OMS-05 drift curve is shown.

Chapter 3

Analysis of Ontong Java Plateau Paleolatitudes and Evidence for Rotation since 123 Ma

Abstract

I have discovered an apparent rotational property inherent in Ontong Java Plateau's basement paleolatitudes. The pattern is evident when comparing differences in Ocean Drilling Program paleolatitudes to differences in their corresponding drill site latitudes. When paleolatitude differences computed among Sites 807 and 1183-1187 are plotted against their respective site latitude differences, a systematic 2:1 slope bias is evident. Of the possible causes of this bias only whole plateau rotation resolves the bias while honoring published paleolatitudes. While it is possible to resolve the bias by introducing *ad hoc* tilt corrections at all six sites, drilling records indicate relatively undisturbed conditions at Sites 1183 and 1185-1187. If my interpretation is correct, it would imply that only Site 807 and 1184 paleolatitudes are erroneous. The 9 degree northward dip observed at Site 1184 appears to stem from inclined deposition rather than post-emplacement deformation. I also estimate an 8 degree southward tilt correction at Site 807 in order to make the data set self-consistent. Reports of unresolved tectonic tilt at Site 807 permit such an estimate. Based on the six sites analyzed, I find that OJP has experienced 25-50 degrees of clockwise rotation since its formation at 123 Ma. In contrast, available Pacific absolute plate motion (APM) models predict less than 10 degrees of rotation. If my analysis is correct it suggests that OJP moved independently of the Pacific early in its history or that Pacific APM models for the Lower Cretaceous are unreliable. While my corrections to Site 807

and 1184 combined with 25-50 degree rotation resolve the internal inconsistencies, the mean paleolatitude value of Ontong Java remains largely unchanged.

3.1 Introduction

The determination that iron-bearing rocks are often magnetized in the direction of the Earth's paleomagnetic field has been paramount among geologic discoveries. Early apparent polar wander paths (APWP) showed some of the earliest physical evidence that plates are mobile [e.g., Runcorn, 1956; Irving, 1956]. Along with the detection of reversing magnetic polarity by land-based geophysicists [Brunhes, 1906; Matuyama, 1929] as well as the "zebra stripe" magnetic anomaly pattern discovered during remote sensing magnetic surveys at sea [Raff and Mason, 1961], these discoveries greatly enhanced our ability to constrain the past movements of tectonic plates.

Paleolatitudes obtained from seamount magnetism [e.g., Sager et al., 2005], anomaly skewness [e.g., Petronotis et al., 1994], and Deep Sea Drilling Project (DSDP) and Ocean Drilling Program (ODP) sediment and basalt samples are widely used in constraining plate motion models, tectonic studies, and in ongoing attempts to define APWP, in particular for the Pacific plate. Models for absolute plate motion (APM) have also been used to predict APWP [e.g., Sager, 2007] and the comparison between observed and predicted APWP is used to assess the validity of the fixed hotspot hypothesis. Of particular importance to the construction of Pacific APWP is the ~ 123 Ma Ontong Java Plateau (OJP) (Figure 3.1). OJP has been recognized as having outlying paleolatitude measurements since a paleolatitude of $\sim 18^\circ\text{S}$ was published for ODP Site 807 [Mayer and Tarduno, 1993]. More recently, ODP Leg 192 drilled basement rocks at Sites 1183 through 1187, all yielding paleolatitudes significantly less than those predicted by APM models and coeval paleopoles from other Pacific sites [Riisager et al., 2003, 2004].

Figure 3.2 shows an adaptation of the Sager [2006] APWP illustrating the $\sim 13^\circ$ discrepancy in OJP’s paleomagnetic pole ($\sim 15^\circ$ according to Sager [2006]). This discrepancy has led previous studies to conclude that OJP could not be connected to any known mantle plume source (i.e., Neal et al. [1997]; Kroenke et al. [2004]) and for others to require true polar wander and octupole effects to link OJP with its only viable source, Louisville Hotspot [Antretter et al., 2004]. This discrepancy was also cited as evidence for Late Cretaceous to Eocene movement of Pacific hotspots, which call into question the validity of the Pacific APM for this time period [Tarduno, 2007].

Furthermore, claims of high internal consistency among OJP ODP-derived paleolatitudes, listed in Table 3.1, have been cited as evidence that other paleomagnetic data of similar ages, such as Mid-Pacific Mountains and MIT Guyot [Sager, 2006], are erroneous [Riisager et al., 2003]. In light of the implications for Pacific plate motion, resolving these contradictions is important. I will show that published OJP ODP-derived paleolatitudes (Table 3.1) exhibit strong internal bias suggesting unaccounted for tectonic tilt at Sites 1184 and 807 and a likely rotation of Ontong Java Plateau.

3.2 Analysis

This analysis begins with a rudimentary observation that differences between paleolatitude measurements (Δ paleolatitude) from Ontong Java’s ODP basement rock samples are in general twice as large as differences between OJP site latitudes (Δ latitude); data obtained from Riisager et al. [2004]. Differences presented in Table 3.3 indicate the pervasiveness of the pattern. As these Δ latitude and Δ paleolatitude differences are so instrumental in revealing the latitude versus paleolatitude bias, I further use them as coordinates in Figure 3.3. Differences for each site pair are computed twice with alternating operand order, hence the symmetry apparent in Table 3.3 and in quadrants one and three of Figure 3.3. Two-tone circles shown in Figure 3.3 indicate the two

ODP sites involved for each data point, with a convention that differences between site latitudes (and paleolatitudes) are determined by subtracting outer site from inner site values. Error bars are computed as $\sqrt{E_{inner}^2 + E_{outer}^2}$, where E are error estimates from Table 3.1. Regression analysis indicates a 2:1 slope (red dashed curve) statistically different from 1:1, with 95% slope intervals indicated by dashed gray lines. Unless significant plateau rotation has been involved, I expect a Δ paleolatitude versus Δ latitude slope of approximately 1:1; however, the OJP ODP paleolatitude data show a clear, significant, and systematic bias.

Furthermore, a geometrically impossible scenario is apparent in the currently accepted OJP paleolatitudes where approximately half of Δ paleolatitude distances exceed their respective inter-site great circle distances (Figure 3.4). Of the eight Δ paleolatitudes exceeding inter-site distances, six pertain to either Site 807 or 1184 and two involve Site 1187. I note that whole plateau rotation alone cannot produce Δ paleolatitude to inter-site distance ratios above 1:1 and that half of the Δ paleolatitudes do not exceed this ratio. Tectonic tilt has been mentioned in drilling reports for both Sites 807 [Mayer and Tarduno, 1993] and 1184 [Mahoney et al., 2001]; I suspect that Site 807 and 1184 paleolatitudes could be at fault.

I explore a multitude of causes for such bias. I eliminated the possibility of whole plateau tilt, which could alter measured paleo-inclinations (and hence paleolatitudes), as I would still find bias in the relationship between differences in ODP paleolatitudes and latitudes which simply removes the effect of constant plateau tilt. I therefore conclude that tilt of the whole plateau cannot account for the observed phenomenon. One can always derive *ad hoc* tilt corrections for each site that completely remove the 2:1 slope bias; however there is a lack of evidence favoring faulting or tilting at Sites 1183, 1185, 1186, and 1187. If we assume instead that these tilts correspond to translational deformation of OJP, the implication is that up to 50% crustal shortening has occurred (see Figure 3.4), constituting a rather unlikely scenario that is unsupported

by regional seismic studies [e.g., Mann and Taira, 2004]. I therefore find differential tilt at each site to be an unlikely cause of the bias.

Although other mechanisms are able to reduce the slope bias, they require that measured paleolatitudes and/or ages be at fault. The only mechanism that allowed for the acceptance of the data involved rotation of the whole plateau. Two paleolatitude corrections were required, however. The literature contains reference to tilted basement rocks at Sites 1184 (9° northward dip [Mahoney et al., 2001]) and at Site 807 (unresolved tectonic tilt [Mayer and Tarduno, 1993]) whereas Sites 1183, 1185, 1186, and 1187 presumably sampled undisturbed rocks. This duality of tilted and undisturbed samples led us to devise a geologic scenario where the observed slope bias would be the result of a combination of rotation of the whole plateau as well as tilt at Sites 807 and 1184.

The rotation method involves the present and past positions of Ontong Java's ODP site locations. Paleo site positions are determined from their published paleolatitudes and from modeled paleolongitudes. I first determine the mean present ODP location (160.137° E, 0.447° S) using the undisturbed OJP ODP Sites, 1183 and 1185-1187. I next determine the mean paleo site position (141.009° W, 24.650° S) by computing the mean of undisturbed published paleolatitudes and by reconstructing the mean present longitude to its 123 Ma location using the WK08-D Pacific APM model (Chapter 2). APM use is limited to mean paleo site longitude derivation in order to minimize its influence on the model; different APM models only affect the results in insignificant ways. The difference in present and paleo mean site positions is the constant (Δ longitude=58.854°, Δ latitude=-24.203°) used for translating present site locations to overlie the paleo site distribution. The mean present site location serves as the vertical axis about which OJP rotations are performed. Rotations about the present mean site location are then translated by the difference in mean site positions to overlie the paleo site distribution. These modeled paleo site locations provide

paleolongitudes for both the observed and modeled data sets (hence differences in predictions from different APM models would cancel out). The interpreted OJP perimeter from Chapter 2 is also translated and rotated by the same amounts. Finally, I produce candidate models at all rotation angles and determine optimum rotations by minimizing modeled paleolatitude versus observed paleolatitude χ^2 misfit, calculated as $\sum\{i = 1 : n\}[(e_i/E_i)^2]$ where $n = 6$, $e_i = \|plat_{obs} - plat_{model}\|$, and E_i are published paleolatitude errors from Table 3.1.

Assuming OJP deformation has been limited to its perimeter and that the interior remains relatively undisturbed, I expect agreement between modeled and observed paleo ODP site positions. In addition to plateau rotation, tilt corrections may also be derived on the basis of this assumption. I therefore compute tilt corrections by determining model versus paleolatitude inclination differences for ODP Sites 807 and 1184. While the study by Mayer and Tarduno [1993] mentioned possible tectonic tilt at Site 807 but made no such correction, the Site 1184 paleolatitude derivation by Riisager et al. [2004] did not mention whether paleoinclination was adjusted. I therefore considered the horizontal and tilted emplacement of Site 1184 tuff deposits due to uncertainty in whether it was applied in previous studies. If beds were deposited horizontally, then the 9° northward tilt observed by Mahoney et al. [2001] would imply a comparable increase in Site 1184's inclination. Conversely, if beds were deposited at an angle, and if the published 1184 paleolatitude was corrected based on the horizontal assumption, then 1184's inclination needs to be reduced.

Figures 3.5 and 3.6 illustrate the improved agreement between modeled and paleo locations that is attained by plateau rotation (ω denotes rotation angle). Unfilled colored circles are paleo site locations as published by Riisager et al. [2004] while filled circles are my tilt-corrected paleo site locations. Arrows show the magnitude and sense of tilt corrections. Open squares are the present ODP sites after rotation and translation and serve as predicted paleo site locations based on the prescribed

rotation angle. Significant reduction in χ^2 misfit is apparent for panels with non-zero rotation angle. Figures 3.5 and 3.6 differ in their handling of Site 1184. In Figure 3.5, I show how removing the Mahoney et al. [2001] 9° tilt adjustment from Site 1184's inclination, coupled with plateau rotation, dramatically improves agreement to its expected location. In Figure 3.6, Site 1184's tilt adjustment is estimated without constraint from the literature as the difference between predicted and observed values.

3.3 Results

The χ^2 results computed for the full range of rotation angles are shown in Figure 3.7. In Figure 3.7(a), I see a reduction in misfit from ~ 1 at 0° rotation to the minimum misfit value of 0.101 occurring at 37° rotation. However, rotation angles between 25° – 50° achieve nearly identical misfit reduction, implying that the true plateau rotation was likely within this range. Figure 3.7(b) shows similar χ^2 misfit results for the alternative scenario in which neither 807 or 1184 are involved in misfit calculations. Based solely on the undisturbed sites which are distributed closer to the mean site location, this scenario suggests a similarly oriented rotation but with a larger range of acceptable rotations. Here, the minimum misfit of 0.057 occurs at 52° rotation angle. Of course, the closer clustering of data points to the rotation axis means the uncertainty in the rotation angle is likely to be higher.

Reconstructions at these preferred rotation angles are shown in Figure 3.8. Improvement between expected (squares) and observed (circles) paleolatitudes is seen at all sites in Figure 3.8(a), however, aside from Site 1186, expected and observed sites do not overlie one another. This scenario implies an $\sim 8^\circ$ southerly tilt correction for Site 807, yielding an estimated -41° inclination and -23.5° paleolatitude. Site 1184, after removing the 9° tilt correction from the published measurement, has -44.9° inclination and -26.5° paleolatitude.

At 52° rotation (Fig. 3.8(b)), further improvement is seen to the point where measured paleolatitudes overlie their expected locations directly at Sites 1183, 1185 and 1186. This scenario implies $\sim 10^\circ$ southerly and $\sim 12^\circ$ northerly tilt corrections for Sites 807 and 1184, respectively. For Site 807, the inclination and paleolatitude corresponding to the 52° rotation tilt correction estimates are -42.9° and -24.9° . For Site 1184, the inclination and paleolatitude would be -41.9° and -24.1° . Therefore, at the 37° rotation angle, Site 807 plots just 3° north of Site 1184, while the 52° rotation scenario suggests Site 1184 was 0.8° north of Site 807 at 123 Ma. This is in stark contrast to the currently accepted 16.5° paleo-separation between Site 807 to the north and Site 1184 to the south, respectively.

The process of slope bias removal by plateau rotation and tilt correction is further illustrated graphically in Figure 3.9. In each graph, two-tone color filled circles are modified by rotations and/or tilt adjustments, while unfilled colored circles are the original biased data, which do not vary. Except in cases of tilt correction, Δ paleolatitudes do not change. In essence, the color filled two-tone circles move only in the horizontal direction as the plateau is rotated. In Figure 3.9(a), the plateau has been rotated 37° , causing the redistribution of Δ latitudes shown. The interior sites (excluding 807 and 1184) now cluster along the $\sim 1:1$ slope line. Similar $\sim 1:1$ slopes are also evident for the subset of Site 1184 points (green) although the 1184 distribution is offset from the origin by a constant vertical offset that is related to its erroneous paleolatitude measurement. Figure 3.9(b) shows the effect of removing the 9° Site 1184 tilt correction from the Riisager et al. [2004] paleolatitude. The 1184 subset of points has now been shifted vertically to the origin and shares a similar $\sim 1:1$ slope with the interior undisturbed points. Figure 3.9(c) shows a similar effect when applying my 8.1° southerly tilt correction estimate to Site 807's paleolatitude, namely that the 807 subset (red points) are shifted down to the origin and share identical slope with the other OJP points. I note that this scenario reduces the slope bias from

slope ~ 2 (as in Figure 3.3) to ~ 1.3 , a substantial improvement given only six ODP sites. The unbiased distribution has slope statistically indistinguishable from 1:1.

Figure 3.9(d) shows the effect of a 52° plateau rotation on the biased background points. A similar observation can be made, that interior points are now aligned along the 1:1 slope line. Site 1184 and 807 subsets are again offset vertically due to their erroneous paleolatitude measurements. Applying my estimated tilt corrections to Site 1184 (Fig. 3.9(e)) and 807 (Fig. 3.9(f)) paleolatitudes results in a further reduction of slope bias from 2 to 1.2. This unbiased distribution also has slope statistically indistinguishable from 1:1, indicating that the slope bias has been resolved.

3.4 Discussion

The OJP rotation hypothesis clearly depends on the accuracy of ODP basement age and paleolatitude measurements for its plausibility. Should ages or paleolatitudes be shown to differ significantly from their currently accepted values, my rotations would be affected and possibly invalidated. Site 1184 age and paleolatitude measurements, in particular, have not been the most reliable according to the literature. Whereas other OJP basement samples were basaltic lavas, mid-Eocene aged fossil-bearing tuff was sampled at Site 1184 [Mahoney et al., 2001]. A subsequent $^{40}\text{Ar}/^{39}\text{Ar}$ analysis of plagioclase crystals separated from the volcanoclastic matrix yielded a Cretaceous age of 123.5 Ma, leading Chambers et al. [2004] to rule out the Eocene age. Similarly, while Site 1184's paleolatitude has been reported as 34.4° S [Riisager et al., 2004], my analysis suggests this measurement is too far south by 8° – 11° . However, I suggest that the 1184 paleomagnetic measurement is likely precise with the bias being in the 9° tilt adjustment. Removing this tilt adjustment reconciles Site 1184's paleolatitude with other undisturbed sites (at 37° rotation) and implies northward inclination of tuff beds at emplacement with a likely vent to the south. I note that, in the event that Site

1184 data are found to be unreliable, the remaining OJP data still support rotation. Indeed, my alternative analysis does not include Site 1184 in χ^2 misfit calculations and suggests 52° rotation although there is less control on rotations. Assuming Site 1184's paleolatitude to be accurate, the 37° rotation scenario is preferable to the less constrained 52° rotation scenario suggesting $\sim 25^\circ$ – 50° of clockwise rotation since 123 Ma.

In exploring potential causes for the observed Δ paleolatitude vs Δ latitude slope bias, I derived a set of six *ad hoc* tilt adjustments that when applied to the published measurements resolved the slope bias without the need for plateau rotation. In support of this interpretation is the fact that these tilt adjustments (see Table 3.2's *ad hoc* column) result in paleolatitudes that are within the published uncertainty range for each of the six sites. However, these *ad hoc* tilt corrections suggest modification of all published paleolatitudes in such a way as to bring them in line with expected values. Therefore the *ad hoc* method holds the model fixed while adjusting the observations. This method is clearly the inverse of my rotation hypothesis, which finds optimum model rotations relative to fixed observations. In addition, inspection of *ad hoc* corrections for the undisturbed sites presented in Table 3.2 reveals magnitudes and directions that correspond to rotation in the opposite sense. While I must acknowledge such a possibility, I consider such a contrived set of inclination adjustments to be much less likely than the rotation hypothesis, which requires tilt adjustment at the two sites that mention tectonic tilt in their original drilling reports. Also shown in Table 3.2 are misfits between modeled and observed paleolatitudes (e_i) at 0° , 37° and 52° . These e_i values exhibit the misfit reductions attained at each of the undisturbed sites through the whole plateau rotation method. I am unable to explain the dichotomy between relatively large paleolatitude measurement uncertainties and the strong agreement between observed and modeled paleolatitude locations. My results apparently indicate that paleolatitude measurements may be better defined

than suggested by their respective and conservative error estimates.

The less likely interpretation requiring tilt adjustments of all OJP basement paleolatitudes implies little change to the tectonic history of the Pacific plate. Ontong Java remains an enigmatic piece of Pacific crust with paleolatitudes that do not conform to the Pacific APWP. Under this scenario, the primary implication is of extensive plateau deformation not previously recognized. In contrast, the rotation hypothesis requires significant revision of Pacific plate history. The rotations predicted by my models are unprecedented among Pacific plate motion models. For instance, the WK08-A, African-derived OMS-05, and WK08-D APMs predict 4° , -2.8° and -13° of OJP rotation to have occurred since 123 Ma [Chapter 2]. The WK08-D APM, favored for including Emperor-stage Hawaiian plume drift, requiring little to no true polar wander, and for best reconciling Ontong Java Nui super-plateau reconstructions with paleolatitude evidence, predicts Pacific-wide rotation in the opposite sense (i.e., counter-clockwise). If this model for Pacific plate motion is reasonable, the implication is that OJP's orientation relative to Pacific was $\sim 50^\circ$ – 65° different than today. Either (a) the APM is unreliable for the Lower Cretaceous or (b) there was relative motion between OJP and the Pacific at the time of OJP formation. While the paleolatitude evidence favors plateau rotation, I am unable to determine whether this rotation involved the whole Pacific or former microplates (e.g., OJP) that were later accreted to the Pacific plate. Although a 37° – 52° rotation of the whole Pacific plate seems unlikely, subduction studies by Shephard et al. [2011, in review] have failed to reconcile mantle tomography profiles with Pacific motion predicted by current APM models, suggesting a possible Pacific history much different than our current understanding. The more likely history involves decoupling between Pacific and Ontong Java although no obvious paleo Pacific–OJP plate boundary is apparent and it is uncertain whether this decoupling took the form of microplate rotation or reflects tectonic interactions with the Pacific or the encroaching Australian plate.

Clockwise OJP rotation is not incompatible with the current consensus that Ontong Java formed simultaneously with Manihiki and Hikurangi plateaus as part of the Ontong Java Nui super-plateau [Taylor, 2006; Chandler et al., 2011, in review]. Manihiki's Site 317a paleolatitude [Cockerham and Jarrard, 1976] is the sole paleolatitude measurement for testing the compatibility of these two hypotheses. Cockerham and Jarrard [1976] reported a 20° paleolatitude difference between DSDP Site 317's volcanoclastic-basalt basement and overlying carbonate sediments. The authors favored the carbonate paleolatitude and offered either tectonic tilt of the basement strata or a failure to average out secular drift as reasons for Site 317's 47.5° S basement paleolatitude. Cockerham and Jarrard [1976] further acknowledged the possibility that compaction of overlying sediments could have altered the sedimentary paleoinclination by $\sim 20^\circ$. Another Site 317 paleolatitude study by Cockerham and Hall [1976] reported more clearly that tectonic tilting likely occurred between the time of carbonate and volcanoclastic sediment deposition and that the carbonate paleolatitude estimate suffered from an inclination error requiring further study. As shown in Figure 3.10(a), the Manihiki carbonate paleolatitude is in good agreement with the super-plateau hypothesis at 37° rotation (1184 is tilt corrected here, Site 317's carbonate paleolatitude is assumed). Furthermore, if I include Site 317 while omitting Sites 807 and 1184 in misfit calculations, I estimate a Site 317-optimized super-plateau rotation of 35° , virtually identical to the OJP-only rotation. However, should the carbonate paleolatitude be erroneous due to tilt or compaction, the 47.5° basement paleolatitude would favor the WK08-D OJN reconstruction from Chapter 2 and not the rotation/super-plateau reconstruction shown in Figure 3.10(a). Higher quality basement paleolatitudes are clearly needed at Manihiki in order to resolve the compatibility of the OJP rotation and OJN super-plateau hypotheses.

Although no clear Pacific/Ontong Java suture is apparent in regional bathymetry, the large magnitude of rotation required by the paleolatitudes and evidence against

such large Pacific plate rotations implies decoupling, as previously suggested by Sager [2006]. These results have implications for studies of Pacific apparent polar wander curves, which have included Ontong Java as a constraint (albeit anomalous) for the ~ 120 - 125 Ma time frame. High internal consistency among OJP paleolatitudes has been used to question the veracity of paleolatitudes at MIT Guyot and the Mid-Pacific Mountains and as evidence against fixity of Pacific hotspots [Riisager et al., 2003]. However, with a decoupled Ontong Java, OJP paleolatitudes would no longer be suitable as constraints for Pacific APWP. MIT Guyot and the Mid-Pacific Mountains, which show much better agreement with the overall Pacific APWP trend (Figure 3.2), would then become the primary constraints for Pacific APWP at ~ 123 Ma. Nevertheless, even after tilt adjustment, the OJP paleolatitudes are still significantly further north than the nearest likely source (Louisville hotspot). If a greatly reduced north-south motion during the Emperor stage is accepted (e.g., Tarduno [2007]) then it is possible that revised Pacific APM would yield reconstructions more in line with the OJP paleolatitudes but at the same time fail to explain the paleolatitudes of MIT Guyot and the Mid-Pacific Mountains. More work is clearly needed on refining the Pacific APM back to 125 Ma.

The tilt adjustment estimates for Sites 807 and 1184 have little impact on OJP's mean paleolatitude. This is largely because these corrections have similar but oppositely oriented magnitudes that move each site closer to the mean. In comparison to the currently accepted 25.2°S mean paleolatitude, I find mean values of 24.8°S and 24.6°S for plateau rotations of 37° and 52° , respectively.

While evidence strongly favors my combined rotation and 807/1184 tilt correction model, I acknowledge that large uncertainties in paleolatitudes allow contributions from other sources including octupole components [e.g., Antretter et al., 2004], insufficient sampling to remove secular drift effects, along with the possibility that a slope statistically similar to 1:1 could be drawn if Site 1184 were omitted from the analysis

or if Sites 807 and 1184 were tilt corrected in the absence of rotation. Figures 3.11 and 3.12 depict the effects of rotationless tilt correction of Sites 807 and 1184 using their respective e_i at 0° tilt correction estimates shown in Table 3.2. A reduction from eight to five invalid Δ paleolatitudes is apparent in Figure 3.11. Although the regression slope apparent in Figure 3.12 is statistically indistinguishable from slope one, internal bias is still evident for three subsets; the undisturbed sites (1183 and 1185-1187) fall along the 2:1 slope curve and the 807 and 1184 subsets remain parallel to the 2:1 slope curve, indicating that the internal bias is not resolved through tilt correction of Sites 807 and 1184 alone.

3.5 Conclusion

I have presented a simple geologic model that reconciles Ontong Java ODP site locations with their respective paleolatitude measurements and that suggests $\sim 25^\circ$ – 50° of clockwise rotation since 123 Ma. Aside from Sites 807 and 1184, of which tilt corrections have been estimated, I find OJP paleolatitudes to be internally consistent when coupled with previously unrecognized rotation of the plateau. The reduction in paleolatitude error and resultant determination that the adjusted paleolatitudes are no longer anomalous, provide evidence for either significant rotation of the Pacific plate at the time of OJP formation or for decoupled movement between the Pacific plate and Ontong Java. The latter hypothesis, favored by other coeval paleopoles, calls into question the suitability of Ontong Java paleolatitudes as constraints for Pacific APWP. Although there is strong support for rotation among the OJP paleolatitudes, the hypothesis is complicated by a lack of an obvious Pacific–OJP paleo plate boundary. Furthermore, Manihiki’s sole basement paleolatitude, although of questionable validity, indicates a paleo position that is incompatible with the rotation magnitudes implied by this analysis. More high quality basement paleolatitudes at Ontong Java,

Table 3.1: Published ODP drill locations and paleomagnetics for Ontong Java Plateau. Refs: [1] Riisager et al. [2003], [2] Mayer and Tarduno [1993], [3] Mahoney et al. [1993], [4] Riisager et al. [2004], [3] Mahoney et al. [2001].

Site	Lon	Lat	Inc	Plat \pm E	Age (Ma)
807 [2]	156.620	3.600	-32.9	-17.9 \pm 3.3	122.3 [3]
1183 [1]	157.015	-1.177	-46.7	-27.9 \pm 7.2	121
1184 [4]	164.223	-5.011	-53.9	-34.4 \pm 5	123.5
1185 [1]	161.668	-0.358	-40.8	-23.3 \pm 2.2	121
1186 [1]	159.844	-0.680	-43.2	-25.2 \pm 3.5	121
1187 [1]	161.451	0.943	-39.2	-22.2 \pm 2.3	121

Table 3.2: Ontong Java paleomagnetic analysis results

Site #	<i>Ad hoc</i>	e_i at 0°	e_i at 37°	e_i at 52°
807	-3.2	-4.2	-8.2	-10.0
1183	2.0	3.0	0.9	0.4
1184	4.7	5.5	9.8	12.0
1185	-1.8	-1.9	-0.5	-0.1
1186	-0.2	0.2	0.2	0.3
1187	-1.6	-1.6	-0.8	-0.7

Manihiki and Hikurangi plateaus will be required in order to confirm or reject the rotation hypothesis.

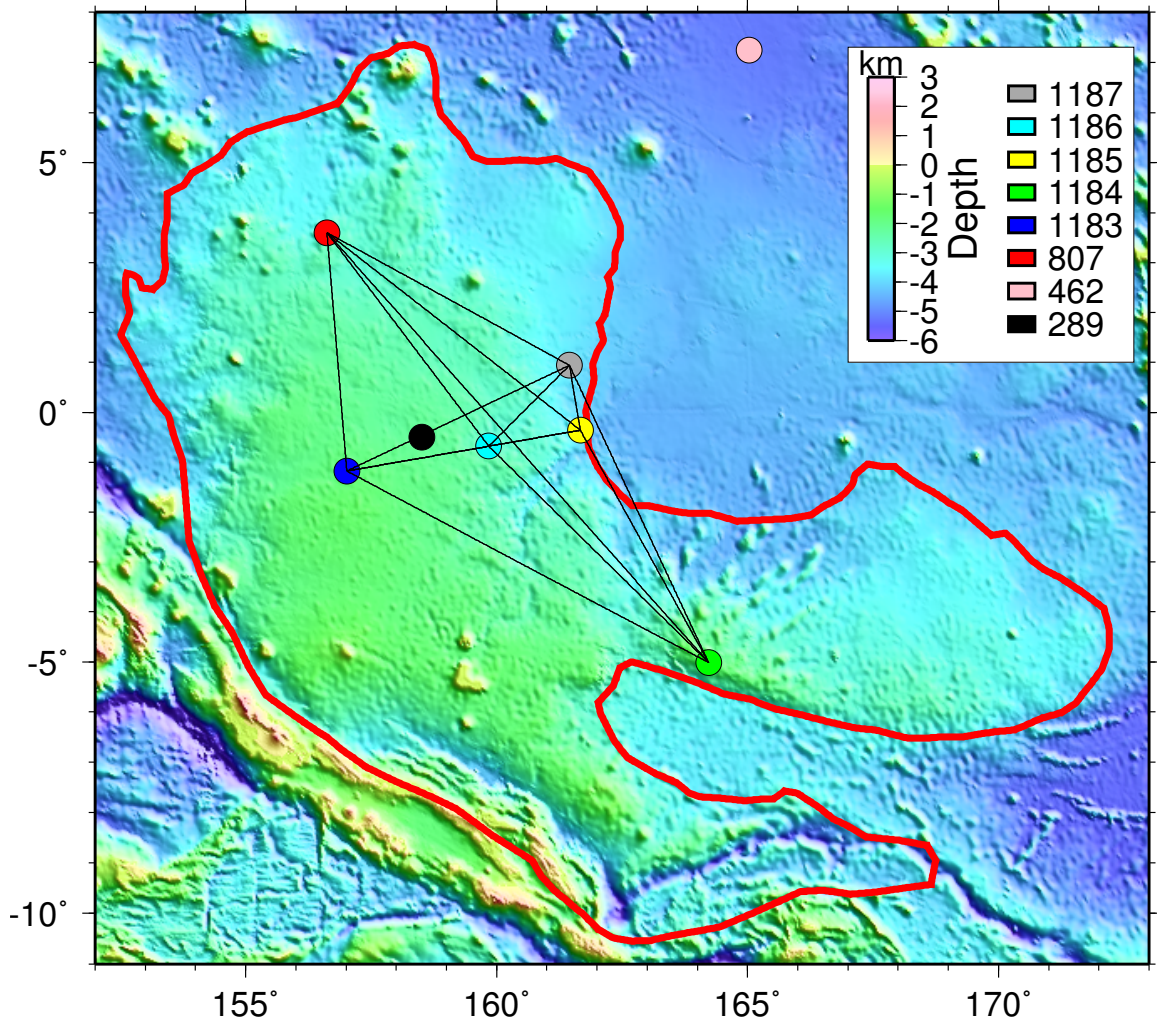


Figure 3.1: Bathymetric map of Ontong Java Plateau (red outline) showing the ODP sites analyzed in this study. Solid lines indicate great circle arcs along which inter-site distances are computed. Although basement rocks from DSDP Site 289 share similar emplacement characteristics, insufficient flows were sampled so these data were not included in this study.

Table 3.3: A clear bias is apparent among inter-site latitude and paleolatitude differences where Δ paleolatitude magnitudes (right) are generally twice their respective Δ latitude (left).

Site	807	1183	1184	1185	1186	1187
807	–	4.8°, 10.0°	8.6°, 16.5°	4.0°, 5.4°	4.3°, 7.3°	2.7°, 4.3°
1183	-4.8°, -10.0°	–	3.8°, 6.5°	-0.8°, -4.6°	-0.5°, -2.7°	-2.1°, -5.7°
1184	-8.6°, -16.5°	-3.8°, -6.5°	–	-4.7°, -11.1°	-4.3°, -9.2°	-6.0°, -12.2°
1185	-4.0°, -5.4°	0.8°, 4.6°	4.7°, 11.1°	–	0.3°, 1.9°	-1.3°, -1.1°
1186	-4.3°, -7.3°	0.5°, 2.7°	4.3°, 9.2°	-0.3°, -1.9°	–	-1.6°, -3.0°
1187	-2.7°, -4.3°	2.1°, 5.7°	6.0°, 12.2°	1.3°, 1.1°	1.6°, 3.0°	–

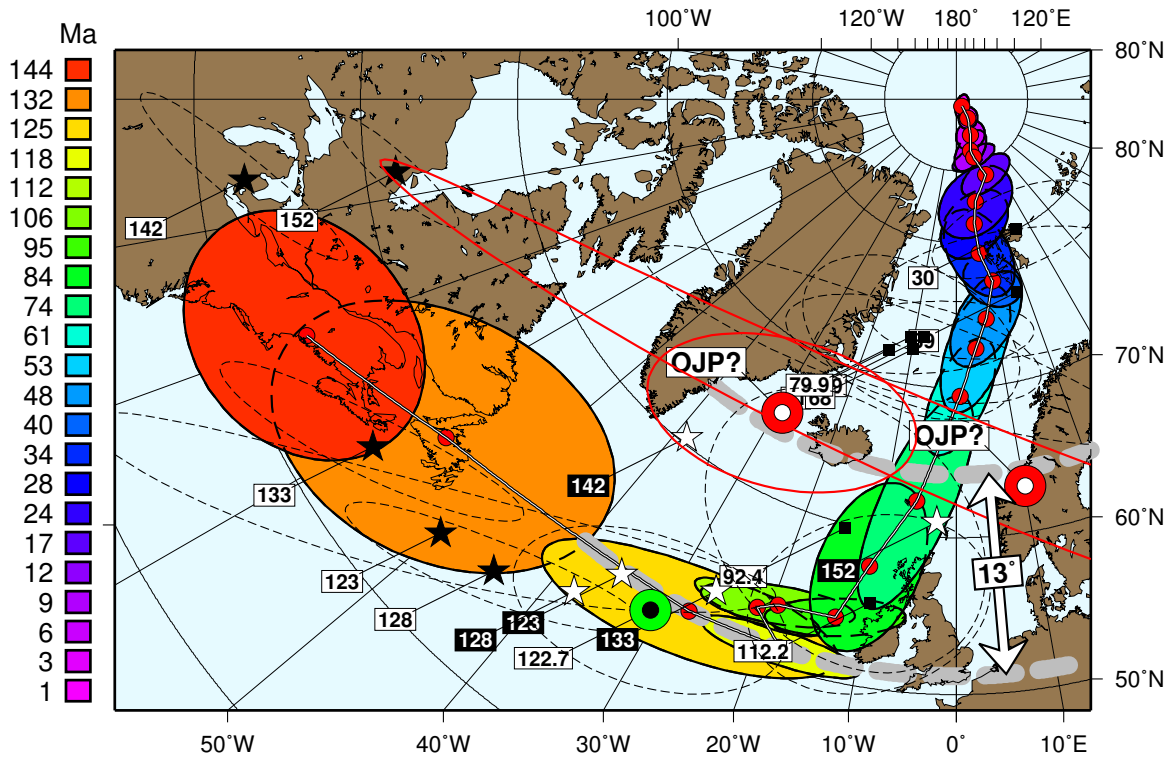


Figure 3.2: OJP diverges from the apparent polar wander path (APWP) for the Pacific plate. Small red circles and corresponding color-filled error ellipses are APWP predictions from the WK08-A APM model Wessel and Kroenke [2008]. Black squares are Cretaceous average group paleomagnetic poles from Sager [2006] with earlier poles from Larson and Sager [1992], here reproduced as stars (black for solutions with anomalous skewness, white without skewness). Anomalous poles for OJP (122 Ma; large red and white circles) from Sager [2006] (left) and Riisager et al. [2004] (right) are also shown, compared to the coeval pole derived from MIT guyot and MidPac mountain samples (Sager [2006]; large green and black circle).

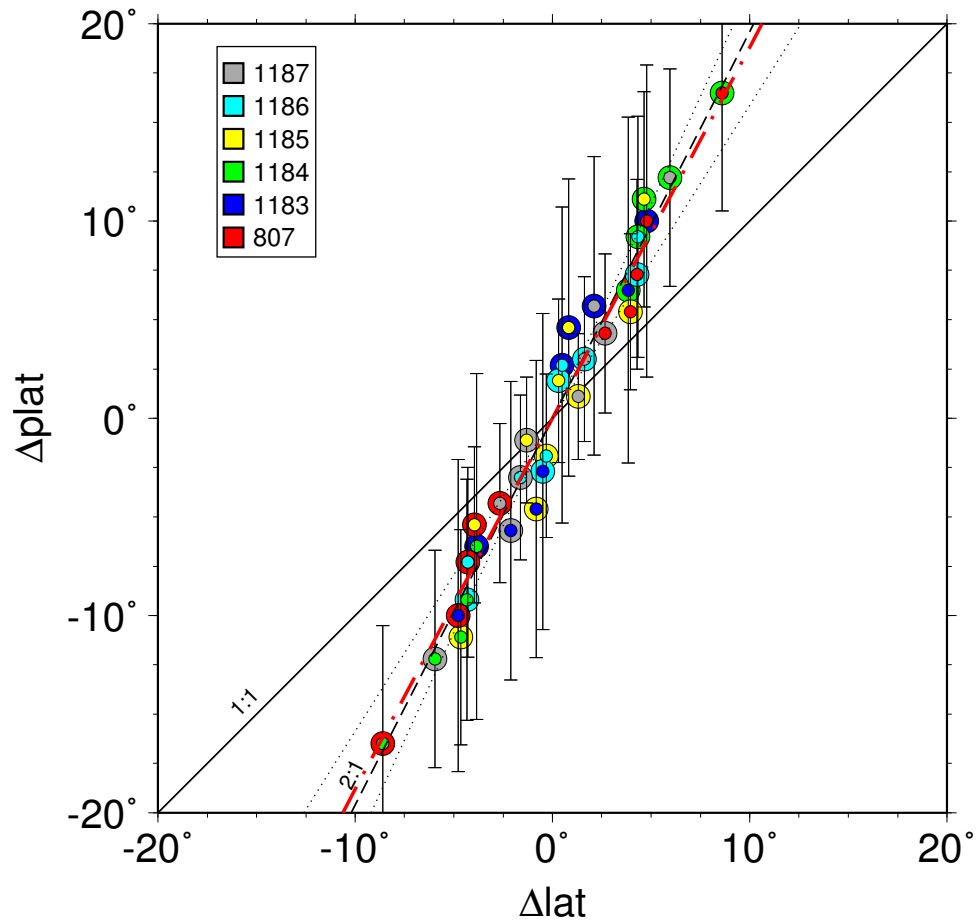


Figure 3.3: $\Delta\text{paleolatitude}$ versus $\Delta\text{latitude}$ shows a 2:1 slope (dashed black line) rather than the expected 1:1 slope (solid line). For each site pair, Δ values are computed by inner minus outer (p)lat. Error bars are computed as $\sqrt{E_{inner}^2 + E_{outer}^2}$. Red dashed least squares regression line indicates statistical difference from slope one while dotted lines indicate 95% slope uncertainty.

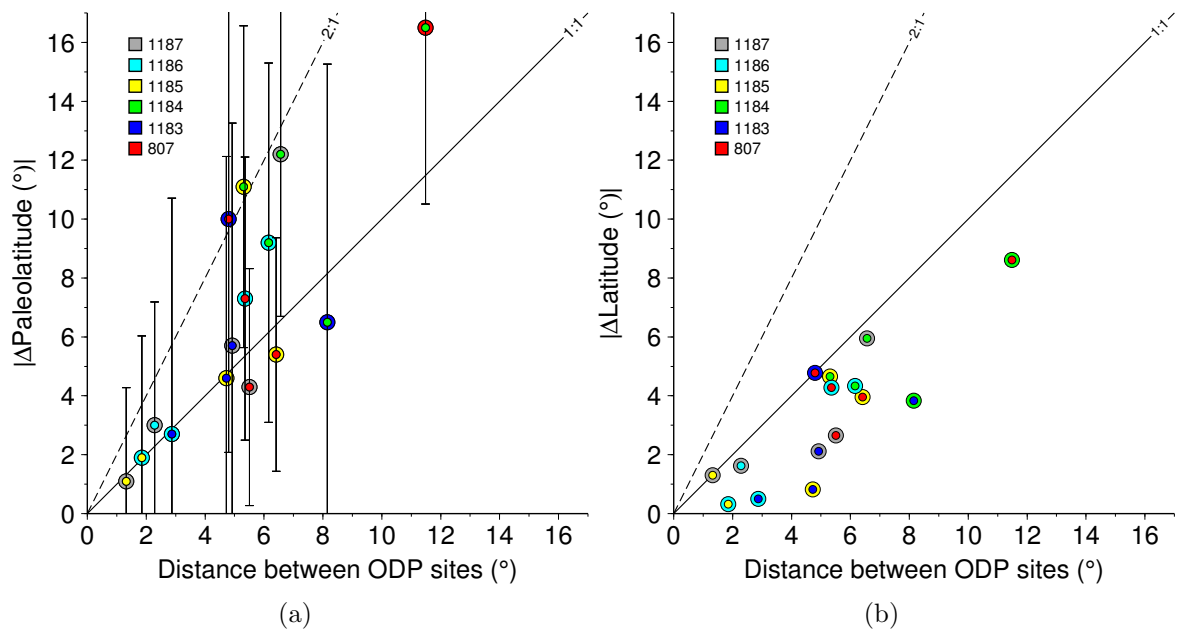


Figure 3.4: (a) About half of OJP Δ paleolatitudes violate the basic geometrical principle that inter-site Δ paleolatitudes cannot exceed their respective great circle distances. (b) Δ latitude versus great circle distance naturally exhibits no such phenomenon. If all paleolatitudes are valid, crustal shortening of $\sim 50\%$ is called for.

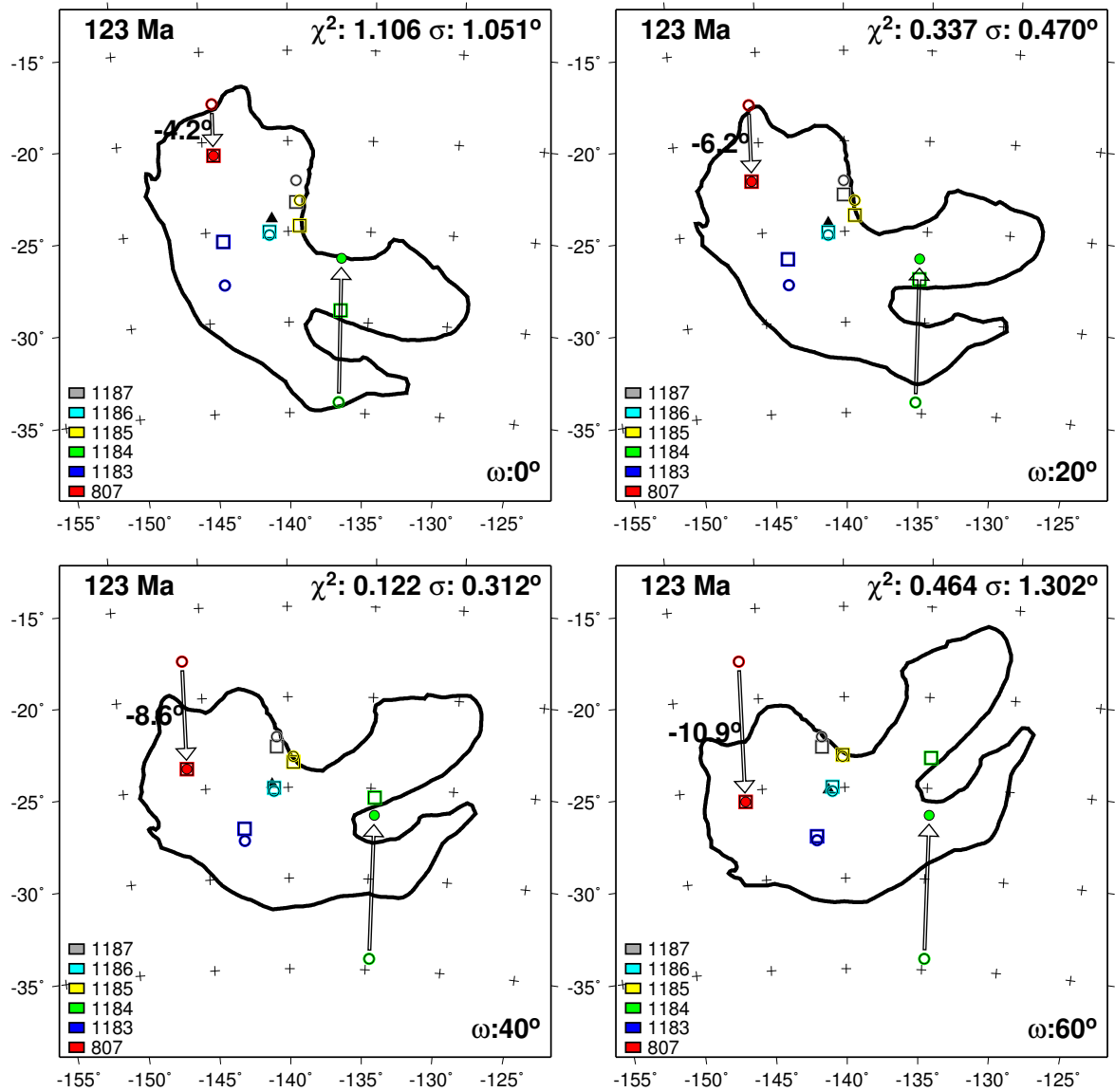


Figure 3.5: Map view comparison of translated and rotated ODP/DSDP drill site positions (squares) to the set of OJP paleolatitude measurements (circles). Rotation is about the mean ODP/DSDP site location (black triangle). Here, Site 807's tilt adjustment is being estimated, hence the site is not included in misfit calculations. Site 1184 is tilt corrected northward by 9° and is a leverage point controlling misfit minimization. Misfit decreases as rotation angle (ω) approaches 40° when it begins increasing.

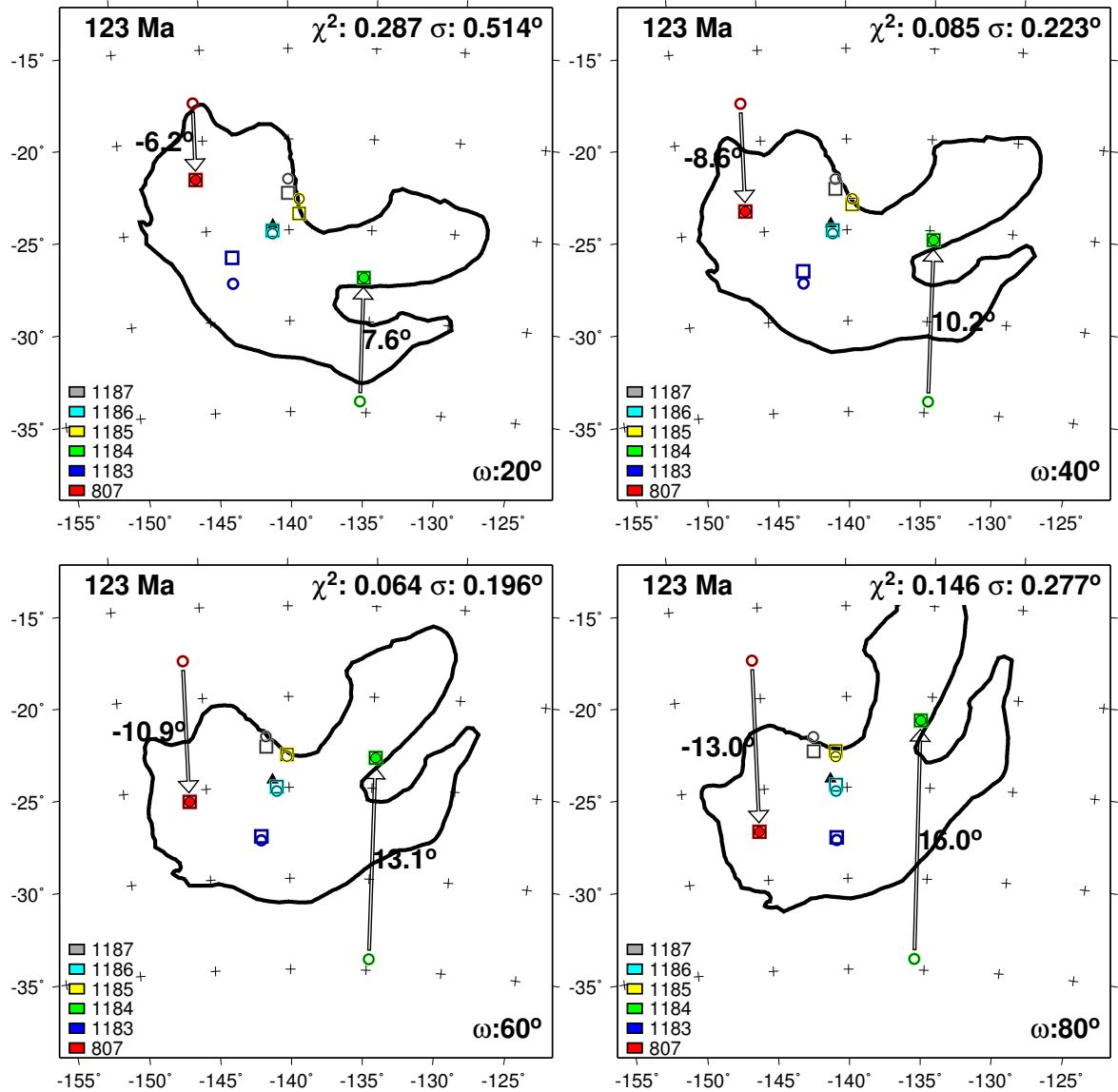


Figure 3.6: The rotational property of the undisturbed sites is determined by excluding Sites 1184 and 807 from misfit calculations. In this case, misfit decreases as rotation angle approaches 60° then begins to increase. Tilt correction estimates for Sites 807 and 1184 are derived as a result. See Fig. 3.5 caption for symbol descriptions.

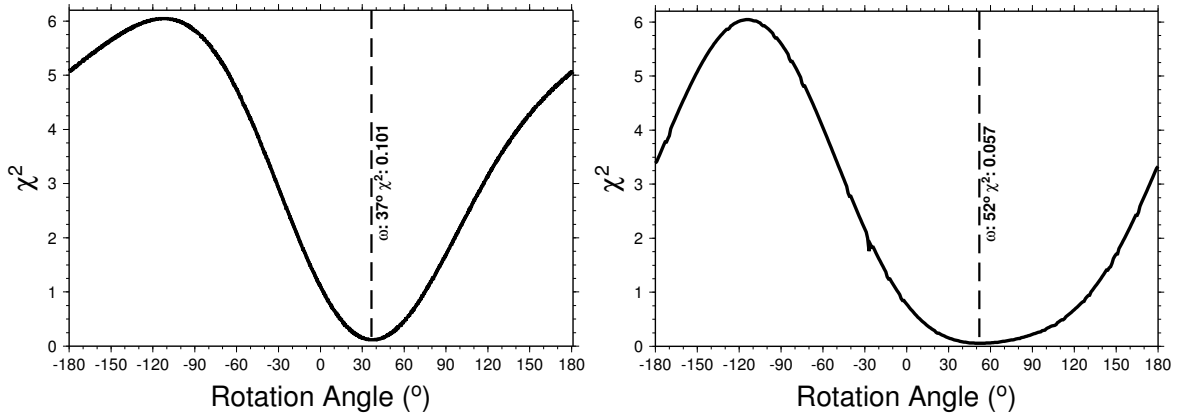


Figure 3.7: χ^2 misfit calculations versus rotation angle shown for both rotation methods. Minimum misfit occurs at 37° clockwise rotation when the tilt-corrected Site 1184 is included in misfit calculations (left). A broader range of low misfit and a global minimum of 52° is found by excluding this site (right).

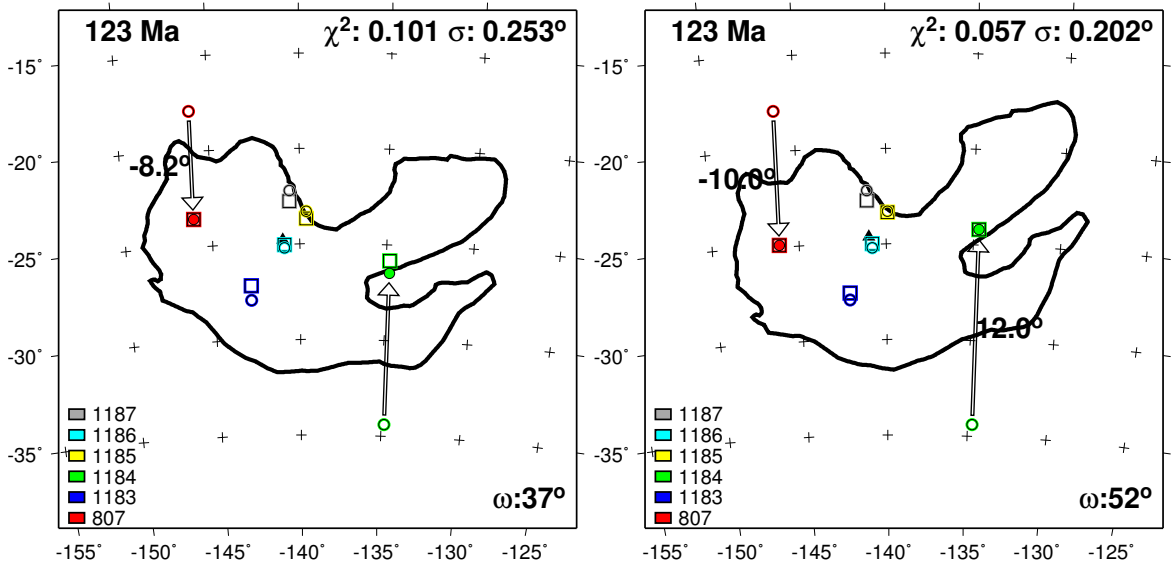


Figure 3.8: Improved agreement between expected and observed paleolatitudes is seen at optimum rotation angles whether Site 1184 is included (left) or not (right).

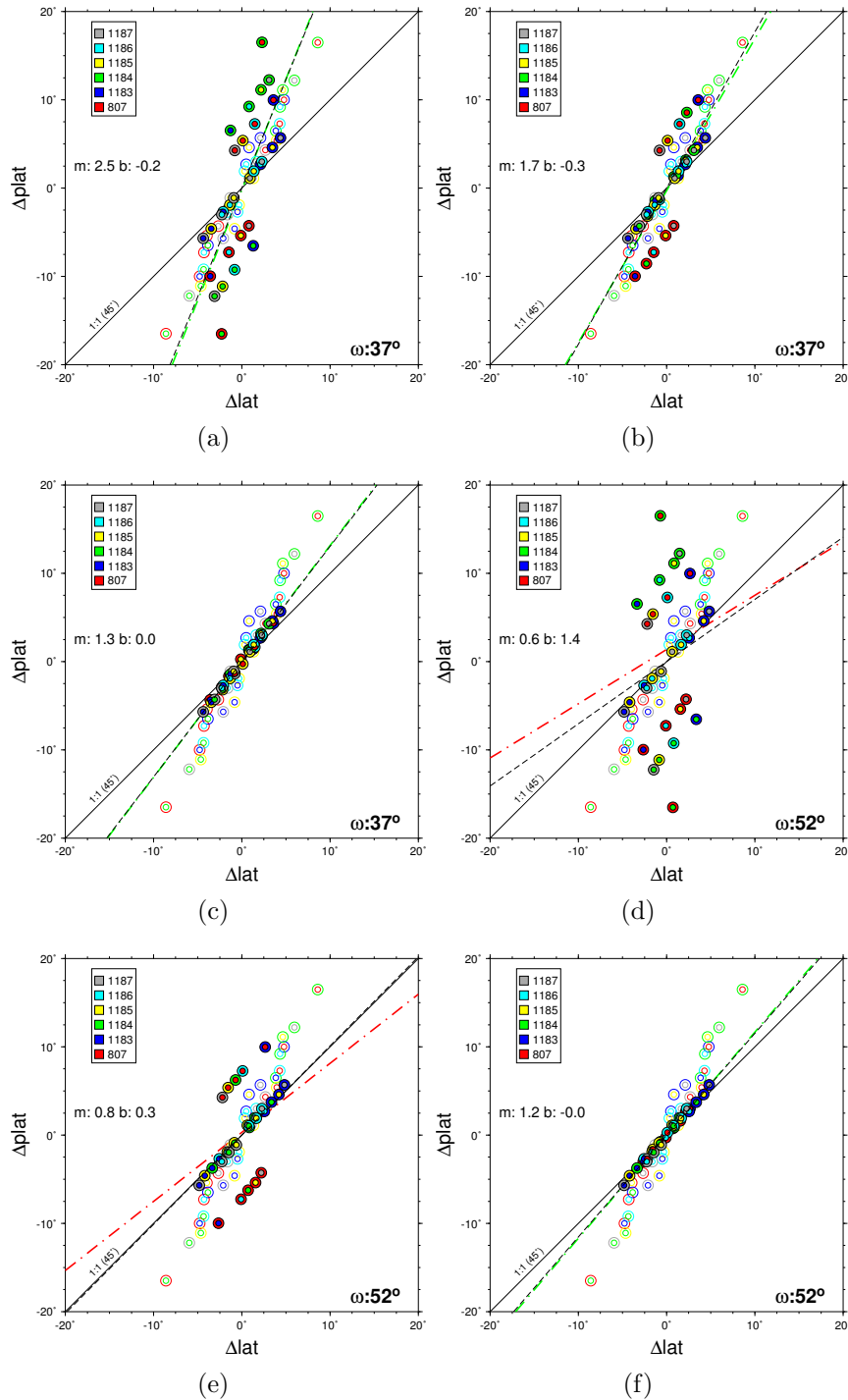


Figure 3.9: Depiction of slope bias removal showing least-squares regression estimates for slope (m) and intercept (b). The slope bias can be removed by (a) rotating OJP 37° , (b) removing Site 1184's published 9° tilt correction (implies emplacement-induced dip), and (c) applying an 8° southerly tilt adjustment to Site 807. (d) Further improvement is seen with 52° plateau rotation along with (e) a 12° northward tilt adjustment for 1184 tuff beds and (f) a 10° southerly tilt correction for Site 807. Original and biased data are plotted as unfilled circles while filled circles are subject to rotation and/or tilt correction.

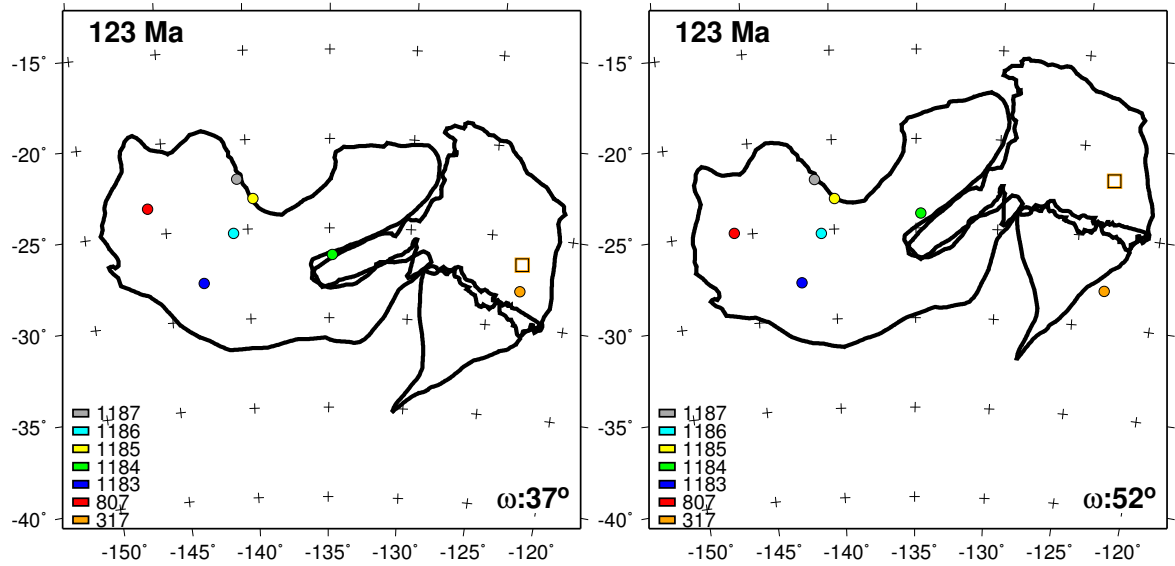


Figure 3.10: 123 Ma reconstruction of the Ontong Java Nui super-plateau [Chapter 2] at 37° (left) and 52° (right) rotation. DSDP Site 317's carbonate paleolatitude [Cockerham and Jarrard, 1976] favors the 37° scenario.

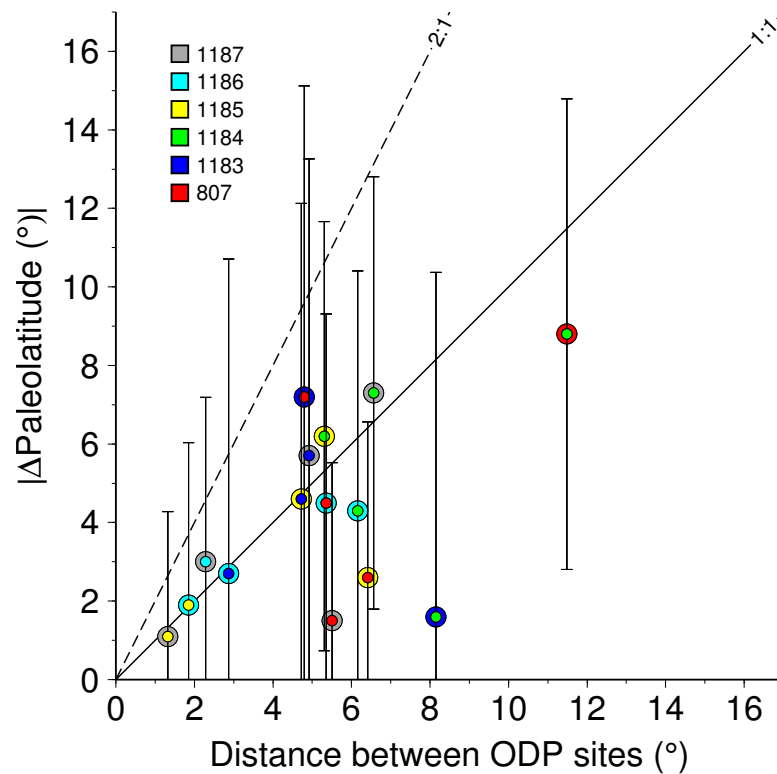


Figure 3.11: ODP Sites 807 and 1184 appear to be erroneous whether or not OJP rotation occurred. Here it is assumed that no rotation occurred so Sites 807 and 1184 are tilt corrected using their respective e_i at 0° tilt correction estimates (Table 3.2). The majority of Δ paleolatitudes no longer exceed their respective inter-site distances.

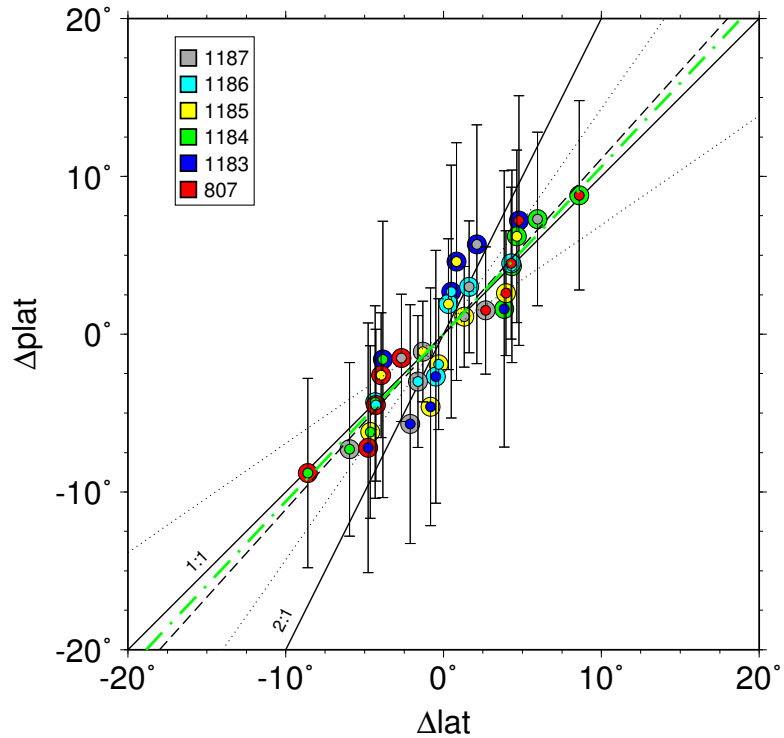


Figure 3.12: Assuming no rotation occurred, Sites 807 and 1184 are adjusted according to their respective e_i at 0° tilt correction estimates from Table 3.2. Although considerably more scatter is seen compared to Figure 3.3, $\Delta\text{paleolatitude}$ versus $\Delta\text{latitude}$ here shows a $\sim 1:1$ slope (dashed black line) when compared to the expected 1:1 slope (solid line). Green dashed least squares regression line indicates statistical equivalence to slope one while dotted lines indicate greatly increased 95% slope uncertainty.

Chapter 4

Errata-based correction of marine geophysical trackline data

Abstract

The National Geophysical Data Center's marine geophysical trackline archive is of primary importance to the scientific community but contains a range of data quality issues that impede its use. The dissemination of archived errors shifts the quality control burden from the few source institutions to the numerous end users. To alleviate this situation, I announce the completion of 5,203 errata correction tables aimed at reducing processing redundancy through removal of extreme and obvious errors. The open source and freely accessible along-track analysis errata system [Wessel and Chandler, 2007; Chandler and Wessel, 2008] is a suitable instrument for deriving, applying and sharing data corrections. Removal of obvious errors is an important initial step that should precede operations that otherwise may proliferate such artifacts, i.e., crossover analysis, interpolation, and gridding. A crossover assessment of these data corrected with errata tables indicates reduction in median crossover errors from 27.3 m to 24.0 m for bathymetry, 6.0 mGal to 4.4 mGal for free air gravity, and 81.6 nT to 29.6 nT for magnetic anomalies. My analysis also indicates widespread tendencies to omit observed gravity measurements and to instead report just the derived anomalies and to submit data containing navigation and geophysical outliers, among other data quality issues. In agreement with prior studies, I also find that residual magnetic anomalies should be recalculated using the latest geomagnetic reference fields whenever possible. These along-track methods may be considered gentler (and more fundamental) than the crossover approach in that along-track corrections affect only

data flagged as erroneous by a reviewer; the vast majority of data are left unchanged.

4.1 Introduction

The existing set of marine geophysical trackline measurements archived at the National Geophysical Data Center (NGDC) reflects an estimated USD 6.5 billion taxpayer investment [e.g., Chandler and Wessel, 2008] and is becoming increasingly valuable as research costs continue to rise. These publicly available data are widely used in constraining bathymetric charts, ground truthing satellite altimetry-derived gravity, inferring seafloor magnetization for plate kinematic studies, performing grid compilations, and in many other investigations of the seafloor, crust, and upper mantle. These data are especially essential in remote localities far from ports and coastlines where researchers are less likely to revisit [e.g., Wessel and Chandler, 2011]. Distributions of gravity, bathymetry, and magnetic tracks are shown in Figure 4.1.

Modern geophysical instruments emit data of increasingly high temporal and spatial resolution. While the task of processing this data has largely been met through the years, the presence of unprocessed and inappropriately scaled and shifted data sets has been confirmed by several workers attempting to identify and remove errors from the global track-line archive. These analyses succeeded in producing improvements in their included data sets. However, considerable time has passed since trackline gravity and bathymetry were analyzed. For instance, Wessel and Watts [1988] examined 834 marine gravity surveys but NGDC now archives more than twice this number at 1,798 legs. Similarly, Smith [1993] examined 2,253 bathymetry cruises although the archive now contains 4,872 depth surveys (see Figure 4.1). More recently, Quesnel et al. [2009] analyzed all but 60 of the 2,471 magnetic tracks available at this time. As these analyses were conducted independently, corrections were made available through publication of crossover adjustments or by downloading corrected

data sets. Unfortunately, crossover analysis derived corrections depend on all other tracks so as new tracks are added to the archive, the published adjustments become less and less relevant.

This dilemma was recognized by Wessel and Chandler [2007] who developed an errata-based system for correcting trackline data stored in NGDC's Marine Geophysical Data Exchange Format (MGD77). The approach recognized NGDC as a data library where users should not overwrite original data, but where errata correction tables should be derived and merged with original values when utilizing trackline data. The study also sought to increase the rigor of quality control checks before adding new cruises to the NGDC archive. The result of this broad undertaking is a set of freely available tools that enable rapid checking of trackline data sets, generation of along-track analysis derived "Errata-77" (E77) correction tables, and merging of original MGD77 data with E77 correction tables to produce corrected data on the fly.

The comprehensive assessment of geophysical values and errors carried out by Chandler and Wessel [2008] served to calibrate the along-track tests. Chandler and Wessel [2008] detailed the range of along-track tests performed by the `mgd77sniffer` quality control checker and illustrated the correction of data using E77 tables. Common errors examined during along-track analysis include excessive survey speed (i.e., > 10 m/s), navigation passing over land, non-increasing or decreasing time, MGD77 header errors, excessive geophysical values and gradients, excessive excursions from global gravity and predicted bathymetry grids, gravity and depth measurements systematically offset from global grids, and comparisons of reported gravity and magnetic anomalies to anomalies recomputed using the latest formulas and reference fields. Unlike ephemeral crossover corrections, along-track analysis derived correction tables depend only on data within the examined cruise and may therefore be considered permanent supplements to the trackline data. Furthermore, whereas crossover analyses

generally consider only one column of geophysical data, the along-track methods of Chandler and Wessel [2008] provide a comprehensive means for locating wide-ranging data problems within individual cruises. In addition to the generation of E77 correction tables for historical data sets, these methods are also suitable for data archivists wanting to quickly detect premature datasets.

I have completed reviewing errata tables for the 5,203 total cruises currently archived by NGDC using the methods of Wessel and Chandler [2007] and Chandler and Wessel [2008] and have made these corrections available online. I anticipate NGDC to archive these errata tables and commence using the quality control tools to encourage submitting agencies to correct such errors before accepting new data into the archive.

4.2 Errata Review Process

I acquire marine geophysical trackline data from NGDC's trackline data portal, amounting to 5,203 at the time of this writing. 93% of archived surveys report depth while 47% and 35% report magnetic and gravity anomalies, respectively. Clearly the majority of magnetic and gravity surveys also report depth data. 280 new cruises have been added to the archive since the analysis by Chandler and Wessel [2008] indicating an approximate archive growth rate of under 100 new surveys added per year excluding revisions of previously archived cruises.

Each time I access the NGDC trackline portal, I ensure that the search region is global, the time frame extends from the previous download to the present, that parameters surveyed include bathymetry, magnetics and gravity (union set to "or"), and that NGDC numbers are used in listings and file names. NGDC numbers contain useful metadata such as a leading two character agency identifier followed by a two character vessel identifier with the remaining four characters identifying individual

cruise legs. The NGDC classification scheme allows the data processor to access all cruises collected by a certain ship, for example, or all data reported by a given agency. I therefore utilize this system, although at times collaborative expeditions have proven difficult to correctly attribute to a single agency. After the online search is complete, I specify that data be saved in multiple survey files, that data be stored in the MGD77 ASCII exchange format [Hittleman et al., 1977], and that uncorrected depths be converted to corrected meters using Carter’s tables [Carter, 1980]. Once downloaded, I extract the data and concatenate the h77 headers with their respective a77 data record files (as NGDC provides them separately) to produce complete MGD77 files.

I organize MGD77 files as specified by Wessel and Chandler [2007] and additionally create an X2SYS database [Wessel, 2010] specific to MGD77 data. The X2SYS database allows me to quickly query for tracks within specific regions and/or having certain data columns. This setup also provides built in crossover analysis capability. Once bookkeeping is complete, errata tables are produced by the mgd77sniffer along-track analysis tool [Wessel and Chandler, 2007]. I specify the following command line arguments for each cruise:

```
mgd77sniffer <ngdc_id> -Rwest/east/south/north -De -Gdepth,topo1.grd  
-gfaa,grav.18.1.img,0.1,1,80.738008628 -Gnav,dist_to_coast_1m_grd.i4
```

The mgd77sniffer reads three 1-minute global grids into memory for each cruise analyzed which can overload systems with limited memory and delay program execution. I avoid this by specifying latitude and longitude extents particular to each cruise using the -R option. The -De option activates E77 errata output. The three -G/g arguments enable depth and gravity comparisons with the specified global grids while the third -G argument activates navigation on land checking. Cruises were examined in lexicographic order between 2008 and the present during which time a variety of global gravity and bathymetry grids were available. I chose an incremental review approach where errata tables were generated and reviewed weekly which allowed me

to upgrade to new global grids and to further develop along-track methods as needed. 50% of errata tables and review plots were generated using the global predictive bathymetry grid of Marks and Smith [2006] while the more recently reviewed half used the 1-minute resolution bathymetry grid by Becker et al. [2009]. Similarly, 24% of errata tables and review plots were generated using the Sandwell and Smith [2005] version 16.1 satellite altimetry-derived global gravity grid after which surveys were reviewed using the version 18.1 gravity grid [Sandwell and Smith, 2009]. All cruises were checked for navigation on land using the 1-minute resolution global distance to coast grid of Wessel and Chandler [2011] which required updating many errata tables that were reviewed prior to the availability of this grid.

Along-track analysis of MGD77 files involves checking every header and data field against physical limits or against limits derived from the data themselves (see Table 4.1). In addition to the error checking methods of Chandler and Wessel [2008] summarized in the introduction, new methods have been introduced to include testing for time zone crossing errors, two-way travel time wrapping effects, as well as testing which gravity formulas may have been used to compute reported free air anomalies. It is important to acknowledge that some valid measurements may be made outside the 99th percentile range. Furthermore, many datasets were collected decades ago and I possess neither the first hand experience nor the acquisition logs to positively assert whether data are valid or not. I therefore employ caution and discretion and flag only obvious outliers and systematic errors.

A sample E77 errata table is shown in Table 4.2. E77 tables consist of an uppermost header line which includes basic MGD77 file information and identifies the version of the MGD77 file analyzed to avoid subsequent merging of incompatible datasets. Following the header line are several commented-out lines reporting when, by whom, command line arguments used, verification status and comments made by the reviewer. Errata files next report detected header errors and results of system-

atic tests, such as regression statistics resulting from depth and free air gravity grid comparisons and regression comparisons between reported and recomputed gravity and magnetic anomalies. These errors are considered global as they pertain to an entire cruise file. Header and systematic messages are led by an error code string, which identifies whether the error should be applied (Y/N/?), whether the message reports an error, warning or information (E/W/I), NGDC cruise identifier and the header record or geophysical field relevant to the message. Each error code string is followed by a brief description of the error. Following these global messages are data warnings, which each report all errors found in an individual record. MGD77 files contain a 24 row header followed by any number of data records. Each data record has a unique time (although on occasion duplicate, decreasing, or no time at all gets reported) along with an array of data codes and geophysical fields. The errata data warnings therefore report errors in a concise manner, allowing many errors to be reported within a given record. The leading field in each error message indicates whether the error is to be applied or not (Y/N/?). As many data warnings are preceded by question marks it is not required that these be toggled to 'Y' or 'N' (however, all E77 header and systematic warnings are required to be toggled to 'Y' or 'N'). For this global review I have chosen to focus on systematic and extreme error correction so many individual data record flags are not applied except in cruises with extreme numbers of obvious outliers. This choice also reflects my desire for corrections to be conservative and, as much as possible, to correct obvious errors. E77 data warnings next report NGDC cruise number, record time and record number, followed by a hyphen-delimited three field error code string. The first error code pertains to navigation errors while the second and third codes pertain to value and gradient warnings, respectively. Following the error code string are brief descriptions of encountered errors. More detailed descriptions of the E77 errata syntax can be found in Wessel and Chandler [2007] and within the Generic Mapping Tools documentation

[Wessel and Smith, 1998].

To decide which errors to apply or reject, a comprehensive review plot is generated for each cruise (see Figure 4.2). These plots show navigation maps and error counts, ship data versus gridded data, reported versus recomputed anomaly regression plots and plots of reported data along-track versus expected values obtained from grids or recomputed anomalies. Information from the MGD77 header is also plotted beneath each regression plot so that MGD77 file processor comments, sampling rates and instrument types can be quickly ascertained. The example E77 file and review plot pertain to a 1970 Hawai'i Institute of Geophysics (HIG) expedition (NGDC id 08040004/survey id 70042204) in the western Pacific aboard the R/V *Mahi*. This example includes many of the marine geophysical data types and illustrates typical issues encountered with the majority of cruises. For instance, the cruise reports high quality navigation with no excessive speeds with just three records found to pass over land. Also typical are the outdated magnetic anomalies which are improved dramatically by recalculation using the latest reference fields (this improvement is clearly illustrated on the review plot). This cruise also reports free air gravity but fails to report the observed gravity measurements and vessel motion (Eötvös) corrections used to generate free air anomalies. This shortcoming is typical of a large number of trackline gravity surveys and unfortunately the omission of the primary gravity measurements impedes our ability to recalculate anomalies. However, this example is intended to illustrate a typical dataset; much more extreme quality issues do exist in the archive.

After choosing which global errors to correct (i.e., after toggling original '?' header error application flags to 'Y' or 'N', the analyst then switches the Errata table verification status flag from 'N' to 'Y' and enters comments and his/her name to facilitate constructive corroboration during future data reviews. The errata table is now said to be reviewed and can be merged with the original data using `mgd77manage` [Wessel

and Chandler, 2007].

4.3 Results

4.3.1 Effects of along-track analysis on global crossovers

I compared the averages of measurement differences at ship track intersections (crossover errors or COE) before and after along-track correction in order to assess the effects of along-track errata tables and to attempt to gauge the overall health of the trackline archive. Large changes in total COE would indicate either highly effective along-track corrections or that the original data quality is suspect, or both. While it is difficult to draw definitive conclusions given such a range of error types, analysis of the averages of discrepancies at ship track crossings enables the abstraction of broad data patterns. More rigorous crossover investigations with error source modeling and crossover corrections are the subject of other investigations as well as future work within this larger quality control project.

As depicted in Figure 4.3, median absolute measurement discrepancies at track intersections decrease for depth, free air gravity and magnetic anomalies as a result of along-track analysis derived corrections. For each histogram, the number of COEs found in each bin is determined and percentages (frequency) are calculated. Bin widths are 10 m for depth, 20 nT for magnetics and 2 mGal for free air gravity. Larger COEs occur less frequently and only the most common percentages are shown. Median depth COEs decrease from 27.3 m to 24.0 m (12.1% reduction), median free air gravity COEs decrease from 6.0 mGal to 4.4 mGal (26.7% reduction), and median magnetic COEs decrease from 81.6 nT to 29.6 nT (63.7% reduction). The numbers of crossovers decrease as well by 6.2%, 11.3%, and 6.8% for depth, free air gravity and magnetic anomalies, respectively. It is difficult to ascertain what causes the reduction in the number of crossovers but the removal of navigation outliers does significantly

affect the perimeters of many cruises, suggesting improvement in navigation as a major cause. Magnetic COE reduction is much more pronounced because of the effect of recalculating anomalies using the latest magnetic reference field [e.g., Quesnel et al., 2009]. This is typically a problem because only preliminary magnetic field models are available while at sea. Furthermore, within the \sim two year window for submitting National Science Foundation-funded data to the archive, magnetic field models rarely mature into definitive models. Figure 4.4 illustrates the dramatic improvement in crossover error magnitudes achieved by simply recomputing magnetic anomalies (for all involved cruises) using the latest reference fields.

4.3.2 E77 errata table review

The mislocation of measurements through bad navigation is perhaps the most insidious error type. These false data may be assimilated by unsuspecting researchers and given equal weight in analyses. One method for identifying navigation outliers is to flag any records with unreasonable velocities. For example, \sim 340,000 out of \sim 72 million velocities in the archive (\sim 0.5%) are found to be in excess of 10 m/s (\sim 20 kts). Approximately half of these errors are from three recent US Coast Guard R/V *Healy* surveys north of the Arctic Circle including cruises 75080002 (HE703), 75080004 (HE405) and 75080007 (HE302). 1,196 cruises (23%) contain speeds in excess of 10 m/s, making this error type one of the most common. The problem occurred fairly often when navigation systems lacked sufficient satellites or stations to maintain consistent vessel location. Extreme cases of this problem have speeds upward of 10,000,000 m/s [Chandler and Wessel, 2008], producing globe spanning ship tracks that impede the utilization of these data.

A prevalent concern relates to the omission of total field gravity measurements. For instance, only 753 gravity surveys report observed gravity measurements while the rest report free air anomalies. Processing errors or outdated gravity formulas are

clearly more difficult to correct without original measurements. According to NGDC's MGD77 format specification [Hittleman et al., 1977], the two most prevalent cases ought to be (a) cruises reporting observed gravity and free air anomalies with the implication that Eötvös corrections *are* included in observed gravity values or (b) cruises reporting observed gravity, Eötvös corrections and free air anomalies where it is implied that Eötvös corrections are *not* accounted for in the observed gravity field. I find, however, that only 183 gravity surveys report observed and free air gravity without Eötvös corrections (case "a") while 504 surveys report observed, Eötvös and free air gravity (case "b"). The clear majority (1,113 surveys) report only free air anomalies, which are presumably corrected for Eötvös effects. However, this problem is mitigated to some extent by relatively minute differences in gravity formulas. Nevertheless, systematic differences of ~ 10 mGal are common for gravity anomalies computed using the International 1930 formula versus International 1967 or 1980, for example [e.g., Jones, 1999].

The omission of total field magnetic measurements is much more severe, however, due to the geomagnetic field's continual and nonlinear secular drift. If an archived magnetic survey lacks total field data, there is a strong possibility that the anomalies will eventually become invalid. Fortunately, only 183 magnetic surveys suffer from this dilemma. Of these, all but 10 were reported by the Japan Hydrographic Department and University of Tokyo. However, Japan Hydrographic Department MGD77 headers indicate the use of a magnetic observatory to account for magnetic variations. This may or may not ensure the relevance of these data depending on how well observatory and survey area conditions correlate. Inspection of anomalies plotted along-track did not suggest contamination by secular drift. However, University of Tokyo MGD77 headers exhibit no magnetic processing comments. Anomaly plots contain long period fluctuations similar to secular drift, although this could also be due to slow-varying seafloor magnetic properties. Also related to magnetic measurements, the diurnal

correction field may be the least utilized with only 24 NGDC data sets containing this field. The geomagnetic field is known to vary within hours, which geomagnetic reference field models generally fail to account for [e.g., Macmillan and Finlay, 2011]. Diurnal variations may be derived from nearby magnetic observatories or computed using comprehensive geomagnetic models such as CM4 [e.g., Sabaka et al., 2004].

Of the 2,471 magnetic tracks, 183 do not report total field data and three joint USGS–WHOI cruises (06780034 (FRNL87-1), 06780035 (FRNL87-2) and 06780038 (FRNL87-5)) stored geomagnetic reference field values rather than magnetic measurements in the total field data column and therefore may not be recomputed. 2,207 errata tables flag magnetic anomalies to be recalculated, making this the most pervasive error type in the archive, affecting $\sim 96\%$ of magnetic anomalies. $\sim 97\%$ of anomalies appear to be suspect including anomalies flagged for recalculation as well as the 24 University of Tokyo surveys possibly affected by secular drift. It is therefore imperative that any magnetic analysis involve anomaly recalculation.

Comparing ship and grid depths yielded 300 flagged offsets exceeding 100,000 m*km each. This non-intuitive unit is best thought of as the area between ship and grid profiles where depths are reported in meters and distances along-track in km. In this case, these offsets are exceeding $1e^8 m^2$, thereby indicating a prevalence of extended loss of bottom tracking or instrument malfunction. 87 ship–grid free air gravity offsets exceeding 50,000 mGal*km ($5e^7 mGal*m$) were also flagged. By examining all ship depths with their predicted bathymetry grid counterparts using regression analysis, I was able to locate 10 depth surveys reported in fathoms rather than meters. These include NOAA cruise 03050023 (POL7106), US Navy cruises 09100014 (KEA08-68) and 09350001 (WW79AL), University of Texas Institute for Geophysics cruise 10020021 (IG2408), Scripps cruise 15020038 (GECS0EMV), UK cruises 19100005 (DI73L1-2) and 19100009 (DI91), NIMA cruise 35120001 (10381), and Orstom New Caledonia cruises 84010001 (COR300) and 84010004 (ZOE100). I

scale these data by 1.8288 (the meters to fathoms ratio). Lamont cruise 01100001 (MMW02) was found to have been erroneously scaled by 1.8288; I scale these data by 0.5468. I further found that USGS cruise 06110022 (S478NC) and Scripps cruise 15020044 (HYPO-1MV) reported depth data scaled by 0.1; I scale these data by a factor of 10. HIGP cruise 08010078 (76010303) apparently reported two-way travel time in milliseconds in the depth field (i.e., cruise “KK078” reported by Smith [1993]); I scale these data by 1.333, the ratio of milliseconds of two-way travel time to depth in meters [Smith, 1993]. Likewise, ship-grid gravity regression tests found 13 gravity data sets scaled by 10. These include UK cruises 19050002 (SHACK375), 19050003 (SHACK475), 19050004 (SHACK376), 19050005 (SHACK676), 19050006 (SHACK877), 19050007 (SHA679L1), 19050008 (SHA679L2), 19110001 (STA179A), 19110002 (STA179B), 19120001 (FAR281L1), 19120002 (FAR281L2), 19120003 (FAR381), and 19120004 (FAR481). I scale by 0.1 to correct these data. Five gravity cruises submitted by the US Geological Survey were found to have been scaled by 0.1 which I scale by 10 to correct (cruises 06050010 (L476WG), 06050017 (L676AR), 06050024 (L678AR), 06050057 (L977AR), and 06050061 (L777WG)).

Whereas Chandler and Wessel [2008] found 3,994 bathymetric, 1,516 magnetic, and 243 gravity surveys reporting values with integer precision, this analysis finds 2,414, 1,862, and 365, respectively. The Chandler and Wessel [2008] analysis may have overestimated the number of bathymetric surveys reporting integer precision. I find 98 depth, 211 magnetic, and 16 gravity surveys reporting values in integer multiples of 5 where Chandler and Wessel [2008] found 79, 213, and 12, respectively. This truncation is unnecessary as the MGD77 format specifies `%.1f` precision (i.e., one decimal place to the right of the decimal) for most geophysical fields. In areas of low geophysical relief, the truncation of precision may cause significant data quality degradation.

Table 4.3 lists 109 trackline surveys that contain errors that I could not cor-

rect using along-track analysis. This list of erroneous surveys includes 63 gravity, 31 depth, and 12 magnetic legs. Uncorrectable gravity errors include anomaly sign errors, reporting only zero magnitude anomalies, bad *Eötvös* corrections, and poor correlation with satellite derived gravity. Depth errors include extremely poor correlation between reported and predicted bathymetry, extreme numbers of outliers, inadequate measurement precision, and instrument malfunction. For magnetics, these errors include unreasonable anomalies with no total field measurements for anomaly recalculation, reporting only zero magnitude anomalies, and completely mislocated navigation.

There remain additional errors that are unique to individual agencies and that are often impossible to repair automatically. For instance, 39 out of 59 gravity surveys submitted by the National Oceanic and Atmospheric Administration (NOAA) contain only negative gravity anomalies. The erroneous portion of one of these surveys (03000001 (DIATTRAV)) was flagged as bad while the other 38 cruises were flagged as entirely invalid and are the NOAA legs (beginning with '03') shown in the left column of Table 4.3. The signs of positive anomalies were reversed so that these anomalies were erroneously reported as negative. This error is obvious when compared to the global gravity grid. Perhaps NOAA is best equipped to resubmit corrected data from their original records. Fortunately for four surveys by Lamont–Doherty Earth Observatory (01010206 (RC2214), 01010207 (RC2215), 01010210 (RC2218) and 01030340 (V1401)), one by University of Texas (10050027 (FM1801)), and one by the Minerals Management Service (60000029 (LSAL6769)), time errors introduced by failing to maintain consistent UTC time while passing over time zone boundaries (i.e., the time zone adjustment changes by one hour but the clock is not changed to compensate) were handled in E77 errata tables. Code for this check was eagerly developed in anticipation of more than just six affected surveys. Although these are relatively trivial errors, the University of Texas survey was found to have 3,450 records having an

erroneous nine hour shift upon crossing a time zone boundary. Not taking this into account could hamper future attempts to accurately apply magnetic diurnal corrections for this leg, for example. I am also able to report the number of cruises suffering from two-way travel time digitization errors (the Precision Depth Recorder wrap-around effects first encountered by Smith [1993]). All of the 46 cruises exhibiting this error were submitted by the Scripps Institute of Oceanography (see Table 4.4). This error typically involves two-way travel time measurements reporting accurate values until reaching 10 seconds (i.e., $\sim 7,500$ meters depth) when values abruptly shift up to 0 seconds. Any measurements beyond 10 seconds are relative to the sea surface rather than the 10 second mark; travel times wrap back once measurements recross the 10 second limit. These errors are now automatically corrected rather than the omittance approach recommended by Smith [1993].

4.4 Discussion

There are no prior studies for directly comparing the effectiveness of these errata tables. I therefore compare along-track error reductions to those attained through crossover error analysis. Wessel and Watts [1988] reported a 38% reduction in marine gravity COE standard deviation from 22.43 mGal to 13.96 mGal for the $\sim 63,000$ crossovers and 834 tracks analyzed. In contrast, my study of 1,798 tracks (537,246 COEs) finds a 34% reduction in COE standard deviation from 44.87 mGal to 29.69 mGal. Whereas the Wessel and Watts [1988] analysis vertically adjusted all but 72 of these tracks and additionally scaled 146 tracks to account for gravimeter drift [e.g., Dehlinger, 1978], my methods provide a comparable data quality improvement while scaling only 18 tracks by 10 or 0.1, removing constant gravity offsets from 15 surveys (Table 4.5) and by disregarding 63 tracks (Table 4.3) as containing erroneous data. Note that these COE values are reduced simply by applying along-track corrections;

no further modeling of systematic COE was done.

The bathymetry quality assessment by Smith [1993] included 2,253 cruises and 329,058 crossovers but focused on error modeling without an error removal component. The Smith [1993] study reported that median depth crossover errors had remained a constant 26 m since the late 1970s and that 95% of cruises had *internal* crossover error standard deviations less than 500 m. The study did not determine a global average of depth COE standard deviations. This study, therefore, reports the first estimate of depth COE standard deviation (1,285.4 m), based on 2,332,048 crossovers. I report a 37.5% decrease in depth standard deviation to 803.14 m using along-track correction methods. Although crossover error source modeling is beyond the scope of this study, these apparently excessive standard deviation magnitudes may result from the tendency of topographic data to be much rougher than potential field data such as gravity and magnetics. I further note that median COE for uncorrected NGDC depth data has increased from 26 m [Smith, 1993] to 27.3 m since 1992, which is unexpected given the considerable improvements to navigation and data acquisition systems during this time.

Quesnel et al. [2009] reported an initial standard deviation for uncorrected magnetic anomaly COEs of 179.6 nT based on analysis of $\sim 427,000$ crossovers. In contrast, my analysis of 494,814 magnetic COEs results in an uncorrected standard deviation of three times this amount, at 567.38 nT. Through their cleaning and anomaly recalculation process, Quesnel et al. [2009] were able to reduce COE standard deviation to 103.9 nT (this study finds improvement in COE standard deviation to 138.6 nT). While the cause of the differences in unprocessed standard deviations between the two studies is unknown, my anomaly recalculation process is likely limited by not correcting for diurnal variation of the geomagnetic field. Incorporation of recent geomagnetic field models, such as the comprehensive model of Sabaka et al. [2004]), which was used in the Quesnel et al. [2009] study, will likely induce a comparable

magnetic COE standard deviation improvement in the along-track method.

Figures 4.5, 4.6 and 4.7 illustrate the distribution of median crossover errors before and after along-track analysis for free air gravity anomalies, depths and magnetic anomalies, respectively. Reductions in median gravity COEs (Figure 4.5) are seen off many high latitude coasts including Kamchatka, Greenland and Antarctica as well as in the sparsely surveyed South Pacific. The pattern of larger magnitude bathymetry COEs over ridges and the sparsely surveyed South Pacific reported by Smith [1993] is apparent in Figure 4.6. Median COE reductions are seen in Figure 4.6 (bottom) in all regions aside from the Arctic where extreme median COEs are seen before and after along-track analysis. These errors are likely related to the three recent *Healy* surveys which could contain erroneous measurements or be poorly located with respect to other surveys in the vicinity; further processing by the source institution is likely required. Figure 4.7 illustrates the dramatic reduction in median magnetic COE achieved through along-track analysis and through recomputing magnetic anomalies using the latest reference fields, in particular.

Many of the errors detected using along-track analysis are not resolvable using crossover methods. Scaling by factors of 0.1 or 10, identifying local offsets from grids, outlier detection, navigation checking, and others are difficult to completely account for in many applications in geophysics, including crossover analysis. Crossover analysis is particularly useful for line-leveling potential field data and for identifying and correcting instrument drift. As along-track analysis do not rely on other tracks and because it identifies and removes obvious errors that hinder crossover studies, along-track analysis should be added to the data processing stream prior to crossover adjustment. Removal of extreme errors should also be performed in general prior to resampling, filtering or gridding geophysical data.

E77 errata tables are available via FTP and for users interested in contributing or maintaining current versions via CVS. In addition, I am hoping to see these

quality control methods and errata tables implemented at NGDC to maximize their availability.

This analysis does not claim to have removed every error from the trackline archive. Indeed, as indicated by median along-track corrected crossover errors, differences remain among different data sets. This conservative approach leaves the majority of outliers untouched due to the ambiguity and increased review time involved in such a review. Furthermore, scientists routinely apply filters to gravity and magnetic anomalies to remove such artifacts prior to their use. In the case of bathymetric data, a study by Sandwell [2011] focused on removing all questionable depth measurements using interactive graphical software. The flags generated by their thorough review will be incorporated into these E77 errata tables to ensure the propagation of their considerable effort.

These first generation errata tables achieve substantial data quality improvement and I encourage their further review and modification by the scientific community at large. I especially encourage incorporation of correction flags derived from studies inspecting shipboard data versus time or distance along track. Data source institutions may also choose to take advantage of these along-track tools and to generate or modify errata tables rather than following the traditional route where updated MGD77 versions are resubmitted to NGDC. Multiple versions of original data sets are occasionally archived under different names and with different geophysical fields, leading to confusion for users. While I certainly do not object to the resubmittal of revised data sets, I suggest the errata-based approach as an efficient and better documented alternative. By incorporating our collective processing efforts into these errata tables, I hope to eliminate processing redundancy and to increase the utility of these valuable data.

4.5 Conclusion

I have initiated an errata-based along-track error correction system for marine geophysical trackline data and compared its performance against prior crossover trackline quality assessments. The along-track methods produce substantial error reduction based on global crossover standard deviations computed before and after along-track correction. Based on the marine geophysical surveys analyzed, I find a strong tendency among source institutions to omit total field gravity measurements and to submit data sets without first removing all navigation and geophysical outliers. I find that 95% of magnetic anomaly data sets require recalculation using the latest reference fields. The tendency to submit preliminary and on occasion unprocessed or erroneous data places a burden on the scientific community, which has resulted in data processing redundancy among data users. The 5,203 errata tables generated in this research serve to mitigate this redundancy and to improve the utility of the world's largest collection of marine geophysical data.

Table 4.1: Along-track analysis outlier thresholds from Chandler and Wessel [2008]. Error checking thresholds for data values and gradients were calibrated using the 99th percentile or known physical limits when available.

Abbrev	Min	Max	maxSlope	maxArea
lat	-90°	90°	–	–
lon	-180°	180°	–	–
twt	0 s	15 s	1 s	–
depth	0 m	11000 m	1000 m	100000 m*km
mtf1	19000 nT	72000 nT	200 nT	–
mtf2	19000 nT	72000 nT	200 nT	–
mag	-1000 nT	1000 nT	200 nT	–
diur	-100 nT	100 nT	20 nT	–
gobs	977600 mGal	983800 mGal	100 mGal	–
eot	-150 mGal	150 mGal	100 mGal	–
faa	-400 mGal	550 mGal	100 mGal	50000 mGal*km

Table 4.2: Sample E77 errata table for HIG cruise 08040004.

```

# Cruise 08040004 ID 70042204 MGD77 FILE VERSION: 19830518 N_RECS: 10686
# Examined: Mon Nov 23 15:26:42 2009 by mtchndl
# Arguments: -R139.45/196.75/-0.55/13.5 -De -Gdepth,/data/GRIDS/S2004_hdr.i2
# -gfaa,/data/GRIDS/grav.18.1.img,0.1,1,80.738008628 -Gnav,/data/GRIDS/dist_to_coast_1m_grd.i4
Y Errata table verification status
# mgd77manage applies corrections if the errata table is verified (toggle 'N' above to 'Y' after review)
# For instructions on E77 format and usage, see http://gmt.soest.hawaii.edu/mgd77/errata.php
# Verified by: M. T. Chandler
# Comments: Recommend recomputing magnetic anomalies - low sample rate.
# Errata: Header
Y-W-08040004-H13-10: Survey year (1970) outside magnetic reference field Unused time range (9999-9999)
Y-E-08040004-H15-01: Invalid Gravity Departure Base Station Value: (0000000) [      ]
Y-E-08040004-H15-03: Invalid Gravity Arrival Base Station Value: (0000000) [      ]
Y-E-08040004-H16-01: Invalid Number of Ten Degree Identifiers: (10) [12]
Y-W-08040004-H16-06: Ten Degree Identifier 3015 not marked in header but block was crossed
Y-W-08040004-H16-06: Ten Degree Identifier 3016 not marked in header but block was crossed
Y-W-08040004-nav-00: Flagged 0.03 % of records with bad navigation
Y-I-08040004-depth-01: RLS m: 1.00 b: 0 rms: 23.30 r: 1.00 sig: 1 dec: 0
Y-I-08040004-faa-01: RLS m: 0.987195 b: -0.79 rms: 8.25 r: 1.00 sig: 1 dec: 1
N-E-08040004-faa-02: Regression slope 0.99 different from 1. Recommended: [1]
Y-E-08040004-mag-07: Anomaly differs from mtf1-IGRF (m: 1.0 b: -184.4 rms: 187.8 r: 0.9 sig: 1 dec: 0). [Recompute]
Y-W-08040004-twt-11: More recent bathymetry correction table available
Y-W-08040004-mtf1-12: Integer precision
Y-W-08040004-mag-12: Integer precision
Y-W-08040004-faa-12: Integer precision
# Errata: Data
? 08040004 1970-10-07T08:46:00.00 3609 0-Q-0 VAL: mag invalid
? 08040004 1970-10-07T08:49:00.00 3610 0-Q-0 VAL: mag invalid
? 08040004 1970-10-07T08:52:00.00 3612 0-Q-0 VAL: mag invalid
? 08040004 1970-10-13T21:14:48.00 5746 0-0-KL GRAD: twt, depth excessive
? 08040004 1970-10-14T21:20:00.00 5994 0-0-OQ GRAD: mtf1, mag excessive
Y 08040004 1970-10-31T20:08:36.00 10682 D-0-0 NAV: on land
Y 08040004 1970-10-31T20:11:48.00 10683 D-0-0 NAV: on land
Y 08040004 1970-10-31T20:13:11.94 10684 D-0-0 NAV: on land

```

Table 4.3: Trackline surveys flagged as invalid in this study.

Free Air Gravity		Corrected Depth		Magnetic Anomaly	
NGDC ID	Survey ID	NGDC ID	Survey ID	NGDC ID	Survey ID
01030237	V3606	01150005	E3D78	02340002	AG044L01
03010003	CMAPPI2A	05990003	VO8806	09030010	SI343619
03010004	CMAPPI3N	06050064	L483BS	09030026	SI932005
03010005	CMAPPI3S	06050065	L583HW	09030049	SI343912
03010006	CMAPPI4S	06050076	L984CP	71010001	RSA72-2
03010007	CMAPPI5A	06050078	L1182CS	71010002	RSA73-1
03010008	CMAPPI5B	06050098	L182NC	71010003	RSA73-2
03010009	CMAPPI5C	06050114	L485WF	71010004	RSA75-1
03010010	CMAPPI5D	06120004	K183AR	71020006	TBD375
03010011	CMAPPI6E	06120009	K176AR	J1010055	HT91T260
03010012	CMAPPI6W	06120012	K177AR	J1010068	HT93T294
03010013	CMAPPI7W	06120015	K180AR	J1010081	HT94T332
03010014	CMAPPI7E	06120019	K382AR		
03020001	POL6202	06910014	P385CB		
03020007	CMAPSU1A	06910021	P1085VI		
03020008	CMAPSU2A	06910022	P1185VI		
03020009	CMAPSU3N	06910023	P1285AG		
03020010	CMAPSU3S	08050029	KI81-2		
03020011	CMAPSU4N	10020023	IG0701		
03020012	CMAPSU4S	15340006	KN138L07		
03020013	CMAPSU5A	19180025	CD7793		
03020014	CMAPSU5B	19370007	20000167		
03020016	CMAPSU5D	19550005	19930092		
03020017	CMAPSU6E	20010014	TT-208		
03020020	CMAPSU7W	29030001	PEGASVII		
03020022	CONMALAS	35140001	02580		
03020024	CONMOREW	58030007	TYDE88 ₅		
03020027	CONMCALF	67010039	73000711		
03030001	DICPVERD	71020006	TBD375		
03030002	DIATLNFZ	88010014	NBP95-6		
03030004	DILANTLS	JA010029	JARE33L4		
03030006	BOMEXDI				
03030015	TAG70				
03040053	POL7004				
03040056	POL7108				
03040057	POL7201				
03040062	OCPANAFZ				
03100002	RAIN394				
06010002	U271GM				
06010003	U371CB				
06010004	U471CB				
06010005	U571AF				
06010006	U671AT				
06050070	L384SP				
06050082	L174SC				
06350004	T274EG				
09030010	SI343619				
09030026	SI932005				
09030045	SI343608				
09030049	SI343912				
12090002	PZGSCXUS				
15040130	MRTN08WT				
15040131	MRTN09WT				
15040160	PPTU01WT				
16030002	HY4-891				
19510009	EGRHECA1				
29030001	PEGASVII				
60000029	LSAL6769				
67010154	85005811				
67010155	85006911				
84010015	EV1300				
88010012	NBP95-4				
J1010061	HT92T273				

Table 4.4: List of surveys submitted by Scripps containing two-way travel time wrap-around errors.

NGDC ID	Survey ID	Survey Year
15010025	LUSI01AR	1962
15010039	MONS01AR	1960
15010052	NOVA05AR	1967
15010053	NOVA06AR	1967
15010055	NOVA08AR	1967
15010056	NOVA09AR	1967
15010060	SCAN03AR	1969
15010062	SCAN05AR	1969
15010073	ZTES2BAR	1966
15010074	ZTES03AR	1966
15010075	ZTES04AR	1966
15010076	ZTES4BAR	1966
15010077	ZTES05AR	1966
15020003	ANTP03MV	1970
15020010	ANTP13MV	1971
15020011	ANTP14MV	1971
15020031	FDRK03MV	1975
15020036	GECS-CMV	1973
15020037	GECS-DMV	1973
15040006	ARES05WT	1971
15040008	ARES07WT	1971
15040010	ERDC02WT	1974
15040015	ERDC07WT	1975
15040017	ERDC09WT	1975
15040043	SOTW03WT	1972
15040044	SOTW04WT	1972
15040049	SOTW09WT	1972
15040055	TSDY03WT	1973
15040059	TSDY07WT	1973
15040060	TSDY08WT	1973
15050017	DSDP19GC	1971
15050018	DSDP20GC	1971
15050019	DSDP21GC	1971
15050028	DSDP30GC	1973
15050043	DSD44AGC	1975
15060009	DNWB-CBD	1957
15060015	JPYN04BD	1961
15080025	NOVA05HO	1967
15080026	NOVA06HO	1967
15100010	STYX09AZ	1968
15150001	HUNT01HT	1969
15150002	HUNT02HT	1969
15150003	HUNT03HT	1969
15180001	SILS01BT	1969
15180002	SILS02BT	1969
15180003	SILS03BT	1969

Table 4.5: These cruises were unresolvable through the usual method for recalculating marine gravity anomalies (i.e., free air anomaly = observed gravity – normal gravity [+ *Eötvös* correction]). To utilize these valuable data, errata tables report correction constants that are added to each survey to account for the apparent failure to properly tie-in gravity measurements at gravity base stations before and after each of these survey. RLS offset is a robust estimate of the systematic difference between shipboard and satellite altimetry-derived gravity (i.e., the best fit y-intercept computed via re-weighted least squares regression of ship and satellite gravity [Chandler and Wessel, 2008]).

NGDC ID	Survey ID	RLS Offset (mGal)	Correction (mGal)
06050075	L884SP	-990.7	990.0
67010135	84001311	348.3	-350.0
88010008	NBP9604	-224.3	220.0
JA010015	JARE30G3	-88.3	88.0
19120005	FARN0687	64.8	-65.0
06780046	FARN0787	61.6	-61.6
19120006	FARN0887	61.4	-61.0
88010010	NBP95-2	53.7	-50.0
88010046	NBP00-2	-49.2	50.0
88010038	NBP96-2	43.7	-40.0
67010200	88003311	-40.0	40.0
67010199	88003211	-38.0	40.0
88010048	NBP00-4	-31.2	30.0
JA010018	JARE30G6	-26.6	26.0
88010029	NBP96-5	22.8	-20.0

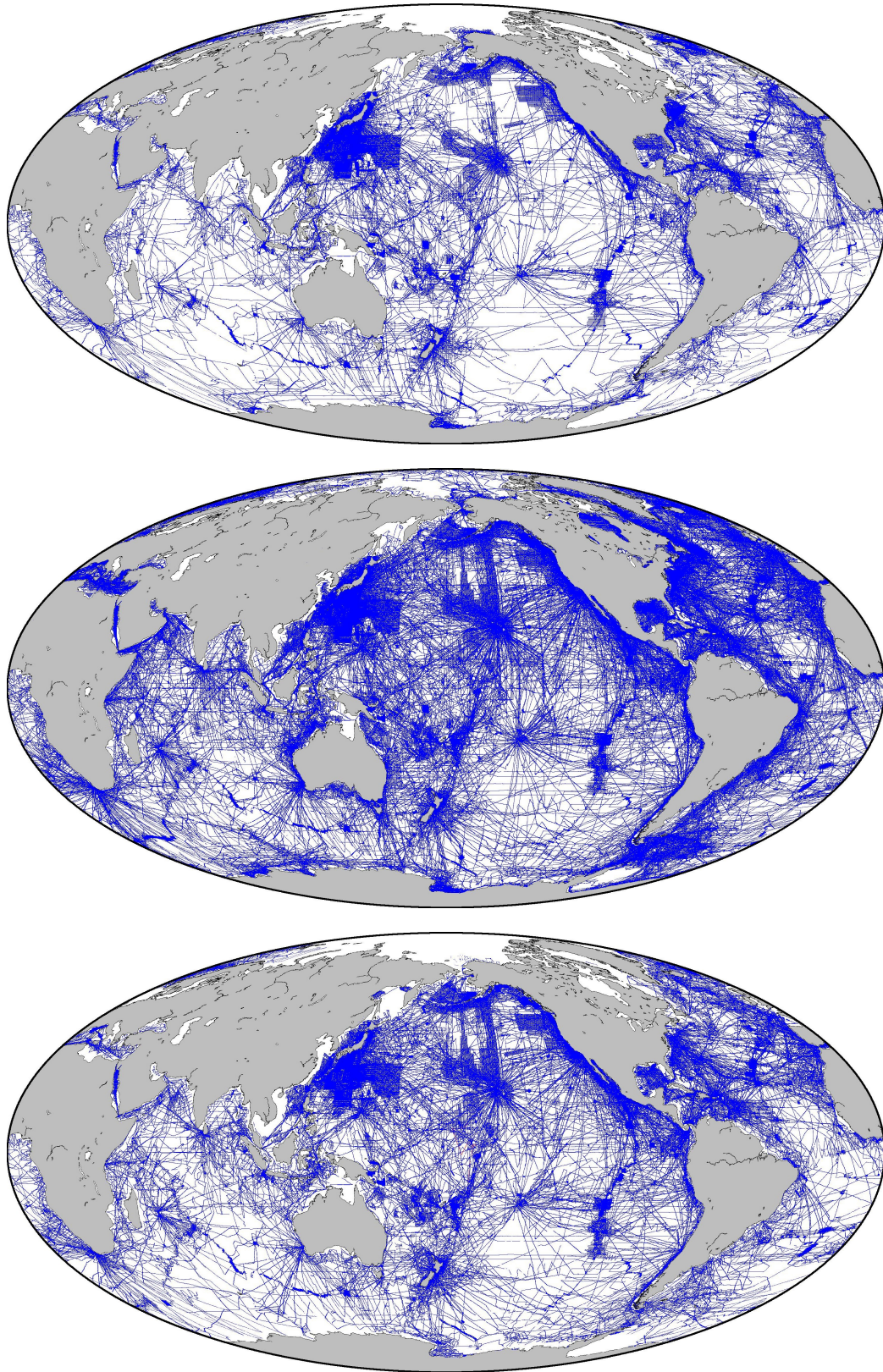


Figure 4.1: Distribution of archived free air gravity (top), bathymetry (middle) and magnetic anomaly (bottom) tracks at NGDC. Blue tracks have passed along-track analysis and overlay original raw tracks plotted in red.

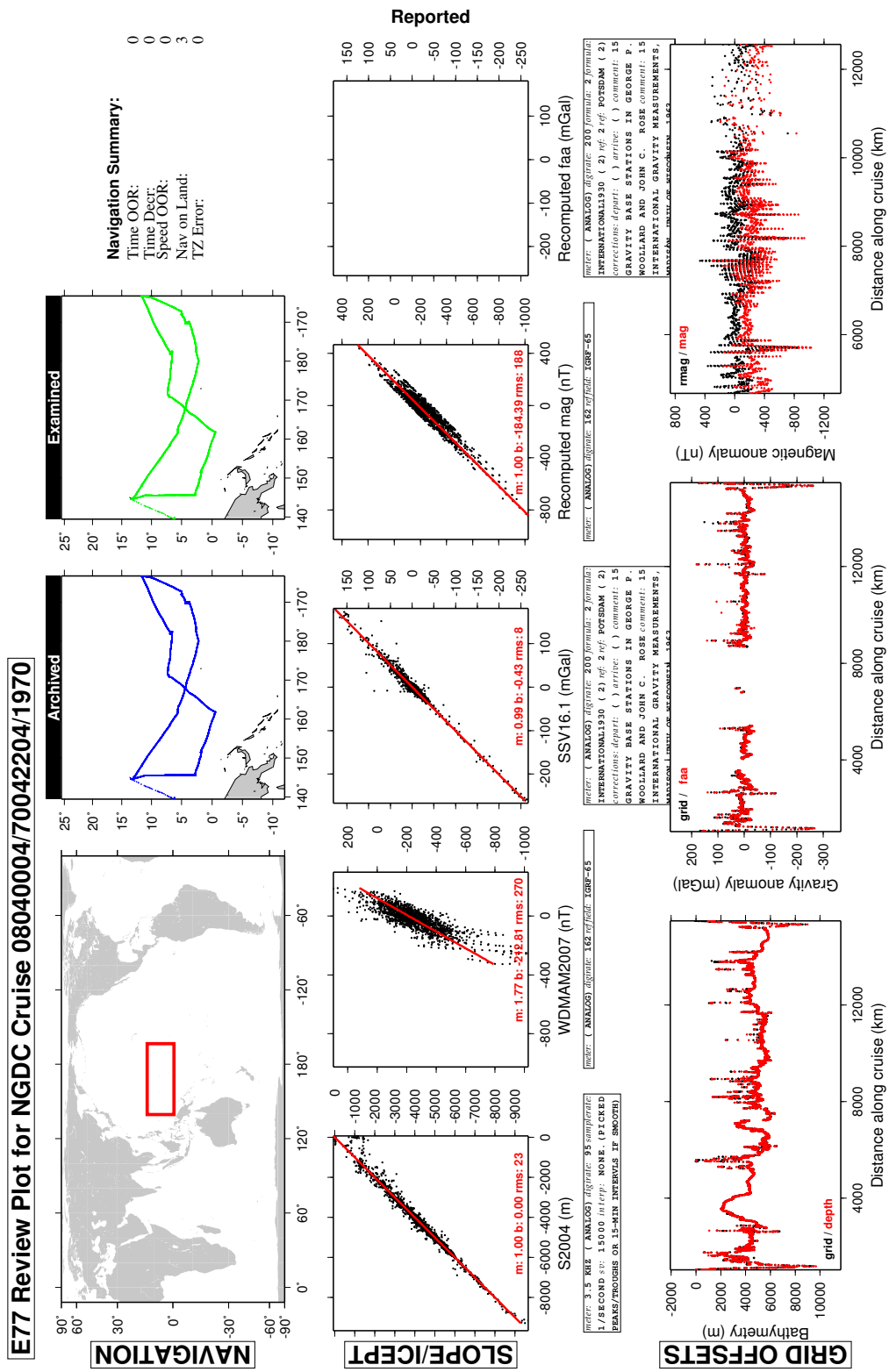


Figure 4.2: Sample E77 review plot for HIG cruise 08040004.

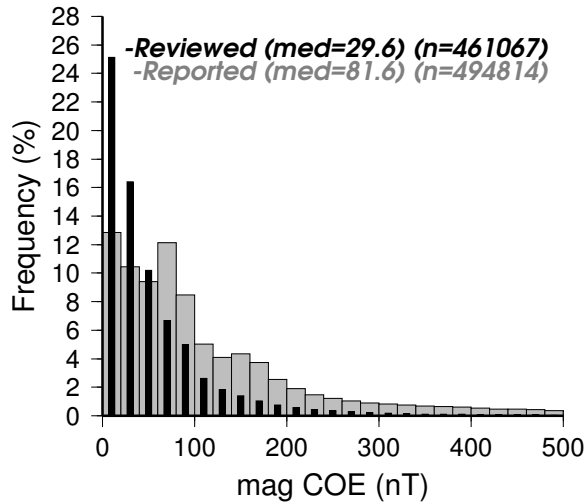
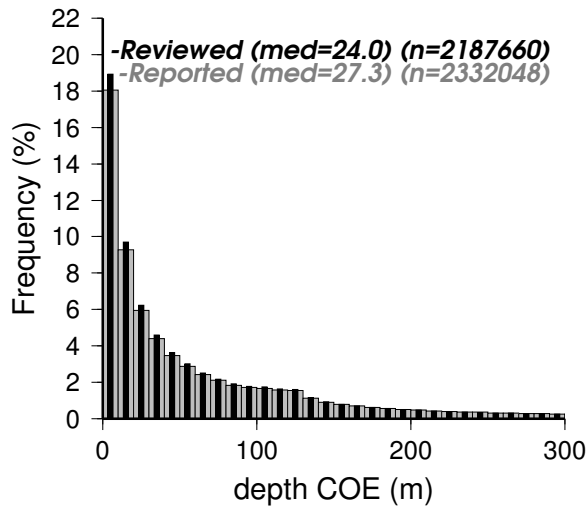
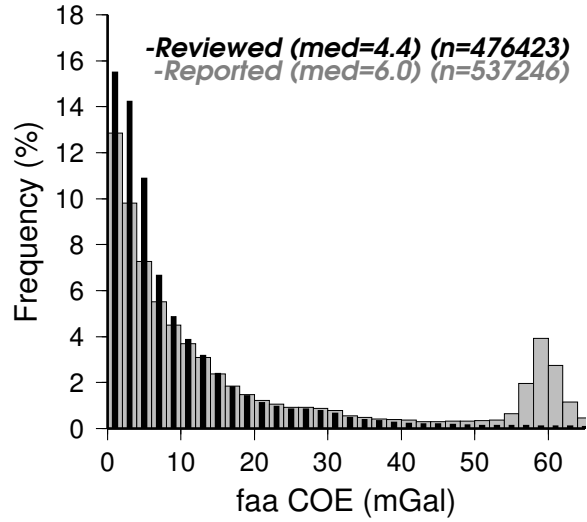


Figure 4.3: Depth, free air gravity, and magnetic anomaly COE histograms before (gray bins) and after (black bins) along-track analysis. The cluster of gray bins near 60 mGal pertains to R/V *Farnella* surveys FARN0687, FARN0787 and FARN0887 listed in Table 4.5.

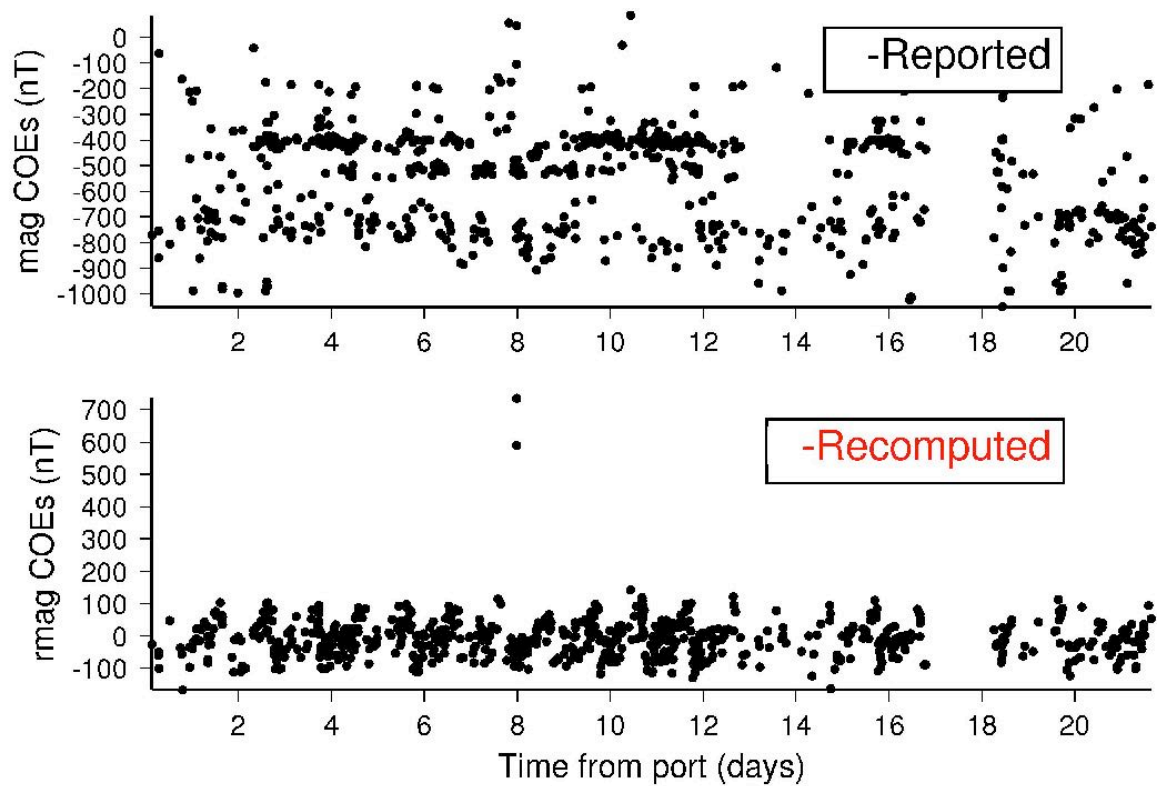


Figure 4.4: Effects of magnetic anomaly recalculations on crossover errors are illustrated by comparing French cruise 67010067 (survey id 77005012) measurements at all intersections before and after calculation of all anomalies.

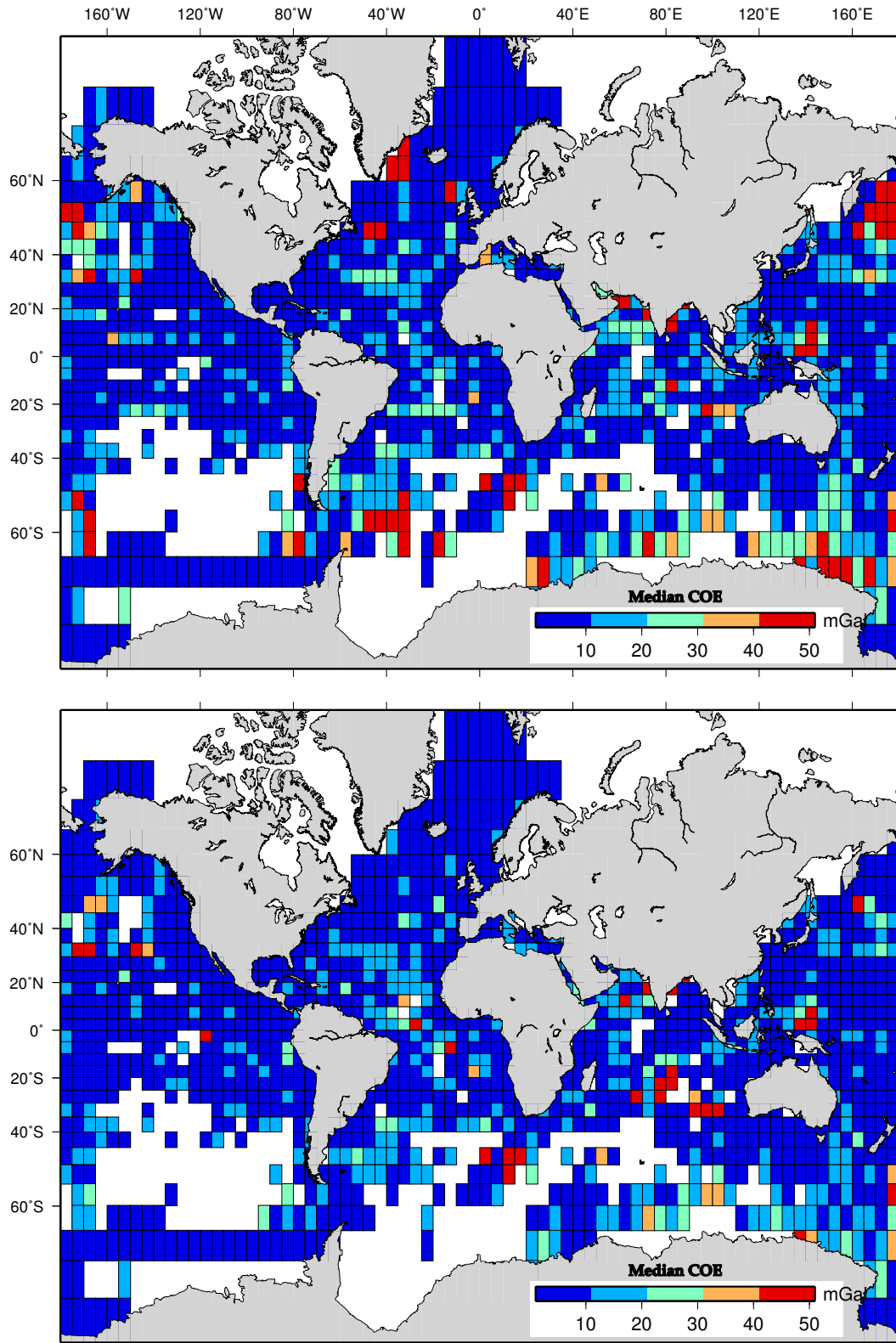


Figure 4.5: Distribution of median free air gravity COEs before (top) and after (bottom) along-track analysis.

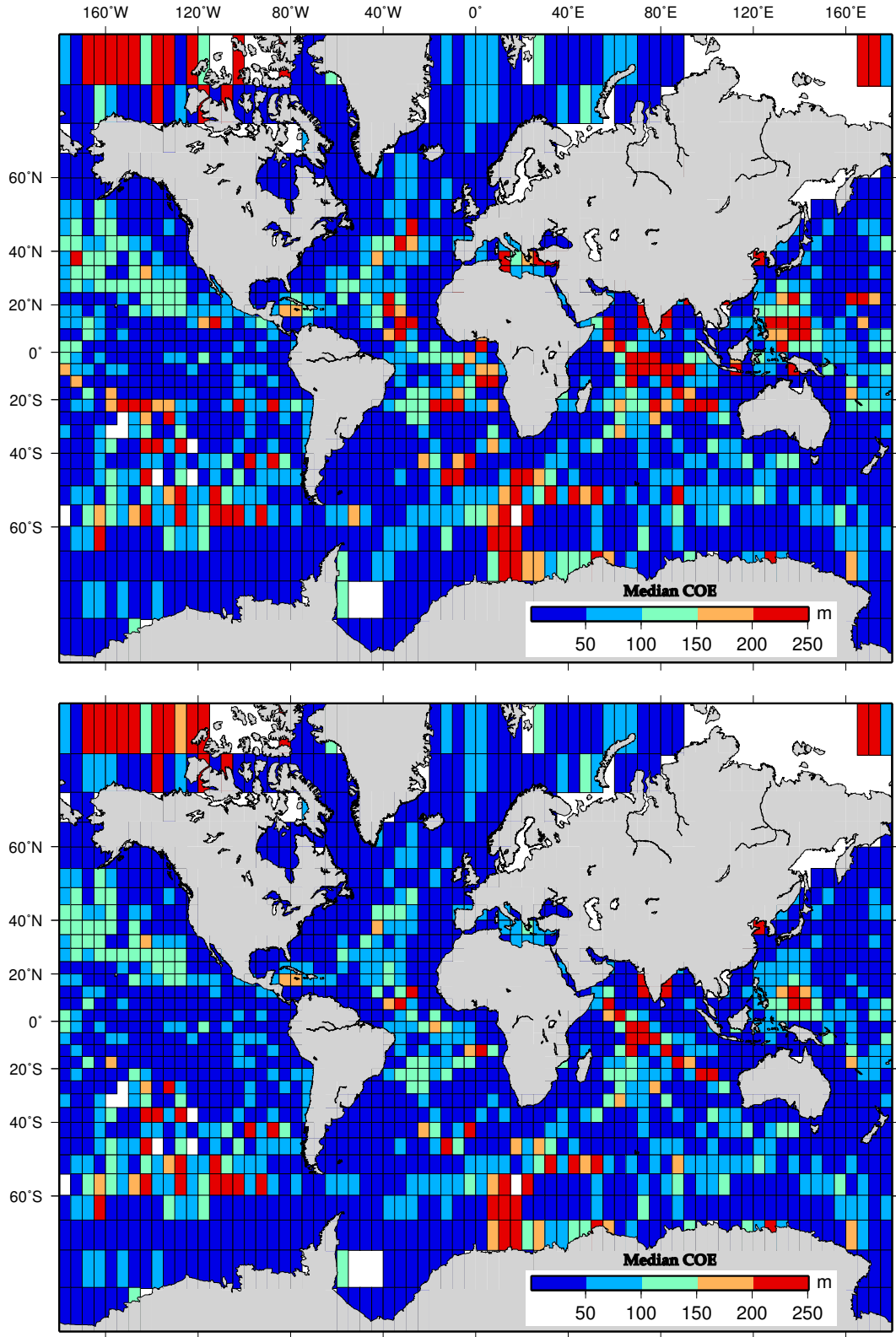


Figure 4.6: Distribution of median depth COEs before (top) and after (bottom) along-track analysis.

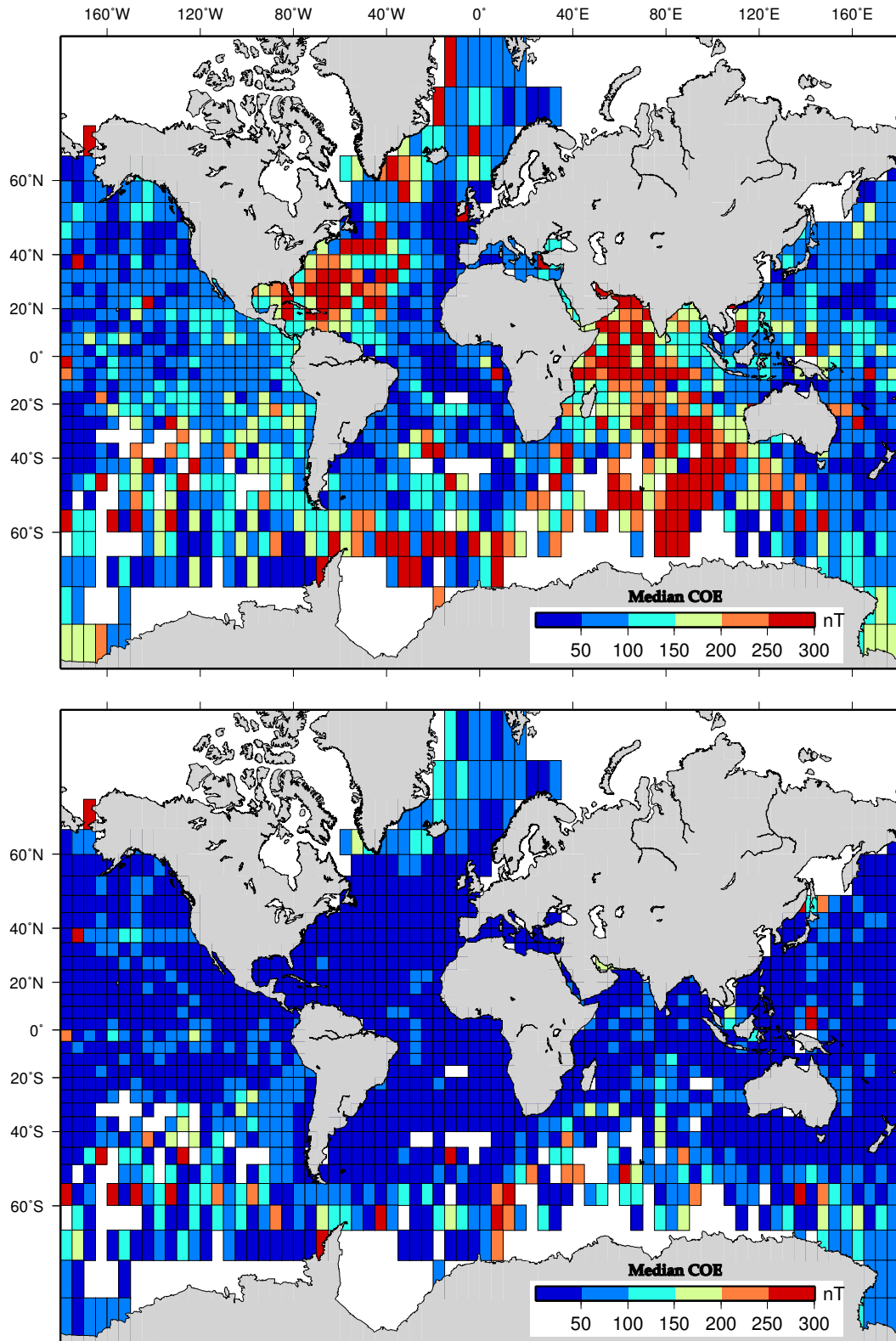


Figure 4.7: Distribution of median magnetic anomaly COEs before (top) and after (bottom) along-track analysis.

Chapter 5

Conclusions

5.1 Pacific absolute plate motion

The three APM comparison presented in Chapter 2 illustrates that no currently available APM can fit all the hotspot trails and simultaneously explain the paleolatitude anomalies. The Africa-based OMS-05 APM projected via a global plate circuit to the Pacific plate fails to predict the Louisville seamount chain using a fixed-Louisville location. Although this predicted chain would show better agreement to the observed chain given a suitable plume drift history, Louisville paleolatitudes obtained during IODP Leg 330 do not support such a drift history. Furthermore, the WK08-A APM models the Emperor chain as a result of more northerly Pacific plate motion from ~ 50 – 80 Ma whereas Emperor paleolatitude evidence opposes this interpretation.

Based on this research, neither OMS-05 nor WK08-A APMs satisfy the geophysical evidence. Of the three APMs considered, the evidence favors the hybrid WK08-D APM developed for this research, which is based on fixed Pacific hotspots with the exception that southward Hawaiian plume drift during the Emperor stage is allowed. Preliminary paleolatitude constraints from the IODP Leg 330 Louisville drilling expedition indicate little, if any, latitudinal motion of the Louisville plume since ~ 70 Ma. These findings further support the WK08-D APM and do not support the Louisville plume history required by the OMS-05 APM.

5.2 Hotspot drift

Hawaiian plume drift during the Emperor stage was alluded to by the anomalous paleolatitude of Suiko at 27°N [Kono, 1980], and it has been apparent since paleo-

latitudes of $\sim 36^\circ\text{N}$ and 27°N were measured at Detroit and Suiko seamounts. More evidence was collected by ODP Leg 197, which was dedicated to the investigation of Hawaiian plume drift [Tarduno et al., 2003]. Tarduno et al. [2009] considered both mantle convection and plume-ridge interaction as drivers of plume drift. Tarduno et al. [2009] favored a scenario in which the Hawaiian plume was captured by the migrating Pacific-Kula spreading system until ~ 80 Ma, when the plume began drifting south until stabilization at ~ 47 Ma.

In the Louisville plume case, although preliminary ODP Leg 330 results indicate little to no Louisville plume drift in the last ~ 70 Ma [Gee et al., 2011], a similar ridge interaction scenario is possible around the time of OJN formation. For example, Figure 2.7 shows that all three APM models reconstruct OJN over the Pacific–Pheonix spreading center at the time of OJN formation. Plume head-ridge interaction may have occurred as the ascending Louisville plume head may have exploited weaker lithosphere at the ridge axis resulting in rapid formation of the plateau and perhaps contributing to its ensuing breakup. Based on the assumption that Louisville hotspot formed Ontong Java Nui, my reconstructions favor $\sim 7^\circ$ – 12° of southward Louisville drift since 123 Ma. However, the excellent agreement between the observed and preferred Louisville seamount chain prediction suggests that drift may have occurred some time prior to 78 Ma. I note that the 123 Ma reconstruction shown in Figure 2.7 also would support plateau formation through entrainment of mantle eclogite as suggested by Korenaga [2005].

5.3 True polar wander

Significant true polar wander for the 123 Ma Ontong Java Plateau vicinity is not supported by my preferred model, nor is it supported by the true polar wander model of Steinberger and Torsvik [2008]. Of the three APMs used to perform absolute

reconstructions, only the WK08-A implies significant magnitudes of true polar wander ($\sim 9^\circ$). However, the preliminary IODP paleolatitude history for the northern Louisville chain may allow moderate TWP to have occurred; more analysis will be needed to resolve this issue.

5.4 Rotation of the Ontong Java Plateau

While each of the three Ontong Java Nui absolute reconstructions indicated rotation, these magnitudes were small, between -4° to $+13^\circ$, and are likely to be poorly constrained due to large uncertainties in APM models for times older than 85 Ma. Results of the paleolatitude analysis in Chapter 3 provide a more compelling case for Ontong Java rotation. Although Site 1184's paleolatitude may or may not be accurate, my rotation models indicate that between $\sim 30^\circ$ and $\sim 55^\circ$ of clockwise rotation has taken place since 123 Ma, regardless of the inclusion of that site in my models. The OJP paleolatitude evidence strongly suggest clockwise rotation of Ontong Java and, in my opinion, supersedes APM-derived rotation estimates. However, the OJP rotation hypothesis currently finds little support in regional geology. Global bathymetry maps predicted from satellite altimetry and constrained by sparse ship track data [e.g., Smith and Sandwell, 1994; Becker et al., 2009] exhibit no clear Pacific–OJP paleo-interface. As compelling as the OJP based rotation hypothesis may be, it is based on only six paleolatitudes whereas Pacific APM rotations are constrained by a large array of hotspot chain geometries and are now being composed to honor paleolatitudes (e.g., WK08-D) and age constraints [e.g., Wessel and Kroenke, 2008]. Should the 2:1 slope bias observed in Chapter 3 turn out to be a misleading artifact associated with large paleolatitude errors, then Ontong Java's anomalous history will remain poorly understood and its rotational history will be better described by the smaller magnitude rotations implied by APM models (e.g., Figure 2.8). We are left with

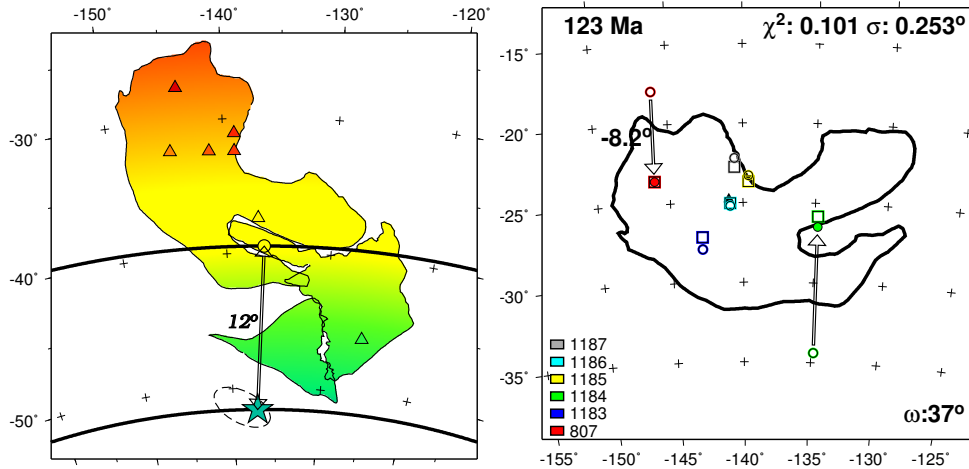


Figure 5.1: The two preferred reconstructions developed in this research. Although the OJP paleolatitude-derived rotation hypothesis (right) is compelling and is likely situated at OJP’s actual emplacement latitude, it is a relatively unconstrained model and requires considerably more data to verify. The WK08-D OJN reconstruction (left) is constrained by hotspot chain geometries and plume drift histories but is reconstructed south of OJP paleolatitude measurements indicating that OJP’s history is not perfectly described by models for Pacific plate motion.

the question of whether Ontong Java shares its rotational history with the Pacific plate (Figure 5.1(a)) or whether it rotated independently at some point in its past (Figure 5.1(b)). Additional basement cores will be needed in order to answer this question.

5.5 Coupling of Ontong Java–Pacific

It is possible that both rotation histories are correct and that the ancient Pacific–OJP paleo-interface is masked by sediments or younger volcanic flows. Because the WK08-D APM suggests Ontong Java rotation (13° counter-clockwise) in the opposite sense as implied by the Chapter 3 analysis (30° – 55° clockwise), a $\sim 40^\circ$ – $\sim 70^\circ$ difference in orientations is indicated. The evidence I have examined suggests decoupling of Ontong Java Plateau from the Pacific plate in OJP’s early history. Prior to the OJP paleolatitude analysis given in Chapter 3, it was assumed that no relative

motion occurred between OJP and Pacific. For instance, Sager [2006] assumed no OJP–Pacific relative motion but acknowledged that it is uncertain whether or not the plateau rotated relative to the Pacific. Also, Pacific magnetic lineations mapped by Nakinishi et al. [1992] appear to extend uninterrupted to the perimeter of OJP (see Figure 2.5). However, OJP’s anomalous paleopole [e.g., Sager, 2006; Riisager et al., 2004] contrasts sharply with other Pacific paleopoles (see Figure 3.2), indicating different OJP–Pacific histories. Although unlikely, I am unable to rule out the possibility that the whole Pacific experienced rotation comparable to OJP rotation and that the two were not decoupled. For instance, Cande and Stegman [2011] proposed that plume head push forces can drive plate motion. Hence, the Louisville plume head may have altered Pacific plate motion during the period of formational volcanism. The many uncertainties involved indicate that a considerable amount of further study and data acquisition will be required to better resolve Ontong Java and Pacific rotational histories. While both preferred models shown in Figure 5.1 cannot simultaneously be correct, I am unable to rule out either scenario. The results of Chapter 3 therefore do not preclude the findings of Chapter 2. It is further possible that Ontong Java shared a microplate-boundary with the Pacific plate and was eventually accreted to the Pacific without significant relative motion, a scenario which allows both OJP rotation and a coupled history of the two plates. The problem remains under-constrained.

5.6 The Greater Ontong Java Plateau Hypothesis

The separation of Hikurangi and Manihiki by seafloor spreading centered at the Osborn Trough is largely accepted by the scientific community. However, the Taylor [2006] hypothesis is not yet fully established. Ambiguities remain and include the southern East Wishbone Scarp, which mysteriously extends south of the East

Wishbone–West Wishbone intersection, as well as complex Tongareva triple junction fabric east of the Osbourn basin. In the Ellice Basin, extensive high resolution mapping will be required in order to image and interpret the basin’s fine scale, complex seafloor fabric and to finally confirm the ~east-west spreading history proposed by Taylor [2006]. The Robbie Ridge–Steward Basin fit appears to be the most contested component of the Taylor [2006] hypothesis. Recent studies by Davy et al. [2008] and Reyners et al. [2011] both omitted the Robbie Ridge–Steward Basin fit (see Figure 5.2 for a comparison of super-plateau fits). The first order rotations derived in this study reconstruct Robbie Ridge into Stewart Basin whether or not their respective conjugate boundaries are included in Hellinger tests. However, excluding this fit does not significantly impact the model as shown in Figure 2.3. A visual inspection of the bathymetry (Figure 2.4) indicates roughly equivalent depths along the Robbie Ridge and within the Stewart Basin. While the Robbie Ridge fit has been used in this study, it is not integral to the model. Whereas the Taylor [2006] study insisted that a gap exist between Ontong Java and Manihiki, I find it unlikely that such a large gap should exist prior to rifting. I note that only a very small interpreted portion of Manihiki extends beyond the Pacific-Ellice Basin suture boundary with my current first order model. A slight modification of the Manihiki boundary is more plausible than a 200–300 km inter-plateau gap as proposed by Taylor [2006]. Progress is being made on establishing a Cretaceous Quiet Zone time scale based on paleointensity variation [Granot et al., 2011] rather than the more common geomagnetic reversal patterns seen elsewhere. Such a time scale could help constrain breakup timing and spreading rates. Furthermore, additional basement paleolatitudes at Manihiki and Hikurangi plateaus will allow further testing of the Taylor [2006] hypothesis.

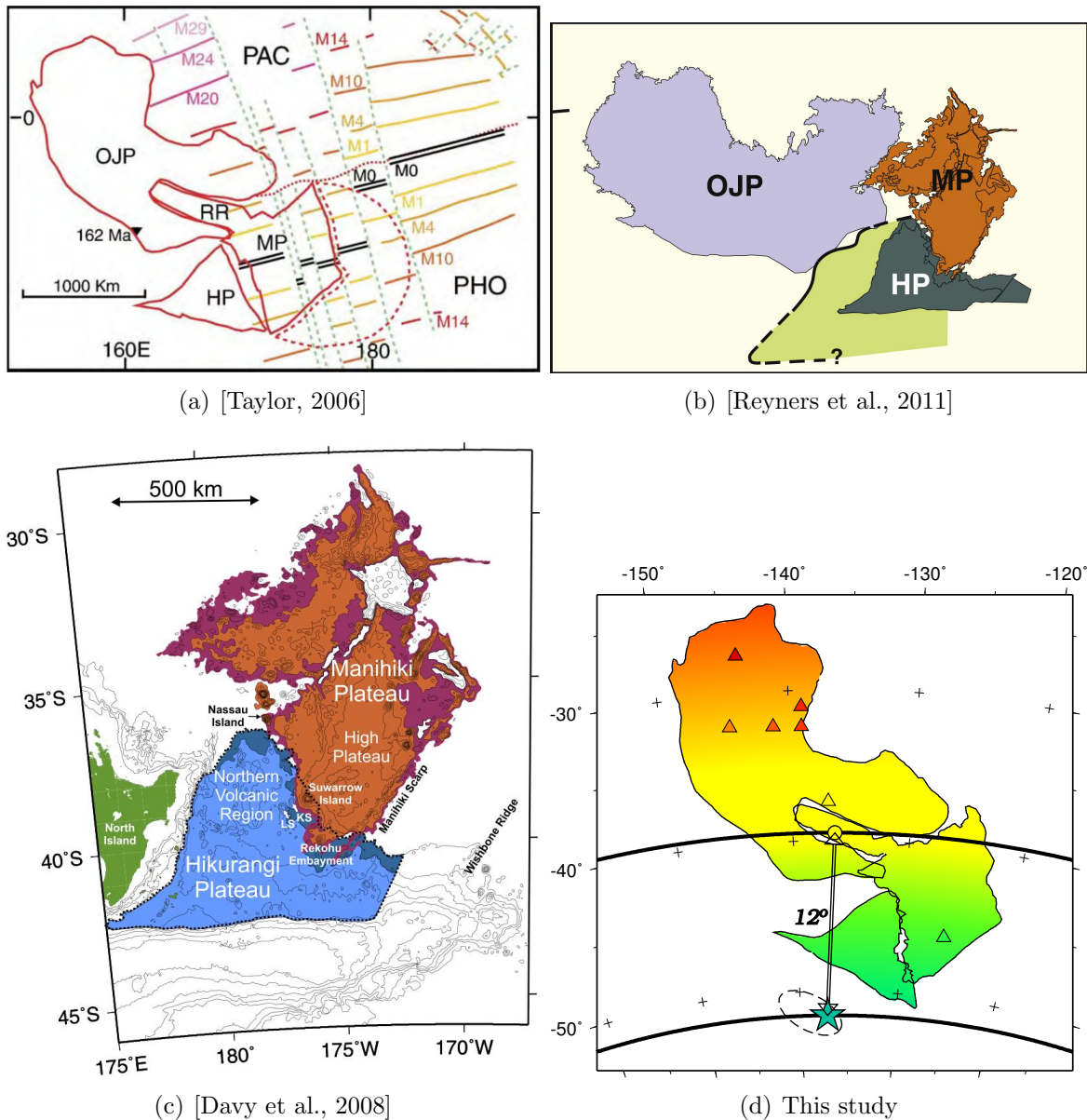


Figure 5.2: Several interpretations of the pre-breakup greater Ontong Java plateau illustrate major differences. For instance, the gap between OJP and MP which is apparent in plots (a) and (b) is not present in plot (d). The geometry of the MP–HP fit also differs (i.e., (d) is intermediate of (a) and (b)/(c)). Another major difference is whether RR is included as part of MP (plots (a) and (d) versus (b) and (c)). Plots (a), (b) and (c) are also qualitative reconstructions whereas plot (d) (this study) is quantitative and based on best-fit spherical rotations. In addition, the Reyners et al. [2011] reconstruction also shows original HP extents inferred from seismic analysis of subducted portions of HP.

5.7 Errata-based correction of trackline data

This analysis has identified a wide range of serious data errors which will hopefully spur renewed efforts among source institutions to revisit and improve erroneous cruises. The errata-based approach is a marked improvement over past marine geophysical trackline quality control efforts. The methods are freely distributed [Wessel and Chandler, 2007] as are the first generation errata tables. Prior studies identified serious quality issues but their analyses relied on discrepancies at intersecting ship tracks so their findings gradually became outdated as more and more tracks became available. In contrast, analysis of trackline data along-track results in data corrections that are independent of other ship tracks. It is my hope that the errata-based system will be utilized by other scientists and that optimum corrections are achieved for as many cruises as possible.

Literature Cited

- Antretter, M., Riisager, P., Hall, S., Zhao, X., Steinberger, B., 2004. Modelled paleolatitudes for the Louisville hot spot and the Ontong Java Plateau. In: Origin and Evolution of the Ontong Java Plateau. Vol. 229. Geol. Soc. Spec. Publ., pp. 21–30.
- Becker, J. J., Sandwell, D. T., Smith, W. H. F., Braud, J., Binder, B., Depner, J., Fabre, D., Factor, J., Ingalls, S., Kim, S.-H., Ladner, R., Marks, K., Nelson, S., Pharaoh, A., Trimmer, R., Von Rosenberg, J., Wallace, G., Weatherall, P., 2009. Global bathymetry and elevation data at 30 arc seconds resolution: Srtm30_plus. *Mar. Geod.* 32, 355–371.
- Bercovici, D., Mahoney, J. J., 1994. Double flood basalts and plume head separation at the 660-kilometer discontinuity. *Science* 266, 1367– 1369.
- Besse, J., Courtillot, V., 2002. Apparent and true polar wander and the geometry of the geomagnetic field over the last 200 myr. *J. Geophys. Res.* 107, 1–31.
- Billen, M. I., Stock, J., 2000. Morphology and origin of the Osborn Trough. *J. Geophys. Res.* 105, 13481 – 13489.
- Brunhes, B., 1906. Research on the direction of the magnetization of volcanic rocks. *J. Physique*, 705–724.
- Bullard, E. C., Everett, J. E., Smith, A. C., 1965. The fit of the continents around the Atlantic. *Phil. Trans. R. Soc.* A258, 41–51.
- Campbell, I. H., 2005. Large igneous provinces and the mantle plume hypothesis. *Elements* 1, 265–269.
- Cande, S. C., Stegman, D. R., 2011. Indian and African plate motions driven by the push force of the Réunion plume head. *Nature* 475, 47–52.
- Carter, D. J. T., 1980. Echo-sounding correction tables. Hydrographic Department, Ministry of Defense, UK 3rd Ed.
- Chambers, L. M., Pringle, M. S., Fitton, J. G., 2004. Phreatomagmatic eruptions on the Ontong Java Plateau: an Aptian $^{40}\text{Ar}/^{49}\text{Ar}$ age for volcanoclastic rocks at ODP Site 1184. In: Origin and Evolution of the Ontong Java Plateau. Vol. 229. Geol. Soc. Spec. Publ., pp. 325–331.
- Chandler, M. T., Wessel, P., 2008. Improving the quality of marine geophysical track line data: Along-track analysis. *J. Geophys. Res.* 113 (B02102, doi:10.1029/2007JB005051).
- Chandler, M. T., Wessel, P., Seton, M., Taylor, B., Kim, S.-S., Hyeong, K., 2011, in review. Reconstructing Ontong Java Nui: Implications for Pacific absolute plate motion, hotspot drift and true polar wander. *Earth Planet. Sci. Lett.*

- Chang, T., 1987. On the statistical properties of estimated rotations. *J. Geophys. Res.* 92(B7), 6319–6329.
- Clouard, V., Bonneville, A., 2001. How many Pacific hotspots are fed by deep-mantle plumes? *Geology* 29, 695–698.
- Cockerham, R., Jarrard, R. D., 1976. Paleomagnetism of some Leg 33 sediments and basalts. In: *Initial Rep. Deep Sea*. Vol. 33. pp. 631–647.
- Cockerham, R. S., Hall, J. M., 1976. Magnetic properties and paleomagnetism of some DSDP Leg 33 basalts and sediment and their tectonic implications. *J. Geophys. Res.* 81, 4,207–4,222.
- Coffin, M., Eldholm, O., 1994. Large igneous provinces: Crustal structure, dimensions, and external consequences. *Rev. of Geophys.* 32, 1–36.
- Coffin, M. F., Duncan, R. A., Eldholm, O., Fitton, J. G., Frey, F. A., Larsen, H. C., Mahoney, J. J., Saunders, A. D., Schlich, R., Wallace, P. J., 2006. Large igneous provinces and scientific ocean drilling. *Oceanography* 19, 150–160.
- Davy, B., Hoernle, K., Werner, R., 2008. Hikurangi Plateau: Crustal structure, rifted formation, and Gondwana subduction history. *Geochem. Geophys. Geosys.* 9 (7), 1–31.
- Dehlinger, P., 1978. *Marine Gravity*. 22. Elsevier Scientific Publishing Company, 322 pp.
- Dietz, R. S., 1961. Continent and ocean basin evolution by spreading of the sea floor. *Nature* 190, 854–857.
- Downey, N., Stock, J., Clayton, R., Cande, S., 2007. History of the Cretaceous Osborn spreading center. *J. Geophys. Res.* 112, doi: 10.1029/2006JB004550, 2007.
- Duncan, R. A., Clague, D. A., 1985. Pacific plate motion recorded by linear volcanic chains. In: *The Ocean Basins and Margins*. Plenum, New York, pp. 89–121.
- Erba, E., Tremolada, F., 2004. Nannofossil carbonate fluxes during the Early Cretaceous: Phytoplankton response to nutrification episodes, atmospheric CO₂ and anoxia. *Paleoceanography* 19, doi: 10.1029/2003PA000884.
- Fitton, J. G., Godard, M., 2004. Origin and evolution of magmas on the Ontong Java Plateau. In: *Origin and Evolution of the Ontong Java Plateau*. Vol. 229. *Geol. Soc. Spec. Publ.*, pp. 1–8.
- Foulger, G., Natland, J., 2003. Is “hotspot” volcanism a consequence of plate tectonics? *Science* 300, 921–922.
- Gee, J. S., Pressling, N., Hoshi, H., T., Y., 2011. Towards a paleolatitude record from the Louisville Seamount trail. *Eos Trans. AGU, Fall Meet. Suppl. Abstr.* DI23B-2089.

- Gradstein, F., Agterberg, F., Ogg, J., Hardenbol, S., Vanveev, P., Thierry, J., Huang, Z., 1994. A Mesozoic time scale. *J. Geophys. Res.* 99, 24051–24074.
- Granot, R., Dyment, J., Gallet, Y., 2011. Geomagnetic field variability during the Cretaceous Normal Superchron obtained from marine magnetic anomalies. *Eos Trans. AGU, Fall Meet. Suppl. Abstr.* DI23B-2089.
- Gurnis, M., Turner, M., Zahirovic, S., DiCaprio, L., Spasojevic, S., Müller, R. D., Boyden, J., Seton, M., Manea, V. C., Bower, D., 2011. Plate tectonic reconstructions with continuously closing plates. *Comput. Geosci.*, doi:10.1016/j.cageo.2011.04.014.
- Hellinger, S. J., 1981. The uncertainties of finite rotations in plate tectonics. *J. Geophys. Res.* 86, 9312–9318.
- Henderson, L., Gordon, R., 1981. Oceanic plateaus and the motion of the Pacific plate with respect to hot spots. *Eos Trans. AGU* 62, 1028.
- Hess, H. H., 1962. History of ocean basins. In: *Petrologic Studies: A volume to honor A. F. Buddington*. Geol. Soc. Amer., pp. 599–620.
- Hittleman, A. M., Groman, R. C., Haworth, T. L., Holcombe, T. L., McHendrie, G., Smith, S. M., 1977. The Marine Geophysical Data Exchange Format MGD77 - key to geophysical records documentation 10, National Geophysical Data Center, Boulder, Colorado, USA.
- Hoernle, K., Hauff, F., van den Bogaard, P., Werner, R., Mortimer, N., Geldmacher, J., Garbe-Schönberg, D., Davy, B., 2010. Age and geochemistry of volcanic rocks from the Hikurangi and Manihiki oceanic plateaus. *Geochim. Cosmochim. Acta* 10.1016/j.gca.2010.09.030.
- Hussong, D., Wiperman, L., Kroenke, L., 1979. The crustal structure of the Ontong Java and Manihiki oceanic plateaus. *J. Geophys. Res.* 84 (B11), 6003–6010.
- Ingle, S., Coffin, M. F., 2004. Impact origin for the greater Ontong Java Plateau. *Earth Planet. Sci. Lett.* 218, 123–134.
- Ingle, S., Mahoney, J. J., Sato, H., Coffin, M., Kimura, J.-I., Hirano, N., Nakinishi, M., 2007. Depleted mantle wedge and seiment fingerprint in unusual basalts from the Manihiki Plateau, central Pacific Ocean. *Geology* 35 (7), 595–598.
- Irving, E., 1956. Palaeomagnetic and palaeoclimatological aspects of polar wandering. *Pure Applied Geophys.* 33, 23–41, 10.1007/BF02629944.
URL <http://dx.doi.org/10.1007/BF02629944>
- Jackson, E., Bargar, K., Fabbi, B., Heropoulos, C., 1976. Petrology of the basaltic rocks drilled on Leg 33 of the Deep Sea Drilling Project. In: *Initial Rep. Deep Sea. Ocean Drilling Program*, Texas A & M University, pp. 571–630.

- Jones, E. J. W., 1999. *Marine Geophysics*. Wiley, 466 pp.
- Joseph, D., Taylor, B., Shor, A., 1992. New sidescan sonar and gravity evidence that the Nova-Canton Trough is a fracture zone. *Geology* 20, 435–438.
- Kerr, A. C., 1998. Oceanic plateau formation: a cause of mass extinction and black shale deposition around the Cenomanian–Turonian boundary? *J. Geol. Soc. London* 155, 619–626.
- Kono, M., 1980. Paleomagnetism of DSDP Leg 55 basalts and implications for the tectonics of the Pacific plate. In: *Initial Rep. Deep Sea*. US Govt. Printing Office, Washington, pp. 737–752.
- Koppers, A., Morgan, J. P., Morgan, J. W., Staudigel, H., 2001. Testing the fixed hotspot hypothesis using $^{40}\text{Ar}/^{39}\text{Ar}$ age progressions along seamount trails. *Earth Planet. Sci. Lett.* 185, 237–252.
- Koppers, A., Staudigel, H., 2005. Asynchronous bends in Pacific seamount trails: A case for extensional volcanism? *Science* 307, 904–907.
- Korenaga, J., 2005. Why did not the Ontong Java Plateau form subaerially? *Earth Planet. Sci. Lett.* 234, 385–399.
- Kroenke, L. W., Wessel, P., Sterling, A., 2004. Motion of the Ontong Java Plateau in the hot-spot frame of reference: 122 Ma-present. In: *Origin and evolution of the Ontong Java Plateau*. Vol. 229. *Geol. Soc. Spec. Publ.*, pp. 9–20.
- Larson, R., 1997. Superplumes and ridge interactions between Ontong Java and Manihiki Plateaus and the Nova-Canton Trough. *Geology* 25, 779–782.
- Larson, R., Olson, P., 1991. Mantle plumes control magnetic reversal frequency. *Earth Planet. Sci. Lett.* 107, 437–447.
- Larson, R. L., Erba, E., 1999. Onset of the mid-Cretaceous greenhouse in the Barremian– Aptian: Igneous events and the biological, sedimentary, and geochemical responses. *Paleoceanography* 14, 663–678.
- Larson, R. L., Sager, W. W., 1992. Skewness of magnetic anomalies M0 to M29 in the Northwestern Pacific. In: Larson, R., Lancelot, Y., et al (Eds.), *Proc. Ocean Drill Program, Sci. Results*. Vol. 129.
- Lonsdale, P., 1997. An incomplete geologic history of the south-west Pacific basin. *Geol. Soc. of Am. Abstr. Programs* 29, 4574.
- Macmillan, S., Finlay, C., 2011. *Geomagnetic Observations and Models*. Springer, Ch. The International Geomagnetic Reference Field, pp. 265–276.
- Mahoney, J. J., Fitton, J. G., Wallace, P. J., et al (Eds.), 2001. *Proceedings of the Ocean Drilling Program, Initial Reports*. Vol. 192.

- Mahoney, J. J., Spencer, K. J., 1991. Isotopic evidence for the origin of Manihiki and Ontong Java oceanic plateaus. *Earth Planet. Sci. Lett.* 102, 196–210.
- Mahoney, J. J., Storey, M., Duncan, R. A., Spencer, K. J., Pringle, M., 1993. Geochemistry and geochronology of Leg 130 basement lavas: Nature and origin of the Ontong Java Plateau. In: *Proc. Ocean Drill Program, Sci. Results.* Vol. 130.
- Mann, P., Taira, A., 2004. Global tectonic significance of the Solomon Islands and Ontong Java Plateau convergent zone. *Tectonophysics* 389, 137–190.
- Marks, K. M., Smith, W. H. F., 2006. An evaluation of publicly available global bathymetry grids. *Mar. Geophys. Res.* 27 (1), 19–34.
- Matthews, K., Müller, R. D., Wessel, P., Whittaker, J., 2011, in press. The tectonic fabric of the ocean basins. *J. Geophys. Res.*
- Matuyama, M., 1929. On the direction of magnetization of basalt. *Proc. Imp. Acad. Japan* 5, 203–205.
- Mayer, H., Tarduno, J. A., 1993. Paleomagnetic investigation of the igneous sequence, Site 807, Ontong Java Plateau, and a discussion of Pacific true polar wander. In: *Proc. Ocean Drill Program, Sci. Results.* Vol. 130.
- McKenzie, D. P., Parker, R. L., 1967. The North Pacific: An example of tectonics on a sphere. *Nature* 216, 1,276–1,280.
- Morgan, W. J., 1968. Rises, trenches, great faults, and crustal blocks. *J. Geophys. Res.* 73, 1,959–1,982.
- Morgan, W. J., 1971. Convection plumes in the lower mantle. *Nature* 230, 42–43.
- Morley, L., 2001. The zebra pattern. In: Oreskes, N. (Ed.), *Plate Tectonics.* Westview Press, pp. 67–85.
- Mortimer, N., Parkinson, D., 1996. Hikurangi Plateau: A Cretaceous large igneous province in the southwest Pacific Ocean. *J. Geophys. Res.* 101, 687–696.
- Müller, R. D., Gurnis, M., Torsvik, T., Cannon, J., 2011. Download GPlates and data.
URL <http://www.gplates.org/download.html>
- Nakinishi, M., Tamaki, K., Kobayashi, K., 1992. Magnetic anomaly lineations from Late Jurassic to Early Cretaceous in the west-central Pacific Ocean. *Geophys. J. Int.* 109, 701–719.
- Neal, C. R., Mahoney, J. J., Kroenke, L. W., Duncan, R. A., Petterson, M. G., 1997. The Ontong Java Plateau. In: *Large Igneous Provinces: Continental, Oceanic, and Planetary Flood Volcanism, Geophysical Monograph* 100. pp. 183–216.

- O'Neill, C., Müller, D., Steinberger, B., 2005. On the uncertainties in hot spot reconstructions and the significance of moving hot spot reference frames. *Geochem. Geophys. Geosys.* 6 (4), 1–35.
- Parkinson, I., Schaefer, B., Arculus, R., 2003. Residue-melt relationships; Os isotopes from the Ontong Java Plateau. *Geophys. Res. Abstr. (Eur. Geophys. Soc.)* 5, 14351.
- Petronotis, K., Gordon, R., Acton, G., 1994. A 57 Ma Pacific paleomagnetic pole determined from a skewness analysis of crossings of marine magnetic anomaly 25r. *Geophys. J. Int.* 118, 529–554.
- Prevot, M., Mattern, E., Camps, P., Daignieres, M., 2000. Evidence for a 20° tilting of the Earth's rotation axis 110 million years ago. *Earth Planet. Sci. Lett.* 179, 517–528.
- Quesnel, Y., Catalan, M., Ishihara, T., 2009. A new global marine magnetic anomaly data set. *J. Geophys. Res.* 114, 1–11.
- Raff, A., Mason, R., 1961. A magnetic survey off the west coast of North America, 40° N to 52.5° N. *Bull. Geol. Soc. Am.* 72 (8), 1267 – 1270.
- Reyners, M., Eberhart-Phillips, D., Bannister, S., 2011. Tracking repeated subduction of the Hikurangi Plateau beneath New Zealand. *Earth Planet. Sci. Lett.* 311, 165–171.
- Riisager, P., Hall, S., Antretter, M., Zhao, X., 2003. Paleomagnetic paleolatitude of Early Cretaceous Ontong Java Plateau basalts: implications for Pacific apparent and true polar wander. *Earth Planet. Sci. Lett.* 208, 235–252.
- Riisager, P., Hall, S., Antretter, M., Zhao, X., 2004. Early Cretaceous Pacific paleomagnetic pole from Ontong Java Plateau basement rocks. In: *Origin and Evolution of the Ontong Java Plateau*. Vol. 229. *Geol. Soc. Spec. Publ.*, pp. 31–44.
- Runcorn, S. K., 1956. Paleomagnetic comparisons between Europe and North America. *Proc. Geol. Assoc. Can.* 8, 77–85.
- Sabaka, T. J., Olsen, N., Purucker, M. E., 2004. Extending comprehensive models of the Earth's magnetic field with Ørsted and CHAMP data. *Geophys. J. Int.* 159 (10.1111/j.1365-246X.02421.x), 521–547.
- Sager, W., Keating, B., 1984. Paleomagnetism of Line Islands seamounts: Evidence for Late Cretaceous and Early Tertiary volcanism. *J. Geophys. Res.* 89, 11,135–11,151.
- Sager, W. W., 2006. Cretaceous paleomagnetic apparent polar wander path for the Pacific plate calculated from Deep Sea Drilling Project and Ocean Drilling Program basalt cores. *Phys. Earth Planet. In.* 156, 329–349.

- Sager, W. W., 2007. Divergence between paleomagnetic and hotspot-model-predicted polar wander for the Pacific plate with implications for hotspot fixity. In: *Plates, plumes, and planetary processes: Geological Society of America Special Paper 430*. Geol. Soc. Amer., pp. 335–357.
- Sager, W. W., Lamarche, A., Kopp, C., 2005. Paleomagnetic modeling of seamounts near the Hawaiian-Emperor bend. *Tectonophysics* 405, 121–140.
- Sandwell, D., Smith, W., 2009. Global marine gravity from retracked Geosat and ERS-1 altimetry: Ridge segmentation versus spreading rate. *J. Geophys. Res.* 114, doi: 10.1029/2008JB006008.
- Sandwell, D. T., 2011. Personal communication.
- Sandwell, D. T., Smith, W. H. F., 2005. Retracking ERS-1 altimeter waveforms for optimal gravity field recovery. *Geophys. J. Int.* 163, 79–89.
- Seton, M., Müller, R., Zahirovic, S., Gaina, C., Torsvik, T., Shephard, G., Talsma, A., Gurnis, M., Turner, M., Chandler, M. T., 2011, in press. Global continental and ocean basin reconstructions since 200 Ma. *Earth-Sci. Rev.*
- Shephard, G. E., Bunge, H.-P., Schubert, B. S. A., Müller, R. D., Talsma, A. S., Moder, C., Landgrebe, T. C. W., 2011, in review. Testing absolute plate reference frames and the implications for the generation of geodynamic mantle heterogeneity structure. *Earth Planet. Sci. Lett.*
- Smith, W. H. F., June 1993. On the accuracy of digital bathymetric data. *J. Geophys. Res.* 98 (B6), 9591–9603.
- Smith, W. H. F., Sandwell, D. T., November 1994. Bathymetric prediction from dense satellite altimetry and sparse shipboard bathymetry. *J. Geophys. Res.* 99 (B11), 21803–21824.
- Steinberger, B., Sutherland, R., O’Connell, R., R., 2004. Prediction of Emperor-Hawaii seamount locations from a revised model of global plate motion and mantle flow. *Nature* 430, 167–173.
- Steinberger, B., Torsvik, T., 2008. Absolute plate motions and true polar wander in the absence of hotspot tracks. *Nature* 452, doi:10.1038/nature06824.
- Steinberger, B. M., O’Connor, J. M., Koppers, A. A., 2011. Motion of Hawaii and Louisville hotspots: Comparison of modeling results with new age and paleolatitude data. *Eos Trans. AGU, Fall Meet. Suppl. Abstr.* V53G-03.
- Sykes, L., 1978. Intraplate seismicity, reactivation of preexisting zones of weakness, alkaline magmatism, and other tectonism postdating continental fragmentation. *Rev. of Geophys.* 16, 621–688.

- Tarduno, J., Bunge, H.-P., Sleep, N., Hansen, U., 2009. The bent Hawaiian-Emperor hotspot track: Inheriting the mantle wind. *Science* 324, 50–53.
- Tarduno, J. A., 2007. On the motion of Hawaii and other mantle plumes. *Chem. Geol.* 241, 234–247.
- Tarduno, J. A., Duncan, R. A., Scholl, D. W., Cottrell, R. D., Steinberger, B., Thordarson, T., Kerr, B. C., Neal, C. R., Frey, F. A., Torii, M., Carvallo, C., 2003. The Emperor Seamounts: Southward motion of the Hawaiian hotspot plume in the Earth’s mantle. *Science* 301, 1064–1069.
- Tarduno, J. A., Slitter, W. V., Kroenke, L. W., Leckie, M., Mayer, H., Mahoney, J. J., Musgrave, R., Storey, M., Winterer, E. L., 1991. Rapid formation of Ontong Java Plateau by Aptian mantle plume volcanism. *Science* 254, 399–402.
- Taylor, B., 2006. The single largest oceanic plateau: Ontong Java-Manihiki-Hikurangi. *Earth Planet. Sci. Lett.* 241, 372–380.
- Tejada, M., Mahoney, J. J., Neal, C. R., Duncan, R. A., Petterson, M. G., 2002. Basement geochemistry and geochronology of Central Malaita, Solomon Islands, with implications for the origin and evolution of the Ontong Java Plateau. *J. Petrology* 43 (3), 449–484.
- Timm, C., Hoernle, K., Werner, R., F., H., van den Bogaard, P., Michael, P., Coffin, M., Koppers, A., 2011. Age and geochemistry of the oceanic Manihiki Plateau, SW Pacific: New evidence for a plume origin. *Earth Planet. Sci. Lett.* 304 (1-2), 135–146.
- Vanderkluisen, L., Mahoney, J. J., Koppers, A. A., Lonsdale, P. F., 2007. Geochemical evolution of the Louisville seamount chain. *Eos Trans. AGU*, 88 (52), Fall Meet. Suppl. Abstr. V42B-06.
- Vening-Meinesz, F. A., 1948. Gravity expeditions at sea 1923–1938: Complete results with isostatic reduction, interpretation on the results. Vol. IV. Nederlandse Commissie voor Geodesie.
- Verhoef, J., Duin, E., 1986. A 3-dimensional analysis of magnetic anomalies over fracture zones in the Cretaceous Magnetic Quiet Zone (Madeira Abyssal Plain. *J. Geol. Soc. London* 143, 823–832.
- Vine, F. J., Matthews, D. H., September 1963. Magnetic anomalies over oceanic ridges. *Nature* 199 (4897), 947–949.
- Viso, R. F., Larson, R. L., Pockalny, R. A., 2005. Tectonic evolution of the Pacific-Pheonix-Farallon triple junction in the South Pacific Ocean. *Earth Planet. Sci. Lett.* 233, 179–194.
- Walker, J., Geissman, J., 2009. Geologic time scale. *Geol. Soc. of America*, doi: 10.1130/2009.CTS004R2C.

- Wegener, A., 1915. The origin of continents and oceans. Braunschweig: Friedrich Vieweg & Sohn Akt. Ges.
- Wessel, P., 2010. Tools for analyzing intersecting tracks: The x2sys package. *Comput. Geosci.* 36, 348–354.
- Wessel, P., Chandler, M. T., 2007. The mgd77 supplement to the Generic Mapping Tools. *Comput. Geosci.* 33, 62–75.
- Wessel, P., Chandler, M. T., 2011. The spatial and temporal distribution of marine geophysical surveys. *Acta Geophys.* 59 (1), 55–71.
- Wessel, P., Kroenke, L. W., 2008. Pacific absolute plate motion since 145 Ma: An assessment of the fixed hot spot hypothesis. *J. Geophys. Res.* 113 (B06101), 1–21.
- Wessel, P., Kroenke, L. W., 2009. Observations of geometry and ages constrain relative motion of Hawaii and Louisville plumes. *Earth Planet. Sci. Lett.* 284, 467–472.
- Wessel, P., Müller, R. D., Sandwell, D. T., Cande, S., 2009. The global fracture zone and magnetic lineation project. *Eos Trans. AGU*, 90 (52) Fall Meet. Suppl., Abstr. T13C–1889.
- Wessel, P., Smith, W. H. F., 1998. New, improved version of Generic Mapping Tools released. *Eos Trans. AGU* 79 (47), 579.
- Wessel, P., Watts, A. B., January 1988. On the accuracy of marine gravity measurements. *J. Geophys. Res.* 93 (B1), 393–413.
- Worthington, T., Hekinian, R., Stoffers, P., Kuhn, T., Hauff, F., 2006. Osborn trough: Structure, geochemistry and implications of a mid-Cretaceous paleospraying ridge in the South Pacific. *Earth Planet. Sci. Lett.* 245, 685–701.